THE ROLE OF ULTRAFINE PARTICULATE MATTER AND NRF2 IN THE PATHOGENESIS OF NEONATAL RESPIRATORY SYNCYTIAL VIRUS DISEASE AT TEXAS A&M UNIVERSITY

A Dissertation

by

CARMEN LAU

Submitted to the Graduate and Professional School of
Texas A&M University
in partial fulfillment of the requirements for the degree of

DOCTOR OF PHILOSOPHY

Chair of Committee,	Natalie Johnson
Co-Chair of Committee,	Aline Rodrigues Hoffmann
Committee Members,	Carolyn Cannon
	Michael Criscitiello
Head of Department,	Ramesh Vemulapalli

May 2022

Major Subject: Biomedical Sciences

ABSTRACT

Despite increasing movements towards cleaner air regulations, air pollution remains a critical factor in millions of deaths globally every year. Particulate matter (PM) is one of the many types of air pollution, and ultrafine particulate matter (UFP) is the highly detrimental and under-regulated smallest fraction of PM. While it is known that PM exposure during pregnancy can lead to harmful neonatal effects, such as stillbirth and low birth weight, little literature exists on the specific effects that UFPs may have during this critical time window. Prenatal PM exposure has also been shown to significantly increase the risk of the infant developing asthma or respiratory infections during childhood, and it is likely, though not confirmed, that UFPs would likely do the same. We undertook to develop a murine model of prenatal UFP exposure, to examine how it might alter neonate's ability to combat respiratory infection, and to examine the possible mechanisms by which prenatal UFPs might exert its influence through the dam to the fetus. This last goal was accomplished by looking at the effect that Nrf2, a major transcription factor controlling antioxidant responses, may play in the neonatal response to UFP exposure. Our findings demonstrated that prenatal UFP exposure did enhance the severity of neonatal respiratory disease, specifically to respiratory syncytial virus (RSV). When examining neonates only exposed to UFPs prenatally, we found that Nrf2 deficient neonates had a reduced ability to respond to oxidative stress than their wildtype counterparts, and that their pulmonary T cell populations had significantly increased levels of Th1 and Th2 immune cells when stimulated by UFPs. This suggests that prenatal UFPs may exert their influence by oxidative stress, perhaps transferred from the mother, and by altering pulmonary T cell differentiation and potential priming for neonatal respiratory infections. Overall, our research shows that UFPs exert negative influences on fetal health that have an impact in the neonatal period, thus demonstrating a need

for increased regulation and public health preventative measures to protect the health of mothers and children in highly polluted regions.

DEDICATION

This work is dedicated in three parts:

First, to the almighty God, who is perfect and just;

Second, to my family, who unceasingly believed in me and loved me unconditionally through many years of school;

Third, to my love, Jonathan, who has held fast and true through joy and storm, and now knows more about mouse breeding than he ever hoped he would;

I love you all.

ACKNOWLEDGEMENTS

Grateful acknowledgement is given to Dr. Ben Morpugo, Dr. Andrei Golovko, and Stephanie King for their assistance, advice, and support through all of these mouse modeling projects. Special thanks are given to Dr. Martin Moore for the chimeric strain of the virus, Dr. Tom Kensler for the $Nrf2^{-/-}$ mouse strain, and Dr. Stephania Cormier's laboratory for constant guidance and assistance.

Much appreciation is given to the NIEHS Outstanding New Environmental Scientist (ONES) external advisory board members Drs. Stephania Cormier, Steve Kleeberger, and Dave Williams for their feedback on building this model.

Immeasurable assistance was provided by the personnel of Dr. Natalie Johnson's laboratory, including Navada Harvey, Drew Pendleton, Ross Shore, Dr. Toriq Mustapha, Jonathan Behlen, and Nicholas Drury.

Lastly, I thank Dr. Natalie Johnson for all the time and compassion that she pours into each of her students, not least of all me. Thank you, Natalie, for your persistent optimism, unflagging support, and boundless ideas that makes you the best of researchers.

CONTRIBUTORS AND FUNDING SOURCES

Contributors

This work was supported by a dissertation committee consisting of Professor Natalie M. Johnson, advisor, of the Department of Environmental and Occupational Health, Professor Aline Rodrigues Hoffmann of the Department of Comparative, Diagnostic, and Population Medicine of the University of Florida, Dr. Carolyn Cannon of the Department of Microbial Pathogenesis and Immunology, and Dr. Michael Criscitiello in the Department of Veterinary Pathobiology.

The exposure chambers were created and maintained by Dr. Renyi Zhang and his laboratory, in particular Dr. Jeremiah Secrest, Dr. Yixin Li, and Jiayun Zhao. Animal breeding, genotyping, and housing was provided by the Texas Institute for Genomic Medicine (TIGM) and the Texas A&M Laboratory Animal Resources and Research (LARR). The flow cytometry analysis was performed by Dr. Gus A. Wright of the Texas A&M University Flow Cytometry Facility. Figure 12 was provided by Dr. Drew Pendleton. All other work conducted for the dissertation was completed by the student independently.

Funding Sources

Graduate study was supported by a National Institute of Environmental Health Sciences grant (RO1 ES028866) and the T32 training grant (5T32OD011083-12), and funding provided by the Department of Veterinary Pathobiology at Texas A&M University.

ABBREVIATIONS

AHR: airway hyperresponsiveness

AhR: aryl hydrocarbon receptor

FA: filtered air

GD: gestation day

HD: high dose

IN: intranasal

IUGR: intrauterine growth restriction

LD: low dose

LRTI: lower respiratory tract infection

Nrf2: Nuclear factor erythroid 2-related factor 2

PM: particulate matter

PND: postnatal day

RSV: respiratory syncytial virus

UFP: ultrafine particulate matter

WT: wildtype

TABLE OF CONTENTS

Page

LIST OF FIGURES

Page

LIST OF TABLES

Page

CHAPTER I

INTRODUCTION*

1.1 Overview

Air pollution and respiratory disease have formed a well-documented and morbid duo in the last few centuries of human health. Yet, knowledge of how these particles affect human health is incomplete and complicated by the diversity of emissions particulate matter (PM) and timing of when exposure occurs. Air pollution is considered the leading environmental risk factor for morbidities and mortalities globally plays a role in approximately 7 million deaths annually. High levels of PM have been linked to disease in every organ system, and effects can differ based on particle characteristics (size, composition, hygroscopicity, etc.), environmental factors (humidity, wind speed, temperature, etc.), and human differences (sex, age, weight, etc.). One of the predominant mechanisms by which PM exerts such harmful influences is by the production of reactive oxygen species (ROS), which cause oxidative stress at a cellular level in numerous tissues throughout the body. Nearly limitless variations on how a target population could be affected requires continued research into the detrimental health effects of PM to better determine appropriate pollution standards and maximize global health.

1.2 Particulate matter with an emphasis on ultrafine characteristics

PM is classified by size as either "coarse" (PM_{10}) with an aerodynamic diameter less than 10 μm, "fine" ($PM_{2.5}$) with a diameter less than 2.5 μm, or "ultrafine" (UFPs, $PM_{0.1}$) with a

* Part of this chapter is reprinted with permission from "Air Pollution and Children's Health—a Review of Adverse Effects Associated with Prenatal Exposure from Fine to Ultrafine Particulate Matter" by Johnson, N. M.; Hoffmann, A. R.; Behlen, J. C.; Lau, C.; Pendleton, D.; Harvey, N.; Shore, R.; Li, Y.; Chen, J.; Tian, Y.; Zhang, R, 2021, *Environ. Health Prev. Med.*, 26 (1), 1–29, Copyright 2022 by Carmen Lau.

diameter less than 0.1 μm. The first two categories are fairly well researched, and reviews have been published on the correlations of each type of particle and various health effects, such as respiratory mortality, cardiovascular mortality, and cancer. The World Health Organization continues to redefine the standards by which air quality must be maintained regarding these two sizes of particles, so much so that when we originally started our research, the recommended maximum standard for $PM_{2.5}$ was 10 $\mu g/m^3$ on an annual basis, but in the new 2021 report, these levels have been decreased to 5 $\mu g/m^3$, while the PM_{10} guidelines have dropped from 20 $\mu g/m^3$ to 15 $\mu g/m^3$; the original guidelines have been kept as interim target levels. These standards are based on reviews and meta-analyses of the literature, examining the lowest levels at which detrimental health effects occur. Therefore, it is little wonder that ultrafine particles (UFPs) are not only understudied but also shockingly under regulated[1], as regulation does not occur without extensive knowledge.

UFPs are defined as particulate matter less than 100 nm in diameter, generally differentiated from the term "nanoparticles" by being environmentally and unintentionally generated[2,3]. The small particle size allows deeper penetration into airways, greater permeability across membranes, including the placenta[4,5] and a comparatively high surface area to volume ratio, allowing for increased adsorption of potential toxins[2,6]. Mounting concern stems from UFPs contributing to a larger number of particles and higher amount of surface area, compared to the larger forms of PM, than was previously thought[7], as UFPs can coagulate and form larger sized particles.[2,8] Additional uncertainty exists in the lack of understanding about UFPs mechanisms of disease, particularly *in utero*:, little is known of whether the effects upon the fetus is a direct result of the UFPs crossing transplacentally or whether the effects arise from maternal oxidative stress.

Current research suggests that UFPs may have a larger capacity for toxicity and delayed, long term health effects than their larger counterparts[2], in part due to their absorptive and pervasive abilities. Polycyclic aromatic hydrocarbons (PAHs) are carcinogenic toxins produced from fossil fuel and wood fires, and these molecules have an affinity for binding to UFPs.[9] Epigenetic modification, such as DNA methylation, is currently under study as another major mechanism by which all PM, not just ultrafine, can modify the health of an organism. Methylation of DNA causes a tightening of the coil-like structure of the histones, preventing genes from being translated and expressed. PM exposure has been frequently shown to hypermethylate DNA involved in circadian rhythms[10], cellular apoptosis, energy metabolism[11], and DNA repair genes, particularly in the placenta[4,12]; this will be discussed later in detail.

Ultrafine particulate matter is not only dangerous in its high level of toxicity and under-regulation, but also in that its smaller size renders many previous models used to predict air pollution movement less applicable. UFPs are also more likely to remain airborne for longer periods of time and permeate into indoor environments from outdoor sources than $PM_{2.5}$ and PM_{10}, and may even coagulate themselves into larger particles[8]. UFPs are also sourced from a number of common indoor household activities, such as burning candles and cooking[13], further complicating our ability to determine the largest sources of UFPs to be reduced and regulated.

Last, it is crucial to understand the long-term effects of UFPs upon the fetus in order that mothers may understand the implications of the environment in which they live, and hopefully be provided with measures with which to prevent and/or counteract gestational exposures. Their effects on the fetus are appreciable even when taking into account such factors as environmental tobacco smoke, residential location, and childhood allergies[3]. During pregnancy, the maternal immune system transitions to immunotolerance and anti-inflammatory so as not to reject the fetus. Our lab

previously showed that in utero UFP exposure caused immunosuppression in the neonates[14], while others demonstrated a similar finding in postnatally exposed mice[15] and adult mice[16]. With a naturally immunosuppressed dam and immunosuppressive doses of aerosolized PM, it is imperative that the neonatal consequences upon the immune system and its capacity to respond to respiratory diseases be examined, for future regulation of UFPs.

1.3 Mechanisms of prenatal PM exposure via the placenta

To understand the connection between gestational air pollution exposure and neonatal health outcomes, one must look at the physical connection between the mother and fetus: the placenta. Barker's hypothesis, written in 1995, is summed up by Luyten et al. as the "etiology of disease in adulthood may have a fetal origin and may be attributed to the effects of adverse environmental exposures in utero"[17]. Though Barker's original theory related to the development of coronary heart disease[18], this theory has been proven in numerous organ systems related to various different exposures (e.g. air pollution, heavy metals, etc.). Evaluating placental changes due to maternal PM exposure is the first step in understanding and countering those fetal effects.

Placental epigenetic modification, specifically hypermethylation, is theorized to be one of the major mechanisms by which adverse birth outcomes may arise. Bhargava et al. used an in vitro model to demonstrate that one of the mechanisms by which UFPs causes increased DNA methylation was by inducing the NF- κB inflammatory pathway, which upregulates levels of DNA methyltransferases[19]. Neven et al. found that both $PM_{2.5}$ and black carbon (BC) caused an increased rate of DNA mutation, measured by Alu, and that multiple genes associated with DNA repair and tumor suppression were hypermethylated, predominantly in the first and second trimesters of pregnancy.[12] Methylation not only occurs in nuclear DNA but also in mitochondrial DNA (mtDNA). In the ENIVR*ON*AGE birth cohort, $PM_{2.5}$ exposure was associated with an

increase in mtDNA methylation in the first trimester and a decrease in mtDNA content in the third trimester, suggesting that the biogenesis of the mtDNA is altered by the methylation early on in pregnancy.[20] The theory that mtDNA copy number could be a potential link between the maternal exposure and adverse birth outcomes is consistent across numerous studies.[21] Tsamou et al., working with the same birth cohort, suggests that this epigenetic alterations may not only be induced by methyltransferases but also by the up- or down-regulation of microRNAs (miRNAs).[22] Increased $PM_{2.5}$ exposure in the second trimester had decreased amounts of miR-21, miR-146a, and miR-222, which are related to the cell cycle, regulation of inflammation, and angiogenesis, respectively. This was followed by a strong association with increased *PTEN* in the third trimester, a mutual gene that these miRNAs all bind, which negatively regulates the pathway promoting cell survival, angiogenesis, and cellular metabolism. Tsamou suggests that these changes in miRNAs in the second trimester are likely directly responsible for the epigenetic modification and placental *PTEN* upregulation in the third trimester, which could lead to placental dysfunction.

Another important placental modification induced by PM is vascular irregularities, often leading to the syndrome preeclampsia. PM, especially UFPs, is well known to cause endothelial dysfunction and vascular inflammation[2], endothelial cell dysfunction being an initiating cause of preeclampsia[23], and an association between maternal exposure and preeclampsia has been made in both humans and mouse models.[24–27] An accepted pathogenesis begins with $PM_{2.5}$ causing altered protein expression which impairs trophoblast invasion (which can also lead to IUGR)[28], leading to unmodified spiral arteries, causing a higher vascular resistance and thus preeclampsia. As a consequence, increased resistance leads to decreased perfusion, thereby leading to a state of placental hypoxia, confirmed by van den Hooven et al.'s study in which PM and NO_2 led to an anti-angiogenic state in late gestation.[29] Placental hypertension and hypoxia not only endanger the

life of the mother, but can increase fetal morbidity and mortality. Naturally, the placental vessels are not the only affected vasculature, and mothers exposed to $PM_{2.5}$ are most at risk in their third trimester for having elevated blood pressure, which predisposes their children to high systolic blood pressures under the age of 9.[30]

Telomere length is an indicator of cellular longevity and senescence; telomeres are shortened with every cell cycle, and cells undergo apoptosis when telomeres are depleted. Shortened telomere length (TL) has been demonstrated after prenatal exposure to PM in umbilical cord blood and placental leukocytes, which has been suggested to predict TL later in life for the offspring, with shortened telomeres generally indicating a shorter lifespan.[31,32] Indeed, even low levels of ambient air pollutants were shown to shorten TL in newborns exposed prenatally.[33] Shortened placental TL may be predictive of placental senescence, which is associated with IUGR and preeclampsia.[32]

1.4 Effects of prenatal PM exposure during infancy and childhood

In utero exposure to air pollution is strongly correlated with increased neonatal and childhood respiratory morbidities, such as asthma and broncho-pulmonary infections[3,34]. Increased infant morbidity and mortality have been linked to increased levels of PM exposure during gestation[35–39], such as stillbirth, preterm birth, low birth weight, and intrauterine growth restriction (IUGR). Glinianaia et al even suggests that exposure may cause an increase in sudden infant death syndrome (SIDS) due to alterations in brain development and maturation.[35] Certainly there is evidence that prenatal PM exposure can cause neurologic abnormalities and has even been associated with behavioral deficits and autism.[40,41] Germ cells and fetal cells are at larger risk for

damage by external factors due to their increased proliferation and sensitivity to their surroundings.[42]

However, the association with post-neonatal mortality is largely driven by respiratory morbidity[43], and fetal exposure to PM affects lung development and respiratory health in a variety of ways that may persist throughout childhood, such as decreased lung capacity and other functional parameters[42]. Prenatal PM_{10} exposure significantly decreased infants' functional residual capacity at 1 year old, while postnatal exposure caused decreased tidal volume at the same age.[44] The same study showed that maternal smoking during pregnancy caused a decreased infant tidal volume at merely 6 weeks of age and dramatically increased the risk of a lower respiratory tract infection during the first year of the infant's life. Studies have shown that an increased risk of recurrent broncho-pulmonary infections in children correlate with prenatal fine PM levels in a dose-response manner[3].

Timing of the exposure also exerts a considerable effect on the neonatal outcome, although the current literature is varied on what type of exposure is the most detrimental at which timepoint. In a Singapore study, higher $PM_{2.5}$ and other pollutant levels in the first trimester were associated with wheezing, while exposure in the second trimester was more associated with bronchitis; this study also examined whether the body mass index of the mothers affected the neonatal outcome, but the evidence was only suggestive and not significant.[45] Lu et al. showed that exposure to SO_2 3 months to 1 year even before conception could significantly increase childhood pneumonia risk, let along prenatal exposure to the pollutant; this was yet another study showing that males were more susceptible to these risks.[46] Korten et al. demonstrated that prenatal exposure was more influential than postnatal exposure, finding that maternal exposure to NO_2 and benzene in the second trimester is associated with decreased lung function parameters when children were 4.5

years old.[42] However, this should not cast postnatal exposure into lesser prominence. MacIntyre et al. showed that PM_{10} and NO_2 were significantly associated with childhood pneumonia, most likely with stronger effect in the first year of life.[47] However, though gestational and neonatal effects are fairly well-characterized in $PM_{2.5}$ and PM_{10} exposures, less literature is available strictly on the effects of gestational UFPs.

Mechanisms for this increased susceptibility following prenatal exposure remain largely unknown. The prevailing theorized pathogenesis characterizes the immune status of the infant perinatally by examining the cord blood. Children have a slightly more Th2-biased immunophenotype than adults, males in particular, and it is believed that the PM exposure enhances this bias to render these children more susceptible to more severe infection or asthma. Baiz et al. found an associated 0.82% decrease in T regulatory cells for a 10 $\mu g/m^3$ increase in PM_{10}, along with decreased T regulatory cells in the second trimester particularly linked to exposure to benzene.[48] As a decrease in T regulatory cells has been associated with a more prominently skewed Th-2 immune response, often leading to allergies or asthma later on in life, this may prove to be a key mediator by prenatal PM exposure.[49]

1.5 Murine models of PM exposure

Models have been developed to look at various size and compositions of particulate matter generally found in air pollution. However, until recent history, it was uncommon that the prenatal murine models have actually aerosolized their compounds in a manner representative of realistic situations for human mothers. The majority of animal models rely on intranasal[50–52], intratracheal[53,54], or intraperitoneal[55,56] routes of exposure to the dams, a less physiologically relevant model for inhalation exposures, though they may ensure more accurate dosing. Hamada

et al. created a model where mice were exposed for 30 minutes a day for three days total[57], while Mauad et al. positioned mice in outdoor settings to inhale real-time aerosolized particulate matter[58], but neither of these offer a long term, high exposure, consistent dosage of uniquely tailored particles. Kulas et al and Cory-Slechta et al both utilized aerosolized UFPs, though the latter dosed neonatally, but both of these models were looking at neurologic and cognitive dysfunction resulting from such exposure.[59,60]

Rodent models employing prenatal fine and ultrafine PM exposure provide substantial evidence on offspring lung dysfunction and increased asthma susceptibility. Features of asthma, or allergic airway disease, can be characterized by measuring airway inflammation and hyperresponsiveness following an allergen exposure. Frequently, mouse models employ sensitization and challenge using the experimental allergen ovalbumin (OVA) or a human relevant allergen, house dust mite. Several models employing various exposure regimens and allergen challenges confirm prenatal $PM_{2.5}$ and $PM_{0.1}$ exposure leads to a characteristic asthma phenotype in offspring. Hamada et al. initially demonstrated pregnant BALB/c mice exposed to aerosolized residual oil fly ash, a surrogate for ambient $PM_{2.5}$, just prior to delivery significantly increased offspring OVA-induced airway hyperresponsiveness (AHR) and elevated levels of eosinophils in bronchoalveolar lavage fluid (BALF) driven by a skewed Th2 response.[57] A primary feature of asthma involves a heightened inflammatory cell influx, largely composed of eosinophils or neutrophils driven via increased Th2 CD4+ T-cell signaling through interleukins (IL) 4 and 5 and/or Th17 signaling via IL-17. IL-4 also drives allergen-specific immunoglobin (Ig) production. Additionally, IL-13 elicits effects related to airway hyperresponsiveness (i.e., bronchoconstriction). Hamada and colleagues further highlight histopathology showing marked pulmonary inflammation and increased allergen-specific IgE and IgG levels. Fedulov et al.

subsequently showed pregnant BALB/c mice exhibit an acute inflammatory response to both diesel exhaust $PM_{0.1}$ and more "inert" particles, titanium dioxide (TiO_2), in contrast to non-pregnant females.[50] Offspring born to mothers exposed to either type of particle went on to develop AHR and display airway inflammation following OVA challenge. These data underscore the state of pregnancy itself affects the host-response to particle exposure and confirm particles increase asthma susceptibly in offspring. In another model of prenatal exposure to diesel exhaust (DE), Corson et al. co-exposed pregnant BALB/c mice to *Aspergillus fumigatus* allergen and DE. Offspring were challenged with this allergen at 9-10 weeks of age.[61] Interestingly, offspring in the prenatal DE + allergen exposure group had decreased IgE production and dampened airway eosinophilia indicating potential protection against allergen-induced inflammation. These results emphasize the influence of co-exposures during gestation on asthma risk. Additionally, Sharkhuu et al. demonstrated prenatal DE exposure altered some baseline inflammatory indices in the lung, which varied based on sex, but changes in response to OVA-induced inflammation were not significant in exposed mice.[62] Manners et al. combined several of the dosing strategies from previously described models to investigate the mechanisms underlying prenatal $PM_{2.5}$ exposure and offspring asthma risk.[52] Researchers showed repeated exposure to DEPs during gestation led to significant OVA-enhanced inflammation and AHR in offspring. Moreover, asthma susceptibility was associated with expression of genes regulated through oxidative stress and aryl hydrocarbon receptor (AhR) pathways. Diesel exhaust PM contains a mixture of polycyclic aromatic hydrocarbons (PAHs), known to upregulate AhR-related genes. The role of AhR in the immune response, including the production of Th2 and Th17, continues to evolve.[63]

Asthma is a complex chronic disease with multiple elements involved in its etiology, including genetic predisposition and a variety of environmental factors. Maternal exposure to

microbial-rich environments is suggested to play a protective role against childhood asthma and allergy development.[64] Using an innovative approach, Reiprich et al. tested the ability of endotoxin (lipopolysaccharide, LPS), representative of microbial exposure, to protect against offspring asthma development.[51] LPS protected against OVA-induced pulmonary inflammation and AHR; however, in offspring prenatally exposed to DEPs, LPS failed to confer protection. Investigators showed the protection was dependent on the epigenetic regulation of IFN-γ expression. Maternal supplementation with the antioxidant N-acetylcysteine reversed these effects suggesting that maternal dietary supplementation may serve as a preventive intervention to combat DEP-induced oxidative stress and downstream consequences in offspring.

Structural alterations in lung development and related functional changes have also been intensely investigated in rodent models of prenatal fine and ultrafine PM exposure. Mauad et al. revealed offspring exposed pre- and postnatally to heavy traffic in São Paulo presented smaller surface to volume ratios and decreased inspiratory and expiratory volumes.[58] Subsequent research by this group substantiates these structural and functional defects.[65] While glandular and saccular structures of fetal lungs were not substantially altered following gestational exposure to concentrated urban $PM_{2.5}$ and $PM_{0.1}$ from São Paulo, offspring showed significantly lower alveolar number and higher lung elastance at postnatal day 40. Genes related to DNA damage, cell proliferation, and inflammation were differentially expressed in the fetal lung suggesting a complex interplay of pathways influencing long-term lung alterations. Research on prenatal $PM_{0.1}$ exposure mirrors work related to manufactured nanoparticles. Paul et al. showed gestational exposure to titanium dioxide (TiO_2), cerium oxide (CeO_2), and silver nanoparticles-induced stereotyped impairment of lung development (decreased radial alveolar count/alveolar surface)

with lasting effects in adult mice.[54] These effects were independent of the chemical nature of the nanoparticles indicating particle size played a primary role.

In a rat model, repeated gestational $PM_{2.5}$ exposure resulted in significant changes in offspring lung structure and function, including increased lung consolidation, airway inflammation, and decreased lung volume and compliance[55]. Additionally, in $PM_{2.5}$-exposed offspring, investigators observed interstitial proliferation, significant oxidative stress in lungs, and upregulation of epithelial-mesenchymal transition (EMT). EMT is a process where fully differentiated epithelial cells undergo transition to a mesenchymal phenotype, thus losing typical epithelial markers like E-cadherin. Transforming growth factor-beta (TGF-β), a key mediator of EMT, can be influenced by oxidative stress/reactive oxygen species (ROS), suggesting the link between $PM_{2.5}$ and aberrant ROS signaling underlying the process of EMT.[66] This phenotype was also characterized in a mouse model of neonatal exposure to radical-containing ultrafine particles.[66] Investigators proposed EMT in neonatal mouse lungs following acute exposure to ultrafine particles may underlie epidemiological evidence supporting PM exposure and increased risk of asthma. Successive research from this group supports the role of early life $PM_{0.1}$ exposure and increased risk of both asthma and respiratory infection risk. Saravia et al. demonstrated an early immunosuppressive phenotype in mice exposed to $PM_{0.1}$ and challenged with house dust mite (HDM).[67] Herein, the PM-HDM group failed to develop the typical asthma-like phenotype; however, offspring developed an allergic phenotype upon re-challenge later in life. The "switching" observed in this study indicates the crucial importance of the timing of exposure, as well as when pulmonary assessment is conducted. Moreover, the initial immune suppression is relevant to respiratory infection risk, which investigators went on to show neonates exposed to $PM_{0.1}$ early in life were more susceptible to severe influenza infection[68]. Likewise, in a mouse

model of prenatal exposure to $PM_{0.1}$, Rychlik et al. demonstrated a dampened response to HDM challenge in offspring from the exposed group.[14] The role of altered adaptive immune response appears to underlie the muted response. Circulating IL-10 was significantly upregulated in offspring exposed to $PM_{0.1}$, suggesting increased regulatory T cell (Tregs) expression and suppressed Th2/Th17 response. Jaligama et al. confirmed the role of IL-10 and Tregs in suppressing the adaptive response following early life $PM_{0.1}$ exposure.[15] Depletion of Tregs reduced morbidity and conferred enhanced protection against influenza virus.

El-Sayed et al. also demonstrated gestational exposure to carbon black nanoparticles induced dysregulation of lymphocyte populations in offspring, indicating neonatal peripheral tolerance. These effects could be predictive of allergic or inflammatory responses in childhood.[69] Importantly, the magnitude of alteration depended on the stage of gestation fetuses were exposed, highlighting the importance in the timing and duration of exposure. In support of the hypothesis that prenatal PM alters immune development and predisposes offspring toward asthma, Wang et al. showed gestational exposure to combustion-derived $PM_{0.1}$ inhibited offspring pulmonary T cell development, with suppression of Th1, Th2, Th17, and Tregs at 6 days of age.[70] Pulmonary Th1 cells remained suppressed up to 6 weeks, leading to enhancement of postnatal allergic responses to OVA evidenced by increased AHR, eosinophilia, and pulmonary Th2 responses. Overall, the bulk of the non-human evidence validates prenatal $PM_{2.5}$ and $PM_{0.1}$ exposure alter offspring lung and immune system development, signifying risk for acute (respiratory infection) and chronic (asthma) pulmonary health outcomes. Since variations in fetal development of lung and immune system vary between humans and rodents, it is sometimes difficult to interpret the translational relevance regarding trimester-specific effects. Nonetheless, combined evidence from human and

non-human studies support reducing exposure may prevent the tremendous burden of respiratory morbidity in infants and children.

1.6 Respiratory syncytial virus in pediatric medicine

RSV is a major pediatric disease in patients under 2 years of age, and is one of the leading causes of pediatric respiratory hospitalizations[71–73], accounting for approximately 1 of 13 visits to a primary care office in the US and approximately 1 of 334 hospitalizations every year in children under the age of five[71]. It has been estimated that 2.1 million children in the U.S. alone require medical attention for RSV infection every year[71]. Likely, this number is even underestimated, both from underreporting and because doctors frequently do not test for the presence of RSV in every case of respiratory disease, as a definitive diagnosis causes no change in clinical therapy. It is estimated that by the age of 1, 70% of all children have been infected with RSV, and by the age of 2, that percentage increases to almost 100%[74], with infection often predisposing children to respiratory issues later in childhood or adolescence. The global burden of disease is estimated at 64 million cases and 160,000 deaths each year[75].

RSV is an enveloped, single stranded, negative sense RNA in the genus Pneumovirus and most frequently manifests as a lower respiratory tract infection with bronchiolitis, rhinorrhea, a dry wheezy cough, fast and/or difficulty breathing, and occasionally a fever[73,74,76]. Children are more at risk for developing severe disease due to two factors. Firstly, their smaller bronchiolar diameter predisposes them to obstruction by mucus, sloughed epithelium, and other debris incited by RSV[73]. Secondly, children, particularly males, have an immunophenotype biased towards the Th2 response[77]. It is well documented that higher RSV disease severity and lung pathology is correlated with a Th2 immune response in humans. Eosinophils, the primary white

blood cell responsible for allergic and Th2 type immune responses, are the predominant cell type found in RSV induced lung pathology. RSV remains difficult to control as it spreads quickly via aerosol or direct contact, children generally do not develop a robust immune response against reinfection, and no efficacious preventive interventions of treatments currently are broadly employed, other than supportive care and preliminary trials with monoclonal antibodies[72,76,78]. Extensive research has associated severe RSV infection with enhanced inflammation with increased Th2 cytokine production and decreased Th1 response[73,74,76]. Additionally, children are often predisposed to more severe RSV infections if they previously had episodes of wheezing or were born premature[71], two risk factors likely to be induced by gestational PM exposure.

Current therapeutic treatment is only supportive, with no vaccine available[73,76]. Thus far, therapeutic options for the treatment of RSV have been limited, nonspecific, and insufficient. In the 1960s, a vaccine for RSV was developed; however, 80% of the recipients became hospitalized after the vaccine enhanced natural RSV infection, with two deaths[76]. Though the idea of a vaccine remains a clinical research priority, little success has been achieved to date. Palivizumab, a monoclonal antibody immunoprophylaxis, has been marketed for high-risk infants, but the efficacy and practicality of this preventative measure has precluded widespread use[78]. For highest efficacy, the antibody treatment needs to be administered before RSV challenge, an impractical approach, and since it is only a passive treatment, must be given repetitively, which remains cost prohibitive. Current treatment regimens consist of supportive therapy, such as oxygen, bronchodilators, and cough suppressants.

1.7 Nrf2 as a key transcription factor in PM-induced oxidative stress

Nrf2 (nuclear factor erythroid 2-related factor 2) is a well-studied transcription factor enmeshed in numerous pathways, the majority of which regulate oxidative stress responses and antioxidant production[79,80]. Though deficiencies of Nrf2 can contribute to many diseases, such as myocardial ischemia[81], Alzheimer's disease[82], and cancer[83], the disruption in Nrf2 production synergistically and detrimentally enhances the severity of many respiratory diseases, such as asthma[84], chronic obstructive pulmonary disease (COPD)[85], and acute respiratory disease syndrome (ARDS)[86]. Adult Nrf2-/- mice are significantly more susceptible to RSV infection than their wildtype counterparts[87]. Additionally, *in vitro* models have demonstrated that bronchial epithelial cells, both human and murine, have significantly increased levels of nuclear translocated Nrf2 induced by incubation with ultrafine diesel particles, as compared to the larger $PM_{2.5}$ or PM_{10} particles[88]. Therefore, our model will be critical in defining the role Nrf2 may play in combatting the combined assaults of *in utero* PM exposure and neonatal RSV infection.

Nrf2 is a powerful antioxidant-inducing transcription factor. Normally bound and led to proteasome degradation by Keap1, numerous stimuli such as reactive oxygen species alter the confirmation of the binding sites between the two molecules and lead to the release of Nrf2[80]. Nrf2 then proceeds to the nucleus to promote transcription of numerous genes that can regulate antioxidant production, apoptosis[83], inflammation[79], and even metabolism[89]. The aromatic and polar groups of UFPs specifically interfere with the proteasomal degradation of Nrf2, allowing for a greater oxidative stress response, compared to larger particulate matter, which generally has a lower organic carbon content[88].

The study of Nrf2 as a potential therapeutic target greatly appeals to many researchers and pediatricians. Nrf2 expression significantly increases in the lungs of wildtype mice with RSV infection[87]. If Nrf2 proves to be a vital anti-inflammatory component of the immune response to

RSV in neonates as well, then the logical conclusion would be to promote overexpression of Nrf2 before and during RSV infection. Nrf2 activators such as sulforaphane, curcurmin[90,91], and BHA (butylated hydroxyanisole) [87] have been used with variable efficacy in murine models and humans, but the usage in neonates of any species lacks empirical data.

PM exposures, both pre- and post-natal, are linked to a number of respiratory diseases in children and murine models, such as childhood asthma[50,52,57,92]. Risk factors for increasingly severe RSV disease in young children include low birth weight, preterm birth, and lung under development[73]; this is an almost complete overlap with the most common effects on fetuses with prenatal PM exposure, aside from stillbirth[35,36]. RSV infection has shown to induce significant decreases in Nrf2 in human infant nasopharyngeal secretions, as well as adult murine lungs, by promoting degradation of the transcription factor[91].

1.8 Significance

Gestational and neonatal clinical research and therapy is safeguarded to protect the vulnerability of the mother and child. Yet, pregnancy remains one of the most immunologically susceptible windows for both patients. Thus, murine models like ours provide one of the safest approaches for studying toxicologic exposures *in utero* and neonatal disease, providing critical knowledge for pediatricians. Our long-term goal is to develop a murine model to closely examine the interplay between aerosolized UFP exposure and the fetal immune system, and particularly, how this affects the neonatal response to respiratory infection.

Our central hypothesis is that *in utero* UFP exposure will enhance the severity of respiratory infection in the neonatal period, which will be further compounded when the host cannot mount a sufficient antioxidant response. Indeed, polymorphisms in maternal genes related

to oxidative stress response pathways, such as the nuclear factor erythroid 2-related transcription factor (Nrf2), have been shown to significantly increase lower respiratory tract infection risk in infants exposed to PM during the prenatal period.[86] The role of Nrf2 in host protection against respiratory infection has been demonstrated in adult mouse models of RSV infection, but information on unique maturation-related neonatal responses are lacking.

The objective of the proposed research is to define the mechanisms by which UFPs affect the neonatal immune system to enhance RSV severity, to elucidate how these exposures might be counteracted or combated. Furthermore, by establishing mechanisms by which UFPs alter the immune system, it may be possible to influence and expedite regulations regarding UFPs. Our rationale is based on preliminary data showing a dose response increase in RSV severity and viral load that correlates with increased levels of UFP exposure *in utero*. Research in this proposal will enhance understanding of the neonate's immune response following UFP exposure, and sequentially examine the effects of RSV within exposed neonates and the role of protective antioxidant genes.

While both placental UFP exposure and neonatal RSV have both been studied, our approach is highly innovative in combining both disease mechanisms to further highlight the toxic potential of UFPs and ultimately promote regulation of these particles. Additionally, our study of neonatal RSV disease severity with Nrf2 deficiencies may provide insight on future therapeutic options, such as supplements or antioxidants given pre- or postnatally to the mother or child.

CHAPTER II

BUILDING A MOUSE MODEL OF PRENATAL ULTRAFINE PARTICULATE MATTER EXPOSURE TO EVALUATE RESPIRATORY DISEASE RISK IN NEONATES

2.1 Introduction

Generally, early life exposure to particulate matter air pollution is associated with respiratory disease in children. Prenatal exposure has been linked with low birth weight and preterm birth[37,93], two factors that commonly lead to increased risk of comorbidities later in life. Moreover, early life exposure has also been associated with increased lower respiratory tract infections in children, and[3] childhood asthma. Numerous experimental models have evaluated offspring responses to different allergens following exposure to prenatal PM exposure.[50,52,57] Offspring response to viral infection following *in utero* PM is not as well characterized.

Respiratory syncytial virus, or RSV, is a major pediatric disease that causes bronchiolitis and wheezing in children, particularly under the age of 2. Though it most commonly manifests as a mild lower respiratory tract infection in young children, and rarely affects adults, its most severe characteristic is the blockage of small airways by mucus and sloughed cells, explaining its biased impact on smaller children. Children are also at a disadvantage due to their slightly Th2-biased immune system; this immune environment predisposes a more severe RSV infection and can be further skewed by PM exposure. No vaccine or efficacious therapy exists for RSV, only symptomatic treatment[73], making therapeutic advancements in this field an ongoing, urgent necessity.

Animal models of prenatal PM exposure and of RSV infection exist in current literature, however, they are infrequently combined. Lee et al made a robust model of neonatal exposure to

free radicals, showing an increased severity of influenza infection afterwards, but this lacks the prenatal component we wish to examine. Prenatal PM exposure in animals has predominantly focused on coarse or fine PM regarding neonatal health, although UFP exposure models are increasing. Wu et al showed UFP prenatal exposure altered metabolism and aortic function in neonates[94], Morales-Rubio et al demonstrated that exposure altered placental function and increased inflammation on both the maternal and fetal side[4], and Kulas et al exhibited neurological changes in offspring after prenatal exposure[59]. Our group looked at prenatal UFP exposure and its suppression of the allergic response due to an upregulation of T regulatory cells, which correlates with Jaligama et al.'s findings of immunosuppression in free radical-exposed neonates, causing an increased severity of influenza.[14,15] Yet the direct correlation of prenatal UFP exposure and neonatal respiratory disease requires more research, not to mention understanding the mechanics behind such susceptibility.

We hypothesized that increased exposure would correspond to increased severity of disease, and to test this hypothesis, we created a mouse model of gestational exposure and neonatal viral challenge. We conducted two different consecutive pilot studies that exposed pregnant mice to varying levels of PM, after which we challenged the neonates with RSV and examined them at various time points to ascertain degrees of viral load and pulmonary changes.

2.2 Methods

2.2.1 PM Generation and Mouse Exposure Model

PM generation followed methods developed by Rychlik et al. [14], with adaptations to accommodate individual housing within whole body exposure chambers and two doses detailed by Behlen et al[95]. Briefly, HEPA filtered air was continuously pumped into three separate

chambers (FA, LD, or HD) within which pregnant dams were group housed. For LD and HD chambers, UFPs were generated using two home-built constant output atomizers where the concentrations of atomizer solutions were adjusted for respective dose. Pilot study 1 exposed dams to FA and LD, while Pilot study 2 exposed dams to FA and HD. We employed a multicomponent aerosol mixture consisting of ammonium nitrate, ammonium sulfate, diesel exhaust PM (NIST, SRM 2975), and potassium chloride, with the mass fractions of 44, 39, 10, and 7%, respectively. Real-time particle size distribution was monitored using a differential mobility analyzer (DMA) in tandem with a condensation particle counter (CPC) where the particle mass concentration was calculated using an average particle density of 1.63 g cm^{-3}. The flowrate of HEPA was adjusted to ensure consistent particle concentrations within chambers throughout the exposure duration. Particle size ranged from 0.02 to 0.5 μm for both LD and HD chambers. The peak particle diameter was 0.049 and 0.066 μm (or 49 and 66 nm) for LD and HD, respectively, over the entire exposure period within the UFP range.

Mice were housed in a climate-controlled room with 12/12h light/dark cycle at an AAALAC approved facility at Texas A&M University. Mice had access to standard chow, 19% protein extruded rodent diet (Teklad Global Diets), and water *ad libitum* except during exposure periods. Male and female BALB/c 8- to 10-week-old mice (Jackson Laboratory, Bar Harbor, ME) were time-mated. The presence of a vaginal plug defined gestational day (GD) 0.5. A schematic of our exposure timeline is shown in Figure 1. Beginning on GD0.5, dams were randomized and placed into exposure chambers where they were exposed to either FA (n=14), LD (n=12), or HD (n=13) from 0800 to 1400 hours (6 hours) daily through GD17.5. Following exposure on GD17.5, mice were removed to individual housing and allowed to deliver spontaneously.

2.2.2 Offspring RSV Challenge

Litters from all three prenatal exposure groups (FA, LD, or HD) were randomly allocated to postnatal groups, including experimental (RSV-exposed) or control (sham-exposed). A chimeric strain of RSV, rA2-19F, previously shown to elicit an aberrant immune response in neonatal mice mimicking human infant infection[96], was provided by Dr. Martin Moore (University of Emory, Atlanta, GA). This strain was passaged in our laboratory in HEp-2 cells (ATCC, Manassas, VA) in serum-free-media (SFM4MegaVir, Hyclone, Logan, UT)[96]. The day of birth was defined as postnatal day (PND) 1. On PND5, offspring were briefly anesthetized with 4.5% isofluorane in oxygen and infected intranasally with either 10 µL RSV (10^6 virus particles/mL) in culture media or 10 µL culture media alone, 5 µL in each nostril for both dosing groups. Body weights were recorded daily. Male and female offspring within each litter were randomly assigned to evaluate viral load 3 days post-infection (dpi) (n=61) and pulmonary immune responses 9 dpi. Immune responses included collection of bronchoalveolar lavage fluid (BALF) (n=71), lung inflation for fixation and subsequent histological analysis (n=65), and T cell profiling via flow cytometry (n=21). Additional collection details provided in supplemental methods.

2.2.3 Pulmonary Viral Load

To determine the number of infectious virus particles in RSV-challenged offspring, 3 dpi pup lungs were quickly excised, frozen in liquid nitrogen, and stored at -80°C until median tissue culture infectious dose ($TCID_{50}$) analysis. The $TCID_{50}$ assay[96] was performed by growing Vero cells (ATCC, Manassas, VA) to confluency in 96 well plates. Media was removed, and 90 µL infection media was added to the wells. Offspring lung tissue was homogenized in 1 mL cold

cell culture media, filtered with a 40 µm cell filter, and the homogenate was added to the wells in duplicate. Samples were serially diluted, and plates were incubated at 37°C with 5% CO_2 for 7 days. Wells were checked at days 4 and 7 for cytopathic effect (CPE), and $TCID_{50}$/mL was calculated as previously described[96].

2.2.4 Pulmonary Immune Responses

BALF cellularity was assessed 9 dpi. Briefly, BALF was collected by tracheal cannulation and washing the lungs with 0.25 mL sterile PBS. Total leukocyte counts and differentials were determined by a board certified veterinary clinical pathologist blinded to treatment group. Additionally, 9 dpi in a separate subset of offspring, lungs were excised, inflated at a constant pressure of 25 cm, and fixed with zinc formalin for histological assessment. Nasal tissues were collected and decalcified in Davidson's solution for 3 days. After fixing, lung and nasal tissue were placed in 70% EtOH and processed and stained with hematoxylin and eosin (H&E) to identify cellular infiltrates and periodic acid-Schiff (PAS) for goblet cell analysis.

All histological assessments were carried out by a board-certified anatomic pathologist blinded to treatment groups. A scoring system, designed by our pathologists, was used as follows to rate inflammation severity: 0 (none to minimal), 1 (mild), 2 (moderate), and 3 (marked). A different scoring system was used to assess the number of goblet cells in 20 different 10x fields corresponding to the percentage of goblet cells in the bronchiolar epithelial cells, as previously described[97].

2.2.5 Statistical Analysis

Statistical analysis was performed using Prism (v8, GraphPad Software, San Diego, CA) to determine differences in offspring outcomes based on exposure group. One-way analysis of variance (ANOVA) with Tukey's multiple comparisons tests were conducted. An adjusted p value of <0.05 was considered statistically significant.

2.3 Results

2.3.1 Pilot Study 1 – BALB/c Dams were Exposed to FA and PM (now designated LD) and Neonates Examined on 6 dpi after RSV Challenge

Our initial pilot study was designed to mimic the World Health Organization standard for PM2.5, which is 25 m^3/day; we initially referred to it as PM, but with our second pilot study including a higher dose, all graphs and tables have been relabeled as LD for clarity in the context of Aim 1.

Maternal metrics were not significantly altered during their gestational exposure to LD (Fig. 1A-B), in either weight gain or final gestational weight. Initial pup metrics also did not differ significantly between dams in different exposure groups, in initial dosing weight (PND5), number of pups per litter, or average weight of pups per litter (data not shown).

At 6 dpi, weights of the neonates were taken again before pups were collected either for BALF or histology, with the lungs of the BAL used for the $TCID_{50}$ assay afterwards. The weights of the neonates did not differ significantly between the prenatal exposure groups or the RSV versus sham infected groups (Fig. 1C), not in the combined data nor in sex separated groups. BAL fluid collected from the pups was analyzed for both total number of leukocytes and a leukocyte differential count. The total leukocyte count did not differ by exposure group or viral

group (Fig. 1D); the differentials showed a predominant mononuclear population with small numbers of the remaining types of leukocytes, but again, no significance was noted (data not shown). The $TCID_{50}$ assay was unsuccessful, as the LD RSV neonatal lungs showed no cytopathic effect (CPE), while some of the sham-infected samples had CPE, likely a result of contamination either from RSV or some other pathogen (data not shown). Selected representations of the histology examined (Fig. 1E-G) showed what we hoped to be the trend in the data, but unfortunately, overall levels of inflammation were minimal even in the PM-exposed, RSV-challenged groups.

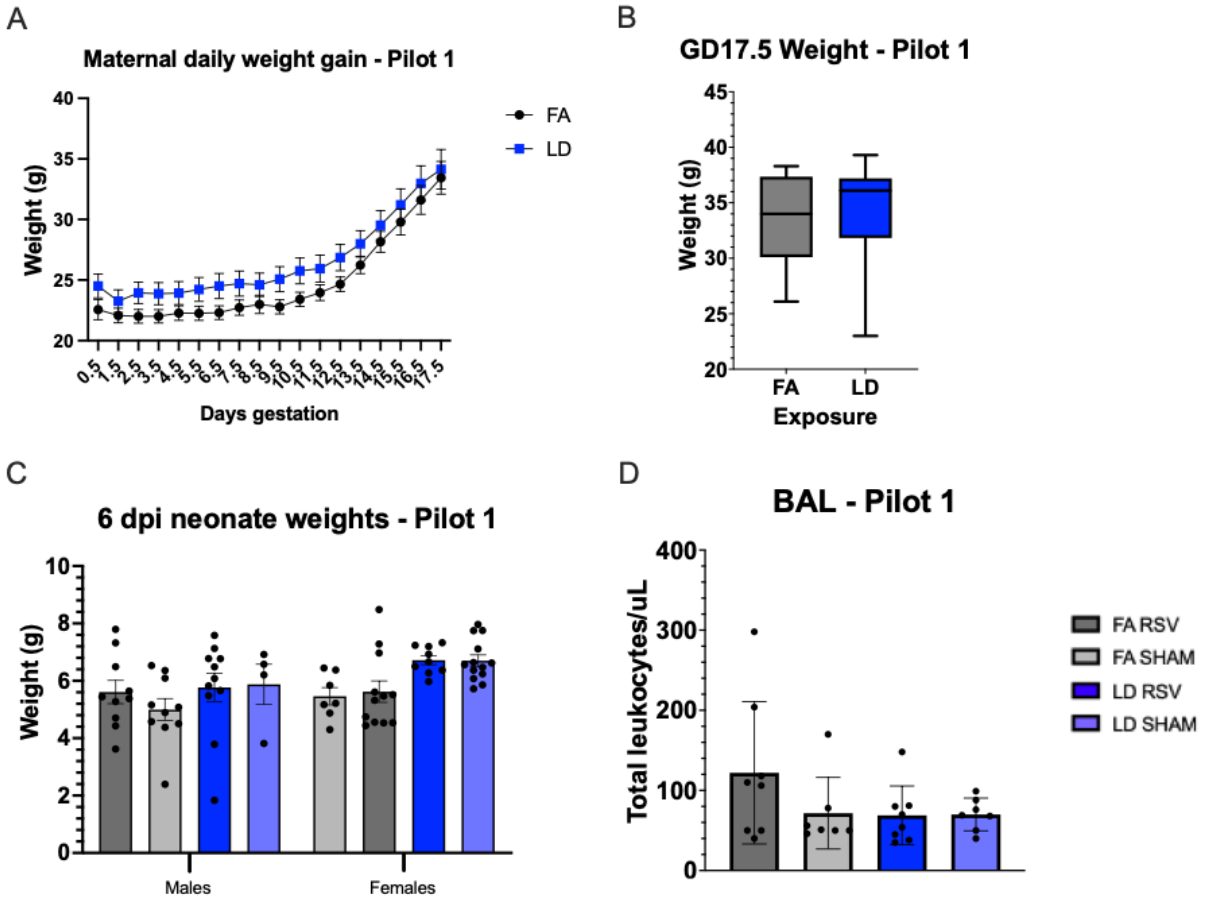

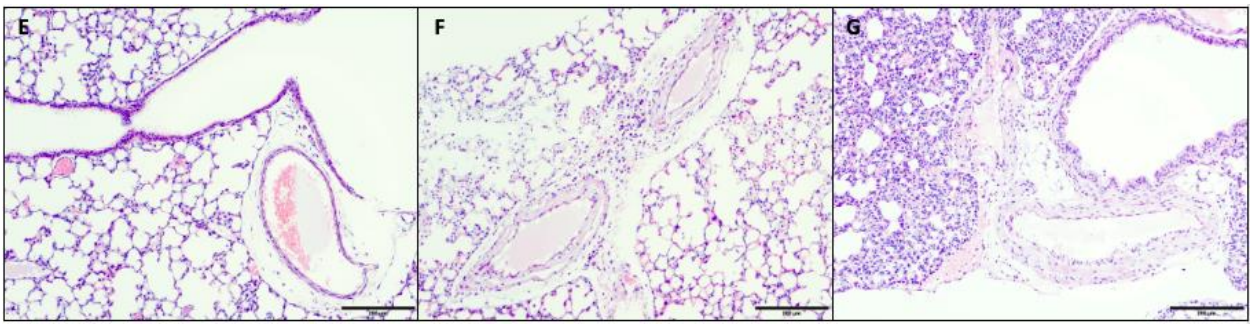

Figure 1. Pilot 1 study wherein BALB/c dams were exposed to either FA (filtered air) or LD (low dose particulate matter) during gestation, pups were challenged with RSV at PND5 (postnatal day), and tissues were collected at 6 dpi (days past infection). Maternal weight gain over gestation (A) and final gestational weight on GD17.5 (gestation day) (B) were not significantly different between the two exposed groups. Neonatal weights taken at collection (C) were not significantly different between any groups. Bronchoalveolar lavage (BAL) fluid showed no significant trends in total numbers of leukocyte per mL (D). Selected histologic sections from the FA-sham (E), FA-RSV (F), and LD-RSV (G) groups were not representative of histologic trends in each group, but rather represent the ideal inflammatory response hypothesized in each group.

2.3.2 Discussion of Pilot 1 Study

As in many pilot studies, our first foray into modeling prenatal exposure and neonatal disease did not yield the results we had hoped. While not entirely surprising that the maternal data showed no differences, it was surprising that the neonatal weights after exposure did not show any differences, as low birth weight is a common consequence of human prenatal air pollution exposure. To not see differences in the weights after infection with RSV signaled a problem in our model, particularly when the lack of trends in the BALF and histology data also confirmed this lack of significance.

Due to the complexity of the model, several factors had to be altered and/or analyzed to determine the true cause of insignificant data. The first parameter to be altered in the second pilot was the PM dosage; we increased the amount of PM exposure by five-fold (thus creating the high dose, HD, group) to simulate a densely polluted environment and hopefully stimulate a more robust response from the neonates. Secondly, we learned that though viral titer of RSV often peaks in neonatal mice at 2-3 dpi, 6 dpi may not be an adequate amount of time in which to see changes in the BALF or histology samples. In our pilot 2 study, we analyzed the mouse samples at 3, 6, and 9 dpi for peak viral load and peak inflammatory presence. We reproduced another FA group in Pilot 2 study, knowing that seasonality can affect the breeding and weights of pregnant mice. With the increased dosage and larger array of endpoints, we hoped to determine the optimal endpoints at which to examine the neonates that represent the most severe peaks of viral load and inflammation.

2.3.3 Pilot Study 2 – BALB/c Dams were Exposed to FA and HD and Neonates Examined on 3, 6, and 9 dpi after RSV Challenge

Our second pilot study mirrored the first study but increased the dose received from 100 ug/m^3/6 hours to 500 ug/m^3/6 hours, five-fold higher than the WHO recommendation for daily exposure to $PM_{2.5}$. To find the best timepoints at which to analyze the neonatal samples for our Aim 2 study, we looked at BALF, histology of lung and nasal tissue, and viral load across 3, 6, and 9 dpi after RSV challenge to the neonates on PND5.

Again, maternal metrics were not significantly altered during their gestational exposure to HD (Fig. 2A-B), in either weight gain or final gestational weight. Initial pup metrics also did not

differ significantly between dams in different exposure groups, in initial dosing weight (PND5), number of pups per litter, or average weight of pups per litter (data not shown).

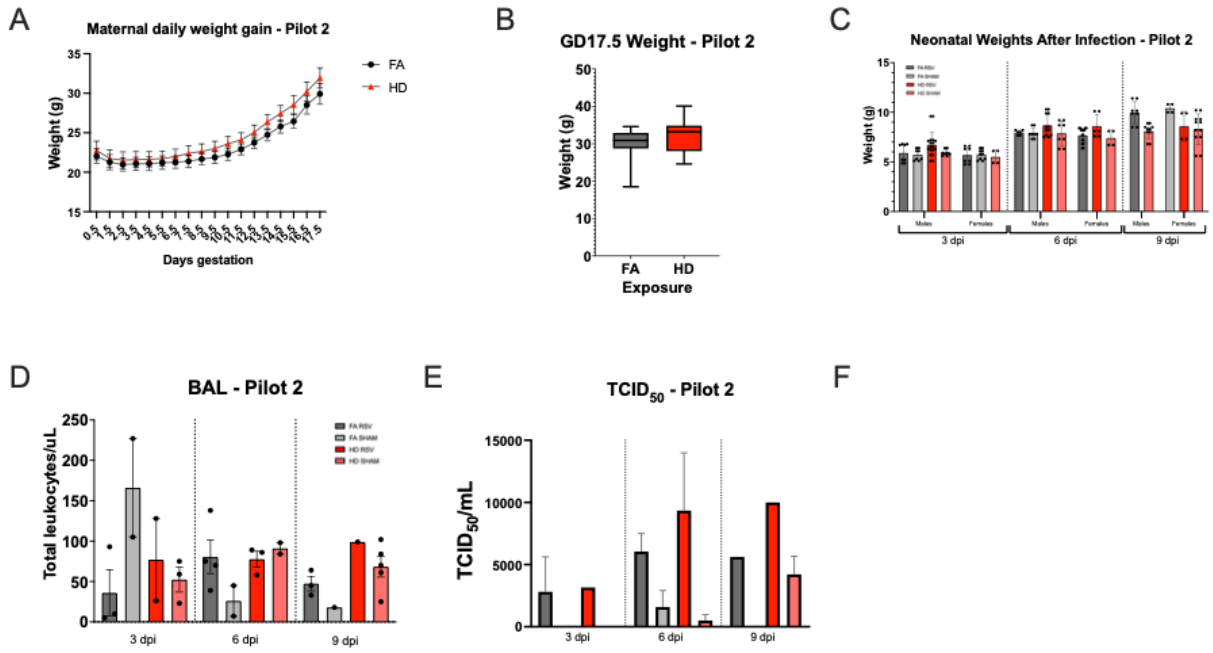

Figure 2. Pilot 2 study wherein BALB/c dams were exposed to either FA (filtered air) or HD (high dose particulate matter) during gestation, pups were challenged with RSV at PND5 (postnatal day), and tissues were collected at 3, 6, and 9 dpi (days past infection). Maternal weight gain over gestation (A) and final gestational weight on GD17.5 (gestation day) (B) were not significantly different between the two exposed groups. Neonatal weight taken at collection (C) did not significantly differ between any groups at any timepoint, although at 9 dpi the HD-exposed groups appear to have slightly reduced weight gain. Bronchoalveolar lavage (BAL) fluid (D) showed no significant differences between groups between days. $TCID_{50}$ assay (E) showed cytopathic effect (CPE) in RSV and some sham infected groups; the viral titer appears to peak somewhere around 6 days. A representative section of nasal histology (F) shows mild neutrophilic inflammation, but this was a non-specific reaction seen in multiple groups.

In the weights taken after infection, though no significance is seen, trends can start to be seen by 9 dpi, where both HD RSV and HD Sham groups seem to have reduced weight gain as compared to the FA groups (Fig. 2C). However, those trends are not seen in the BAL fluid (Fig. 2D), which has no discernible patterns within or between dpi endpoints for total numbers of leukocytes. As in Pilot 1, the differential counts of the leukocytes were predominantly mononuclear cells, and there was no significant difference in differential distribution between any of the groups (data not shown). The $TCID_{50}$ assay showed a trend of increasing titers in the RSV mice that were HD-exposed, and the titers seemed to possibly increase from 3 to 6 dpi but did not appear to change at 9 dpi (Fig. 2E). However, these trends are not significant. RSV-infected mice occasionally showing no titers and sham-infected mice having occasional CPE; again, this could demonstrate either cross-contamination, contamination by another pathogen, or simply user error. The nasal and lung histology were even less rewarding than the Pilot 1 samples, showing very mild histiocytic and eosinophilic inflammation in 5 of 32 mice, not correlated to exposure or viral group. The nasal histology occasionally showed neutrophilic infiltrates (Fig. 2F), but again, these findings were not specifically associated with either exposure or viral group.

2.3.4 Discussion of Pilot Study 2

Similar to the first pilot study, we did not observe any significant changes in the maternal data between groups exposed to PM and HD. However, in this pilot study, we started to note a slight decrease in the weight gain in the 9 dpi HD-exposed neonates as compared to the FA-exposed neonates, regardless of viral status. While the lack of weight reduction in the viral

groups is surprising, the reduction caused by exposure, even though not significant, mirrors those trends in human infants where prenatal exposure can frequently cause low birth weight, which can predispose to many other morbidities later in life, not necessarily respiratory-related.

The BALF and histology results remained frustratingly mild and non-significant even at the high dose and varying time points. The viral load assay did successfully show CPE in both FA- and HD-exposed groups at all three time points for RSV challenged neonates. Cormier et al. found that neonates tended to have a peak viral load in the first 2 days after infection, which our results are not consistent with, showing a peak and possibly a plateau around 6 dpi. This could have been due to sampling technique, as lungs washed for BAL were also used for viral load to maximize tissue use; our next studies separated the two end points to ensure no skewing of data.

2.4 Conclusions

We learned several valuable lessons from both pilot studies that we applied in aims 2 and 3. First, though the low dose may stimulate a small response, a higher concentrated dose of the ultrafine particles is necessary to see more overt changes in the neonatal lungs. We learned that it would be possible to expose the dams to GD18.5, instead of GD17.5 as previously thought, as our mice rarely gave birth until GD19.5. We learned that timing of the various endpoints is critical, such that viral load should be taken earlier and BALs and histology should be measured later, when inflammation has had time to set in. Though our data would suggest that 6 dpi is the optimum time to measure viral load, according to Cormier's group and by understanding the pathophysiology of most viral diseases, it is likely that 3 dpi would be a more appropriate time point for us to evaluate.

During critical evaluations of our pilot studies, we noticed that the dams in the exposure chambers tended to cluster in one or more corners together, particularly in the HD exposure chambers. This caused major concerns as to whether the dams were getting equally exposed to the aerosol, and whether communal grooming and oral ingestion of the ultrafine particulate matter might be increasing exposure in an unquantifiable manner. The corners where the dams congregated also naturally accumulated solid and fluid waste material, of which the volatile gases may have also contributed to exposure. Our solution was new, individual mesh housing units into which mice were placed for the duration of exposure, with units being elevated on racks so that no dam was resting in her own waste. Though these do not remove the confounding factor of the mouse being able to groom herself and have oral exposure to the particulate matter, it does allow for a more consistent exposure and is less stressful than a head or nose-cone type apparatus.

Our last, and most pressing, concern is that of strain. We had chosen the BALB/c mouse because it is a moderate to strong responder to RSV and should be naturally predisposed to more severe pulmonary damage due to the Th2-biased immune system. However, our group previously found that the C57BL/6 strain had a stronger immune response to prenatal exposure than the BALB/c. This is likely due to the fact that C57BL/6 mice have a more profound response to oxidative stress. Therefore, in aim 2, we use only C57BL/6 mice, and in aim 3, we will work with a knockout mouse on this background as well to keep the maximum sensitivity to the PM exposure.

Overall, our pilot studies were beneficial in defining and reshaping our murine model of gestational air pollution exposure. These studies were necessary in determining changes to the mouse strain, pollution levels, and endpoints for maximizing exposure and capturing the highest

severity of changes. Aims 2 and 3 take a definitive look at the effects of combining PM exposure and RSV challenge, as well as beginning to look at the mechanisms behind the prenatal exposure to ultrafine particulate matter.

CHAPTER III

IN UTERO EXPOSURE TO ULTRAFINE PARTICLES EXACERBATES SEVERITY OF NEONATAL RESPIRATORY SYNCYTIAL VIRUS INFECTION

3.1 Introduction

Maternal exposure to air pollution (such as particulate matter or PM) represents a major cause of global infant morbidity and mortality, which are driven by preterm birth, infant low birth weight, and lower respiratory tract infections (LTRIs)[35–37,98,99]. For example, early life exposure to fine PM (diameter smaller than 2.5 μm or $PM_{2.5}$) impacts fetal lung development and pulmonary health in a variety of ways that may persist throughout childhood[42]. Epidemiological studies have demonstrated that children are subjected to high susceptibility for severe respiratory infections following early childhood and prenatal $PM_{2.5}$ exposure[3,100]. Darrow et al. observed significant associations between the organic carbon fraction of $PM_{2.5}$ and hospitalizations for pneumonia and upper respiratory infections (URIs), suggesting associations with bronchiolitis/bronchitis among children aged 1-4 years[100]. Correlations were also observed between the sulfate fraction and URIs, also in association with bronchiolitis/bronchitis, which had notably lower cases of hospitalization. Jedrychowski et al. observed an increased risk of recurrent broncho-pulmonary infections in children correlated with prenatal $PM_{2.5}$ exposure in a dose-response manner, highlighting the 24-h mean level 20 $\mu g/m^3$ could better protect infants in comparison to the U.S. EPA standard (35 $\mu g/m^3$)[3].

Fine PM is either directly emitted (primary) into or formed via gas-to-particle conversion (secondary) in the atmosphere[101]. For example, sulfate represents a key ingredient for secondary PM primarily from coal-fired power plant emissions. Also, while contributing negligibly to the

total PM mass concentration, ultrafine particles (diameter less than 100 nm or UFPs) typically exist in high concentrations from direct emissions and new particle formation[102,103]. In particular, traffic emissions represent a major source for UFPs under urban environments[104]. Currently, there are no regulatory standards for the UFP fraction, despite evidence that UFPs can penetrate through the placental barrier and directly reach fetal circulation in humans and animal models[5,94,105,106]. The underlying mechanisms on how *in utero* exposure enhances infant respiratory morbidity risk remain uncharacterized in response to viral infections.

Previous *in vivo* models probing mechanisms of skewed immune responses have combined neonatal PM (mean diameter 0.2 μm, with or without an environmentally persistent free radical component) with influenza infection. Lee et al. showed neonatal exposure to radical containing-PM significantly enhanced pulmonary oxidative stress and influenza infection severity via increased presence of regulatory T cells (Tregs)[68]. In follow up work, increases in the immunosuppressive cytokine IL-10 and pulmonary Tregs were confirmed to suppress adaptive T cell responses, this suppression likely underlying enhanced infection severity[15]. Analogous to these findings, our laboratory developed an *in utero* exposure model, wherein pregnant mice were exposed to 100 $\mu g/m^3$ UFPs (ranging in size from 20-200 nm, with a peak diameter ~50 nm) generated from diesel exhaust PM, ammonium nitrate, ammonium sulfate, and potassium chloride[14]. In this model, offspring prenatally exposed to UFPs and challenged with an allergen demonstrated an immunosuppressive phenotype, evidenced by histopathology and loss of IL-13 and IL-17 pulmonary cytokine expression and increased IL-10 levels in serum. Building off our model, the objective of this study was to evaluate the impact of *in utero* UFP exposure on disease severity in response to respiratory syncytial virus (RSV) infection, an important cause of infant bronchiolitis/bronchitis.

RSV is an enveloped, single stranded, negative sense RNA virus that has a high morbidity and significant mortality among pediatric patients characterized by bronchiolitis and respiratory failure[73,74,76]. RSV infection is the leading cause of infant hospitalization, and it has been estimated that 2.1 million children in the U.S. alone require medical attention for RSV infection every year[71]. The global burden of disease is estimated at 64 million cases and 160,000 deaths each year[75]. Children are much more susceptible due to their diminutive bronchi and bronchiolar diameter that easily become obstructed with mucus, inflammatory cells, and sloughed epithelium[73]. Moreover, infant RSV infection presents with increased Th2 cytokine production and decreased Th1 response[73,74,76], which has been modeled in neonatal mice to replicate key features of infant viral infection[96]. We hypothesized *in utero* UFP exposure may alter offspring pulmonary immune responses, and possibly enhance RSV disease severity. To assess this hypothesis, we exposed time-mated C57BL/6N mice to filtered air (FA) or UFPs at a low dose (LD, 100 μg/m^3) and high dose (HD, ~500 μg/m^3) and challenged their offspring with RSV or sham (control) shortly after birth. Exposure levels for LD and HD equate to 24-hour average values of 25 μg/m^3 and 125 μg/m^3, respectively. The low dose, previously employed by Rychlik et al., is at the acceptable level set by the World Health Organization guidelines for $PM_{2.5}$ and under the 35 μg/m^3 limit for $PM_{2.5}$ set by the U.S. EPA[14]. In addition, our study included 500 μg/m^3 (HD) to evaluate dose responses.

3.2 Methods

3.2.1 PM Generation and Mouse Exposure Model

PM generation followed methods developed by Rychlik et al. [14], with adaptations to accommodate individual housing within whole body exposure chambers and two doses detailed

by Behlen et al[95]. Briefly, HEPA filtered air was continuously pumped into three separate chambers (FA, LD, or HD) within which pregnant dams were individually housed. For LD and HD chambers, UFPs were generated using two home-built constant output atomizers where the concentrations of atomizer solutions were adjusted for respective dose. We employed a multicomponent aerosol mixture consisting of ammonium nitrate, ammonium sulfate, diesel exhaust PM (NIST, SRM 2975), and potassium chloride, with the mass fractions of 44, 39, 10, and 7%, respectively (Fig. 3). Real-time particle size distribution was monitored using a differential mobility analyzer (DMA) in tandem with a condensation particle counter (CPC) where the particle mass concentration was calculated using an average particle density of 1.63 g cm^{-3}. The flowrate of HEPA was adjusted to ensure consistent particle concentrations within chambers throughout the exposure duration. Particle size ranged from 0.02 to 0.5 μm for both LD and HD chambers. The peak particle diameter was 0.049 and 0.066 μm (or 49 and 66 nm) for LD and HD, respectively, over the entire exposure period within the UFP range.

Mice were housed in a climate-controlled room with 12/12h light/dark cycle at an AAALAC approved facility at Texas A&M University. Mice had access to standard chow, 19% protein extruded rodent diet (Teklad Global Diets), and water *ad libitum* except during exposure periods. Male and female C57BL/6N 8- to 10-week-old mice (Jackson Laboratory, Bar Harbor, ME) were time-mated. The presence of a vaginal plug defined gestational day (GD) 0.5. A schematic of our exposure timeline is shown in Figure 1. Beginning on GD0.5, dams were randomized and placed into exposure chambers where they were exposed to either FA (n=14), LD (n=12), or HD (n=13) from 0800 to 1400 hours (6 hours) daily through GD18.5. Following exposure on GD17.5, mice were removed to individual housing and allowed to deliver spontaneously.

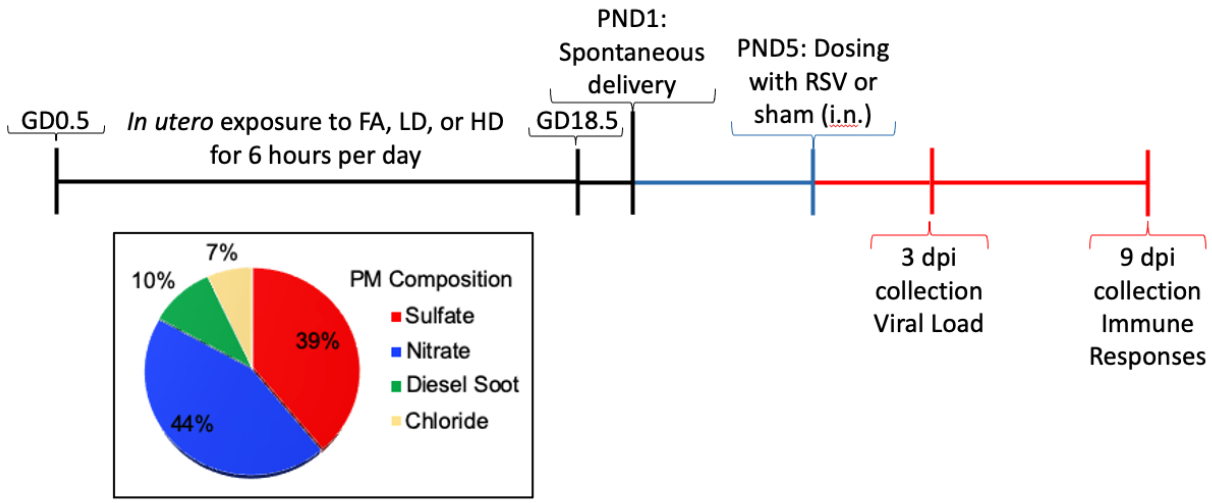

Figure 3. Experimental timeline for mouse exposure model. Each dam had a one-week acclimation period to exposure system (with filtered air) before time-mating. Upon the presence of plug (termed GD 0.5), dams were randomized into an exposure group, filtered air (FA) or UFPs at a low dose (LD, 100 μg/m^3) or high dose (HD, 500 μg/m^3), and exposed throughout gestation until GD 18.5. After delivery, offspring were infected with culture media (sham) or a chimeric RSV strain, rA2-19F via intranasal (i.n.) instillation. Endpoints, including pulmonary viral load and pulmonary inflammation/flow cytometry were determined at 3- and 9-days post infection (dpi), respectively. GD: gestation day; PND: postnatal day; RSV: respiratory syncytial virus.

3.2.2 Offspring RSV Challenge

Litters from all three prenatal exposure groups (FA, LD, or HD) were randomly allocated to postnatal groups, including experimental (RSV-exposed) or control (sham-exposed). A chimeric strain of RSV, rA2-19F, previously shown to elicit an aberrant immune response in neonatal mice mimicking human infant infection[96], was provided by Dr. Martin Moore (University of Emory,

Atlanta, GA). This strain was passaged in our laboratory in HEp-2 cells (ATCC, Manassas, VA) in serum-free-media (SFM4MegaVir, Hyclone, Logan, UT)[96]. The day of birth was defined as postnatal day (PND) 1. On PND5, offspring were briefly anesthetized with 4.5% isofluorane in oxygen and infected intranasally with either 10 μL RSV (10^6 virus particles/mL) in culture media or 10 μL culture media alone, 5 μL in each nostril for both dosing groups. Body weights were recorded daily. Male and female offspring within each litter were randomly assigned to evaluate viral load 3 days post-infection (dpi) (n=61) and pulmonary immune responses 9 dpi. Immune responses included collection of bronchoalveolar lavage fluid (BALF) (n=71), lung inflation for fixation and subsequent histological analysis (n=65), and T cell profiling via flow cytometry (n=21). Additional collection details provided in supplemental methods.

3.2.3 Pulmonary Viral Load

To determine the number of infectious virus particles in RSV-challenged offspring, 3 dpi pup lungs were quickly excised, frozen in liquid nitrogen, and stored at -80°C until median tissue culture infectious dose ($TCID_{50}$) analysis. The $TCID_{50}$ assay[96] was performed by growing Vero cells (ATCC, Manassas, VA) to confluency in 96 well plates. Media was removed, and 90 μL infection media was added to the wells. Offspring lung tissue was homogenized in 1 mL cold cell culture media, filtered with a 40 μm cell filter, and the homogenate was added to the wells in duplicate. Samples were serially diluted, and plates were incubated at 37°C with 5% CO_2 for 7 days. Wells were checked at days 4 and 7 for cytopathic effect (CPE), and $TCID_{50}$/mL was calculated as previously described[96].

3.2.4 Pulmonary Immune Responses

BALF cellularity was assessed 9 dpi. Briefly, BALF was collected by tracheal cannulation and washing the lungs with 0.25 mL sterile PBS. Total leukocyte counts and differentials were determined by a board certified veterinary clinical pathologist blinded to treatment group. Additionally, 9 dpi in a separate subset of offspring, lungs were excised, inflated at a constant pressure of 25 cm, and fixed with zinc formalin for histological assessment. Nasal tissues were collected and decalcified in Davidson's solution for 3 days. After fixing, lung and nasal tissue were placed in 70% EtOH and processed and stained with hematoxylin and eosin (H&E) to identify cellular infiltrates and periodic acid-Schiff (PAS) for goblet cell analysis.

All histological assessments were carried out by a board-certified anatomic pathologist blinded to treatment groups. A scoring system, designed by our pathologists, was used as follows to rate inflammation severity: 0 (none to minimal), 1 (mild), 2 (moderate), and 3 (marked). A different scoring system was used to assess the number of goblet cells in 20 different 10x fields corresponding to the percentage of goblet cells in the bronchiolar epithelial cells, as previously described[97]. Lastly, lungs from a separate subset of offspring sacrificed 9 dpi were perfused with sterile PBS for single cell suspension processing for flow cytometry analysis (details in Supplemental Methods). Cells were stained with antibodies for CD3, CD4, CD8, IFNγ and IL-4 to determine CD8+ and CD4+ Th1/Th2 responses, respectively. Additionally, to evaluate Tregs, cells were stained with antibodies for CD25 and FOXP3. Stained samples were analyzed using a Beckman Coulter Moflo Astrios high speed cell sorter. Data was analyzed using FlowJo Software. Gating strategies are depicted in Supplemental Figures 5-8.

3.2.5 Gene Expression

Total RNA was extracted from 9 dpi lungs using TRIzol reagent according to manufacturer's protocol (ThermoFisher Scientific). RNA was quantified with a DeNovix DS-11 FX+ Spectrophotometer/Fluorometer with ≥1.8 260/280 nm absorbance values. Following purification, cDNA was reverse transcribed (Qiagen QuantiTect® Reverse Transcription), and transcription levels of key genes related to oxidative stress (*Nrf2, Nqo1)* and inflammatory responses (NF-κB) were analyzed using SYBR Green qRT-PCR (Applied Biosystems™ *Power* SYBR™ Green PCR Master Mix) on a Roche LightCycler® 96 System. Relative expression was calculated using $2^{-\Delta\Delta CT}$ with *Gapdh* as the reference gene.

3.2.6 Statistical Analysis

Statistical analysis was performed using Prism (v8, GraphPad Software, San Diego, CA) to determine differences in offspring outcomes based on exposure group. One-way analysis of variance (ANOVA) with Tukey's multiple comparisons tests were conducted. An adjusted p value of <0.05 was considered statistically significant.

3.3 Results and discussion

3.3.1 In utero UFP exposure and RSV infection suppresses weight gain in female offspring

Dams were exposed to one of three exposures throughout gestation (Fig. 3), including FA, LD, or HD. The mean PM mass concentration for the LD and HD exposures over the time course of each exposed pregnant dam averaged 101.40 ± 2.76 (mean ± SEM) and 492.47 ± 10.53 $\mu g/m^3$ as determined by our real-time mass concentration system (Appendix 1, Sup. Fig. 1). Our initial murine

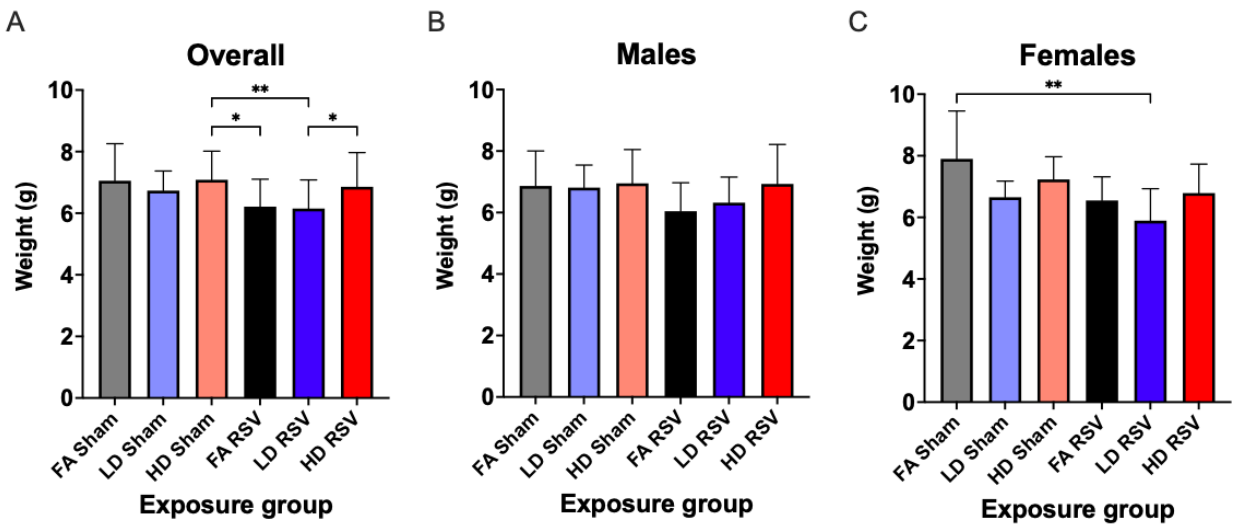

Figure 4. Offspring weights measured 9 days post-infection expressed as mean ± SEM. (A) Overall, offspring body weights were significantly lower in the LD RSV group, as compared with the HD RSV group (p=0.0324). (B) Differences between body weights post-infection were not significantly different in male offspring. (C) In females, offspring from the LD RSV group weighed significantly less than the FA Sham group (p= 0.0132) highlighting RSV morbidity after UFP exposure sex-specific differences. Offspring sample sizes from 3-6 litters, listed (n=Male, Female), include FA Sham (9, 2), LD Sham (16, 15), HD Sham (10, 9), FA RSV (16, 8), LD RSV (20, 13), and HD RSV (16, 16). Data analyzed using one-way ANOVA with Tukey's multiple comparison test (*P<0.05; **P<0.01).

---

model created by Rychlik et al. established a daily UFP exposure (low dose, LD, 100 $\mu g/m^3$) throughout gestation, which is an equivalent dose of 25 $\mu g/m^3$/24 hours[14]. In that model, offspring challenged with house dust mite allergen demonstrated an immunosuppressive phenotype, more pronounced in the C57BL/6 strain than the BALB/c strain. We adapted this model to our current study utilizing C57BL/6 mice by adding in a five-fold increase in exposure (HD), exposed to an

equivalent of 125 $\mu g/m^3$/24 hours. Maternal exposure in the LD and HD groups were maintained close to their target levels of ~100 $\mu g/m^3$ and ~500 $\mu g/m^3$, respectively, with slightly more variability in the HD group.

The average litter size of the LD-exposed dams (9.1±2.2 pups) was significantly higher than HD-exposed dams (6.7±0.8 pups) (P=0.028). However, average maternal weight gain did not vary significantly across exposure groups (P=0.107, Appendix 1, Sup. Fig. 2). We have consistently observed no impact on maternal weight gain in our other exposure experiments employing LD and HD exposures [14,95]. Initial offspring body weights measured on PND 5 showed no significant differences among mean pup weights across exposure groups (P=0.899, Appendix 1, Sup. Fig. 3). This was surprising because human observational studies support an impact on infant birth weight[93]. Rychlik et al. also did not observe offspring weight changes in response to *in utero* UFPs, and Behlen et al. only noted reduced female fetal crown to rump lengths in the LD-exposed group. Weights evaluated at the time point in the current model (PND5) could be more affected by litter size or do not manifest at this stage.

Offspring body weight was also measured after viral (or sham) challenge at either 3 dpi or 9 dpi, corresponding to PND 8 or 14, respectively. No significant differences were detected 3 dpi among exposure groups, even when sex was taken into consideration (P=0.340, data not shown). Notably, 9 dpi mean pup body weight (6.15±0.16 g) in the LD RSV group was significantly lower than the HD RSV group (6.86±0.20 g) (P=0.032, Fig. 4). This was reflected in the female offspring, which showed a significant decrease (~12.9%) in the LD RSV mean weight in comparison to the experimental control (FA Sham, 7.06±0.36 g) (P=0.008). In their model of neonatal PM exposure and influenza infection, Lee et al. also noted PM-exposed pups gained significantly less weight in comparison to control groups, highlighting enhanced morbidity[68].

Interestingly in our model, we did not observe a linear dose-response relationship in decreased weight gain. The non-monotonic dose-response with sex-specificity indicating female susceptibility was also pronounced according to Behlen et al. using the same exposures paradigm. The authors indicate distinct changes in placental morphology and signaling pathways related to lipid homeostasis in placental tissue in the female LD-exposed offspring that was modulated in the HD group[95]. This U-shaped curve or a potential threshold effect is also observed for some, but not all, of the additional phenotypes described below.

3.3.2 In utero UFP exposure induced higher pulmonary viral load in offspring and caused enhanced inflammation

The $TCID_{50}$ assay, evaluating the presence of replicating RSV, was assessed in offspring lung 3 dpi, a time point selected due to peak levels based on viral load kinetics[96]. As expected, none of the sham-exposed pups across any PM exposure group showed evidence of any cytopathic effect that would signify viral replication (data not shown). Overall, lungs from RSV-infected offspring demonstrated an increasing trend in $TCID_{50}$/mL in correlation with exposure: FA-RSV (6,576±5,020), LD-RSV (14,326±6,240), and HD-RSV (33,035±14,665 $TCID_{50}$/mL) (P=0.094, Fig. 5). One outlier (56,2341 $TCID_{50}$/mL) within the LD-RSV group had an exponential difference from the mean of the group and was removed. When separated by sex, this trend was observed only in females (P=0.163), which overall had higher viral load as compared to males.

Allowing for time for a sufficient immune response, offspring BALF was collected 9 dpi and evaluated for a total leukocyte count and leukocyte differentials. Overall, BALF from the LD RSV group demonstrated the highest leukocyte/μL total (118.4±9.1), and although not

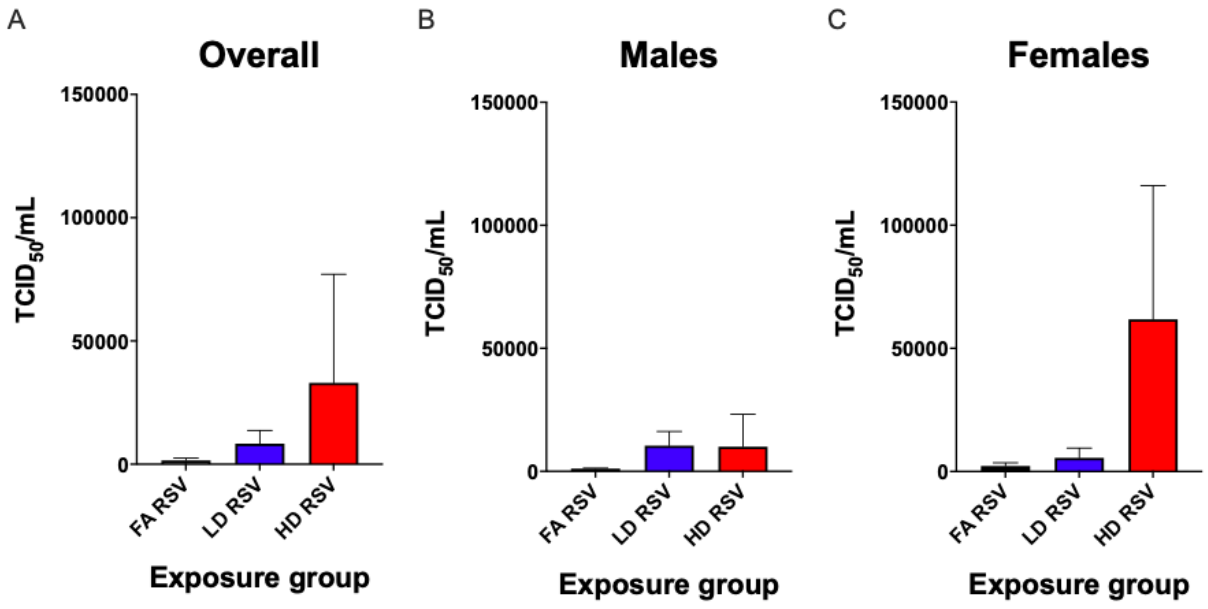

Figure 5. Pulmonary viral load evaluated using the $TCID_{50}$ assay in offspring lungs 9 days post-infection expressed as mean ± SEM. (A) Overall, the number of infectious $TCID_{50}$/mL trended higher in response to UFP dose (P=0.094). (B, C) This trend was mirrored in male and female offspring; however, females exhibited higher infectious titers compared to males. Offspring sample sizes from 4-6 litters, listed as (n=Male, Female), include FA RSV (3, 2), LD RSV (4, 3), and HD RSV (5, 4). Data analyzed using one-way ANOVA with Tukey's multiple comparison test.

---

significant, varied the most drastically from the FA RSV group (81.0±11.5) (P=0.268, Fig. 6A-C). The total number of leukocytes within all sham groups were similar, all close to 100 leukocytes/μL. The HD RSV group had a surprisingly lower total number of leukocytes in the BALF. No significant differences were observed among any of the sex-separated groups, although the female LD RSV (136.1±14.18) and HD RSV (102.5±29.59) groups were greater

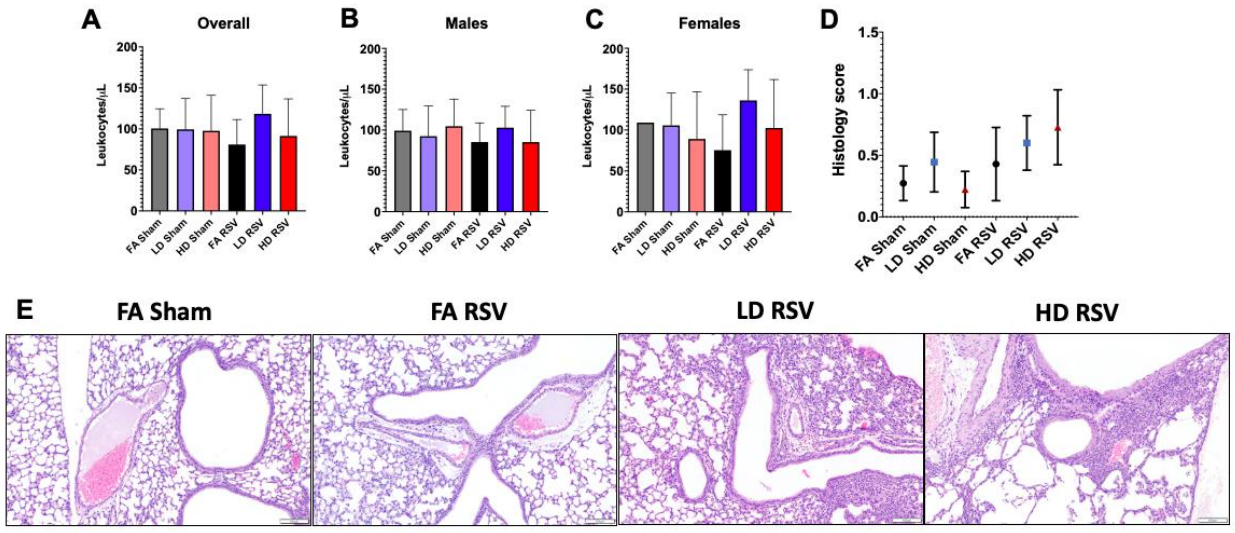

Figure 6. Pulmonary inflammation assessed in offspring lungs 9 days post-infection by bronchoalveolar lavage fluid (BALF) cellular infiltrates expressed as mean ± SEM. (A) Overall, leukocyte infiltration was mild in BALF, indicating a slight increase in the LD RSV group (P=0.268). (B, C) This trend was observed in male and female offspring, but mainly driven by the female LD RSV group. (D) A pulmonary inflammation scoring system was applied to evaluate severity. Overall, more severe inflammation was seen in response to increasing UFP dose as indicated by average histology scores ± SEM (P=0.603). (E) Representative photomicrographs of H&E-stained sections of lungs in offspring show no inflammation (grade 0) in the FA Sham group, mild inflammation (grade 1) in the FA RSV group, moderate inflammation (grade 2) in the LD RSV group, and marked inflammation (grade 3) in the HD RSV group. Scale = 100 µm. Offspring sample sizes from 3-6 litters, listed as (n= Male, Female), for BALF include FA Sham (6, 1), LD Sham (4, 3), HD Sham (7, 8), FA RSV (8, 7), LD RSV (5, 4), and HD RSV (7, 4). Offspring sample sizes for histopathology include FA Sham (7, 4), LD Sham (5, 4), HD Sham (5, 4), FA RSV (3, 4), LD RSV (7, 3), and HD RSV (6, 5). Data analyzed using one-way ANOVA with Tukey's multiple comparison test.

than the FA RSV (75.33±24.97) average level (P=0.293 and P=0.828, respectively). Leukocyte differentials demonstrated a predominance of mononuclear cells, typical of BALF samples, with lower and variable numbers of lymphocytes, neutrophils, and eosinophils (data not shown). No statistical significances were observed across groups within the mononuclear cells, lymphocytes, neutrophils, or eosinophils (P=0.718, P=0.734, P=0.342, P=0.342, respectively).

Histological score (Table 1, Fig. 6D) and representative images (Fig. 6E) overall indicate *in utero* UFP exposure enhanced lung pathology. Peribronchiolar and perivascular infiltrates of eosinophils and macrophages were the most common inflammatory finding, with eosinophilic alveolar infiltrates and hyperplasia of the bronchiole associated lymphoid tissue (BALT) being less common. Mild alveolar histiocytosis was seen in nearly every specimen (n=54), with moderate alveolar histiocytosis (n=4) being associated with moderate to marked levels of inflammation in 3 of 4 samples. An increasing trend in average histology inflammation scores is seen in the FA RSV (0.43±0.30), LD RSV (0.60±0.22), and HD RSV groups (0.73±0.30), though no groups were significantly different (P=0.603). In summary, the FA RSV group had 1/7 mice (14.3%) classified as mild, 1/7 (14.3%) moderate, and 5/7 (71.4%) as no inflammation. The LD RSV group had 4/10 mice (40%) classified as mild, 1/10 (10%) as moderate, and 5/10 (50%) as no inflammation. The HD group had 3/11 mice (27.3%) classified as mild, 1/11 (9.1%) as moderate, 1/11 (9.1%) as marked, and 6/11 (54.5%) as no inflammation. In all of the sham-exposed groups, almost all mice were classified with either mild inflammation (FA 27.0%, LD 22.2%, HD 22.2%) or no inflammation (FA 73.0%, LD 66.6%, HD 77.8%), with the exception of 1 mouse in LD Sham group that scored moderate (11.1%). No statistical differences were detected between males or females for severity of inflammation (P=0.323 and P=0.7932, respectively).

Lung sections were also stained with periodic acid-Schiff (PAS) stain to examine the goblet cells and mucus production of the bronchi and bronchioles. The PAS stain infrequently highlighted aggregates of mucus within the lumen of airways (n=2) but did not reveal any significant association between severity of inflammation and mucus production (R^2=0.145), nor were there statistical differences between exposure groups (P=0.970, Sup. Fig 4). According to the scoring system listed in the methods, the highest scoring group was LD-RSV (0.91±0.17), followed by HD-Sham (0.86±0.14) and LD-Sham (0.79±0.15).

Our model demonstrated the successful infection of neonates with a chimeric strain of RSV, with histologic evidence of an inflammatory response predominated with eosinophils and mononuclear cells. RSV is historically problematic in inducing infection in mice, with most researchers preferring to use the murine analogs such as Sendai virus [107]. However, the $TCID_{50}$ assay demonstrated cytopathic effect within cells cultured with infected lung homogenates, indicating pathogenicity of the virus within our *in vivo* model. Both viral load (Fig. 5) and histology (Fig. 6) showed a trend of increasing infection and severity in correlation with increasing *in utero* UFP exposure (P= 0.094 and P=0.603, respectively). Higher histological scores in the male HD and female LD groups dosed with RSV may suggest differential dose effects by sex, but repeating the experiment with a higher number of pups would be necessary for confirmation. Overall, these findings support prenatal UFP exposure enhances neonatal RSV infection severity. Outcomes from our model corroborate findings from human observational studies[3,100]. Importantly, our low dose maternal exposure, under the U.S. EPA 24-hour exposure level for $PM_{2.5}$ implied increased offspring risk, as did findings from Jedrychowski et al. showing risk for acute bronchitis and pneumonia in children prenatally exposed to levels below 35 $\mu g/m^3$.[3] Moreover, our findings also agree with associations observed by Darrow et al. citing increased risk of hospitalization for

pneumonia and associations with bronchiolitis/bronchitis among children aged 1-4 years exposed to various PM fractions, including organic carbon and sulfates, both represented in our exposure model[100]. A recent study published by Fang et al. showed increased childhood respiratory emergency room visits among children under 14 years old living in Beijing in association with exposures to particles in size fractions of 5–560 nm, mainly from traffic emissions[108]. Significant associations of respiratory emergency room visits were also found to be associated with secondary aerosols and emissions from gasoline and diesel vehicles. The findings by Fang et al. corroborate our model findings specific to UFP-exacerbated childhood respiratory risks.

Early life UFP exposure may exert a detrimental influence over the neonate's ability to combat RSV infection. Mucous metaplasia and hypersecretion are commonly seen in children with RSV and is one of the main components of airway obstruction [73,109]; these findings are mirrored in animal models [110]. However, in our model when comparing the goblet cell counts, no upward trends were seen within the UFP-exposed groups (R^2=0.142, Appendix 1, Sup. Fig. 4), though a few individual mice were noted to have accumulations of mucin within bronchi. This lack of goblet cell metaplasia is most likely due to the short duration of infection in mice, even with chimeric strain of the virus, and would likely be more pronounced in a re-infection study [84].

3.3.3 In utero UFP exposure altered offspring T cell response to RSV infection

Offspring lungs challenged with RSV were also collected 9 dpi to evaluate T cell differentiation (Fig. 7), with data represented as a percentage of each subset within the CD3 or

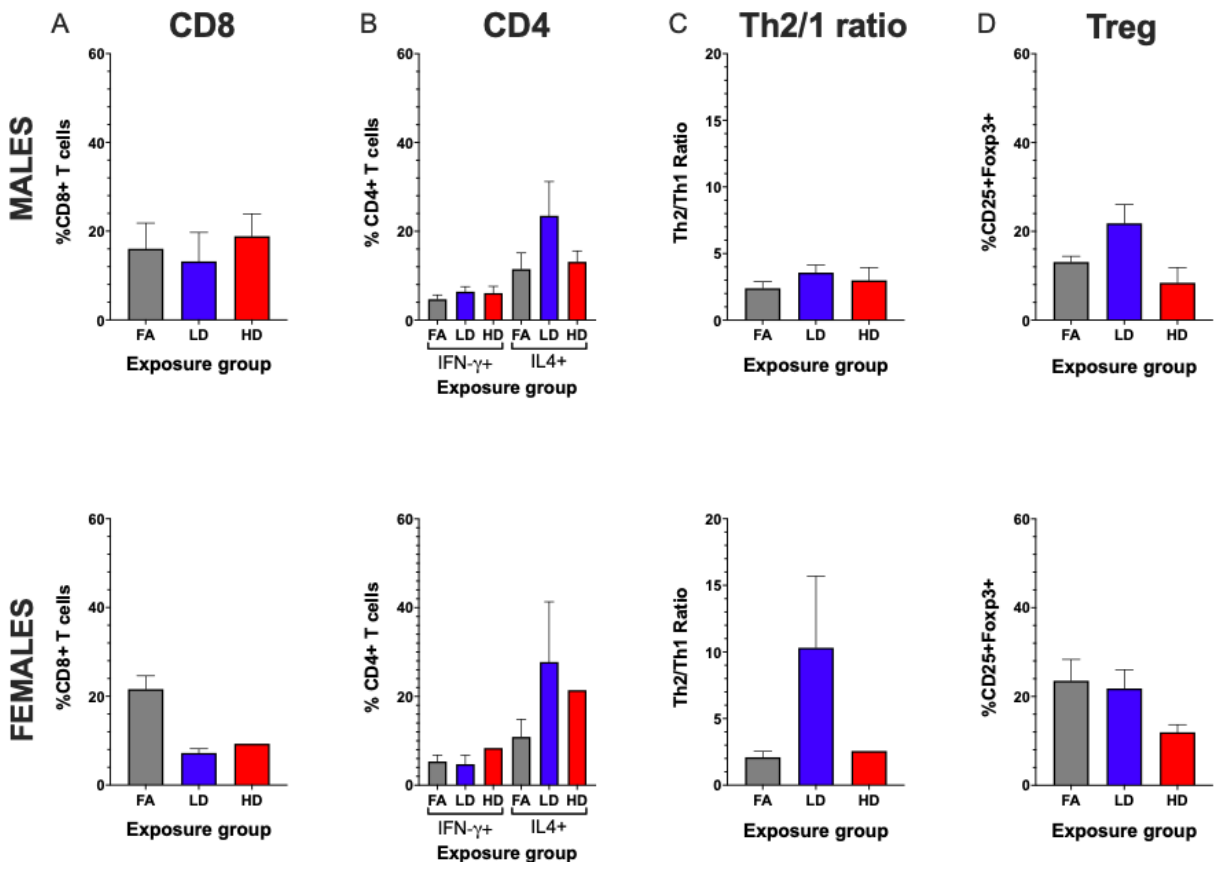

Figure 7. Flow cytometry analysis of neonatal lungs of offspring 9 dpi dosed with RSV, separated by sex. (A) CD8+ T cells. (B) CD4+ cells differentiated by Th1 (IFN-γ+ cells) and Th2 (IL-4+ cells). (C) Th2/Th1 ratios determined that all groups are minimally to moderately Th2 biased. (D) T regulatory cells. Offspring sample sizes from 3-6 litters, listed as (n= Male, Female) for A-C and D, respectively, include FA RSV (3, 5) and (4, 6), LD RSV (2, 2) and (6, 6), and HD RSV (6, 1) and (3, 3). Error bars represent SEM. Data analyzed using one-way ANOVA with Tukey's multiple comparison test.

CD4 positive cells, where appropriate. Within the combined sex data (not shown), there were no significant differences among the CD8+ T cell population among exposure groups, although a

slight decrease in the LD group (12.54±3.40) was observed as compared to the FA (19.51±2.80) and HD (17.49±4.49) groups, indicating possible decreased Th1 response. This coincided with a trend toward Th2 bias (i.e., increased CD4+IL4+ T cells), especially in the LD group. CD4+IFN-γ+ cell levels were consistently low across the FA, LD, and HD groups, and the percentage of CD4+ cells staining for IL-4 was higher in all groups, with LD-RSV group average (26.06±7.88), higher than both the FA and the HD groups by 15% and 11%, respectively (P=0.057 and P=0.167, respectively). Within the Treg panel offspring average CD25+Foxp3+ cells did not differ significantly across groups overall (P=0.090, data not shown). However, a slight decrease in Tregs was observed in the FA and HD groups as compared to the LD group (P=0.867 and P=0.101, respectively). Sex-separated data (Fig. 7) show similar trends, with more pronounced reduction in CD8+ cells in female (LD and HD groups), and more pronounced Th2 skewing in the LD female group. Overall, the flow cytometry data mirrors our histopathological findings indicating again a potential non-monotonic dose-response or "thresholding" effect. An altered Th1/Th2 ratio, skewed toward Th2 response reflects the typical pattern of immune response in children who have increased RSV severity due to an enhanced Th2/allergic immunophenotype [111]. Human observational studies support $PM_{2.5}$ affects the immune system, although only a handful of human studies relevant to early-life exposure are published to date[4,34]. Herr et al. observed that prenatal exposure to $PM_{2.5}$ shifted lymphocyte distributions in umbilical cord blood, where exposure during early gestation resulted in increased T lymphocytes, decreased B lymphocytes, and decreased natural killer cells, and late gestation exposure was associated with decreased T lymphocytes, increased B lymphocytes, and increased natural killer cells[49]. Evidence of shifting immune responses over different developmental stages is also reflected in mouse models. Wang et al. showed that gestational exposure to combustion-derived $PM_{0.1}$ inhibited offspring pulmonary T

cell development, with suppression of Th1, Th2, Th17, and Tregs at six days of age[70]. Pulmonary Th1 cells remained suppressed up to six weeks, leading to enhancement of postnatal allergic responses to ovalbumin (OVA) evidenced by increased airway eosinophilia driven by Th2-bias responses. In another model, Sharkhuu et al. demonstrated prenatal diesel exhaust (DE) exposure caused sex-specific alterations in lung protein and inflammatory cells, as well as splenic T cell subsets, even though allergen challenge did not enhance inflammation[62]. These findings mirror data in our previous UFP-allergen model (using 100 μg/m^3 of UFPs and house dust mite challenge), wherein Rychlik et al. also did not observe prenatal UFP to enhance inflammatory response to allergen. Overall, this window of immune suppression may in fact underlie increased susceptibly to viral infection. Findings from the current research add to the body of basic research showing prenatal $PM_{0.1}$ exposure alters offspring pulmonary immune system development, signifying risk for acute respiratory infection risk.

3.3.4 Sex- and dose-specific effects of in utero UFP exposure on inflammatory and oxidative stress-related gene expression

qRT-PCR was performed in lung samples collected 9 dpi to evaluate inflammatory (*NF-κB*) and oxidative stress-related (*Nrf2, Nqo1*) gene expression (Fig. 8). Expression was greater in all three genes in male offspring across multiple exposure groups in comparison to female offspring levels. For *NF-κB* expression, HD sham and HD RSV groups had significantly higher expression (~4-fold) versus FA Sham control. Similarly, for *Nrf2* and its downstream gene *Nqo1*, HD Sham and HD RSV male offspring had significantly higher expression as compared to FA Sham. The females had notably lower gene expression in all exposure groups. *NF-κB* is a redox-

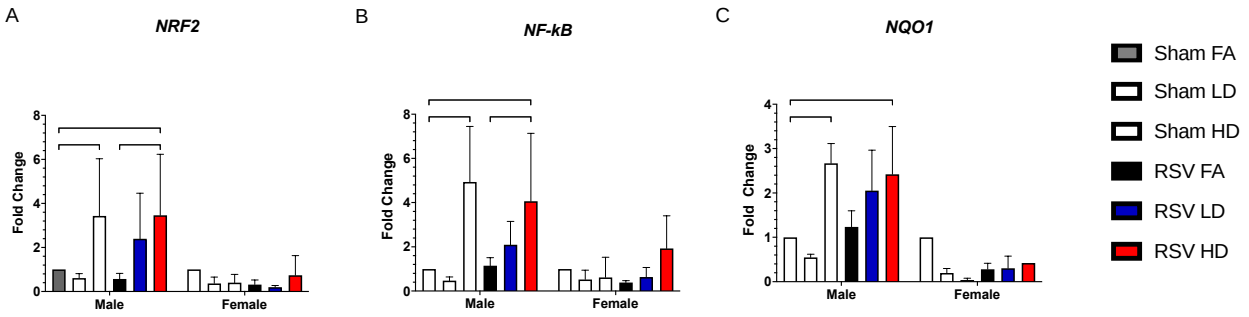

Figure 8. Genes related to inflammation and oxidative stress were evaluated by qRT-PCR. HD Sham and HD RSV males show significant increases in expression, up to 4-fold, from their controls in NF-κB (A), Nrf2 (B), and NQO1 (C), while no groups of females displayed increased or significantly different levels of expression. Offspring sample sizes from 3-6 litters, listed as (n= Male, Female) include FA Sham (6, 1), LD Sham (4, 3), HD Sham (7, 8), FA RSV (8, 7), LD RSV (5, 4), and HD RSV (7, 4). Error bars represent SEM. Data analyzed using one-way ANOVA with Tukey's multiple comparison test (*p<0.05; **p<0.01; ***p<0.001).

---

sensitive transcription factor that activates pro-inflammatory cytokines and other immune response genes[112]. Activation of this pathway is associated with increased levels of the pro-inflammatory enzyme COX-2 and cytokines like IL-1β and TNF-α. Since the HD RSV-infected male offspring showed such a pronounced inflammatory response as indicated by histopathology score, perhaps this is the main driver of inflammation. Nrf2 is a redox sensitive transcription factor regarded as the master regulator of the antioxidant response[80]. Nrf2 binding to the antioxidant response element (ARE) in promoters upstream of phase II enzymes and other oxidative stress-related enzymes, including *Nqo1*, drives transcription in response to oxidative stress. Disruption of Nrf2 has been shown to enhance susceptibility to allergic airway inflammatory responses induced by chronic exposure to diesel exhaust PM[88]. In our model,

Table 1. Pulmonary inflammation following *in utero* exposure to UFPs and offspring RSV challenge.

	Overall	Males	Females
FA Sham	0.27 ± 0.14	0.14 ± 0.14	0.50 ± 0.29
FA RSV	0.43 ± 0.30	0.67 ± 0.67	0.25 ± 0.25
LD Sham	0.44 ± 0.24	0.60 ± 0.40	0.25 ± 0.25
LD RSV	0.60 ± 0.22	0.57 ± 0.30	0.67 ± 0.33
HD Sham	0.22 ± 0.15	0.20 ± 0.20	0.25 ± 0.25
HD RSV	0.73 ± 0.30	1.17 ± 0.48	0.20 ± 0.20

Histological evaluation was performed on H&E stained slides using a scoring system ranging from 0-3 (0-no lesions; 1-mild; 2-moderate; 3-marked). Average scores, shown above ± SEM, were compared among groups and sexes. Offspring sample sizes from 3-6 litters, listed as (n= Male, Female) include FA Sham (7, 4), LD Sham (5, 4), HD Sham (5, 4), FA RSV (3, 4), LD RSV (7, 3), and HD RSV (6, 5).

---

males appear to mount an effective Nrf2 antioxidant response, which is lacking in female offspring. Data on differential effects of *in utero* UFP exposure on placental pathways highlight the role of altered lipid metabolism, especially in female LD-exposed offspring (Behlen). Novel pathways in the lung are yet to be validated and necessitate further research to identify mechanisms. In this study, we only surveyed three candidate genes, so it is entirely possible that another gene network not evaluated here is responsible for the unique effects observed in female offspring.

3.3.5 Implications for human health effects during early infancy

Our work demonstrates that *in utero* UFP exposure alters offspring pulmonary immune responses in a sex- and dose-specific manner, exacerbating neonatal RSV infection in early infancy. Our results show that offspring body weights are significantly reduced in response to infection, markedly in the female LD group. Pulmonary viral load is higher in the LD and HD groups and is greatest for females. Peribronchiolar and perivascular infiltrates of eosinophils and macrophages represent the most prominent histopathological response to RSV. In both sexes, increasing severity of inflammation correlate with increasing UFP exposure. Notably, the highest degree of inflammation is observed in the HD group for males, whereas the LD group show the most inflammation alongside increased leukocyte counts in bronchoalveolar lavage fluid for females. Pulmonary inflammation is characterized by an enhanced Th2 but reduced Th1 cellular response, particularly in the female LD group.

Our model has several advantages, including a controllable maternal inhalation throughout gestation representing urban UFP exposure. This model lays the foundation for future mechanistic investigations to characterize sex differences in respiratory responses to prenatal UFP exposure. Likewise, there also exist limitations in our model, which require further investigation. For example, a few of our measures with small sample sizes likely prevent robust statistical analysis, especially sex-separated analysis. The selection of the background strain, the C57BL/6, likely corresponds to a Th1-biased immune system. Our choice for this strain follows Rychlik et al., which showed higher strain susceptibility to prenatal UFP exposure. C57BL/6 mice are considered moderate responders to RSV according to the ranking done by High et al [113]. The inherent Th1-biased immunophenotype may mask the difference among various endpoints. On the other hand,

the presence of statistical significance and trends demonstrates that UFPs exhibit notable effects even in mice that may be less susceptible to exaggerated Th2 responses. In addition, the viral titer employed in our work is slightly lower than that in other previous studies [87,96].

Since RSV infection represents a significant cause of infant morbidity and mortality, it is imperative that future mitigation policies and interventions are developed and implemented to reduce early life exposure to air pollution and to protect the health for the most vulnerable population. Lastly, our findings of suppressed pulmonary immune response from *in utero* UFP exposure likely have implications for other respiratory virus infections in early infancy, including the novel severe acute respiratory syndrome coronavirus 2 (SARS-CoV-2)[114], which clearly warrants future investigations.

CHAPTER IV

NRF2 PROTECTS AGAINST NEONATAL OXIDATIVE STRESS FOLLOWING *IN UTERO* ULTRAFINE PARTICULATE MATTER EXPOSURE

4.1 Introduction

Early life exposure to particulate matter (PM) air pollution is linked with numerous adverse developmental outcomes, impacting global neonatal morbidity and mortality, and increasing risk for chronic health effects later in life.[1,2] PM is classified by size into coarse (PM_{10}, <10 μm), fine ($PM_{2.5}$, <2.5 μm), and ultrafine particles (UFPs, diameter <0.1 μm). The World Health Organization recently lowered its guideline values for PM_{10} and $PM_{2.5}$ aimed at promoting reduced risks for acute and chronic health effects.[3] Conversely, no guidelines or regulations exist for UFPs. The small diameter of the UFPs allows for a deeper penetration into airways, the ability to translocate systemically, and a higher surface area to volume ratio that allows increased absorption of potentially toxic chemicals generating systemic oxidative stress responses.[4] Evidence from experimental models and human placentae demonstrates UFPs can cross the placental barrier into fetal circulation.[5,6]

Since fetal development is a period of rapid differentiation and growth, *in utero* exposure to UFPs, and also more broadly PM, represents a unique window of susceptibility. Prenatal exposure to PM_{10} and $PM_{2.5}$ has been consistently linked with preterm birth, infant low birth weight[7–9], and respiratory morbidities, including risks for respiratory infection and childhood asthma[10–12]. Emerging evidence supports prenatal UFP exposure is independently linked with childhood asthma incidence.[13,14] Additional observation studies demonstrate early life exposure to various PM fractions, including organic carbon and sulfates, and particles in size fractions of 5–560 nm

mainly from traffic emissions, are associated with increased risk of hospitalization for respiratory infections among children in the U.S. and in China.[15,16] In the latter study, significant associations of respiratory emergency room visits were also found to be associated with secondary aerosols and emissions from gasoline and diesel vehicles. Findings from a birth cohort study in Korea demonstrate increased susceptibility of lower respiratory tract infections in infants prenatally exposed to $PM_{2.5}$ and second-hand smoke was significantly modified by polymorphisms in maternal genes related to oxidative stress response pathways, especially in the nuclear factor erythroid 2-related factor (Nrf2) gene.

Nrf2 regulates and enhances the cellular response to oxidative stress.[17] A transcription factor in the Cap n' Collar family with a basic leucine zipper, Nrf2 is bound in the cytoplasm by the Keap1-Cul3 complex.[18,19] In traditional canonical activation, oxidative stress initiates the oxidization of cysteine residues of the dimerized Keap1 protein, altering its conformation to prevent it from binding Nrf2. The freed Nrf2 translocates to the nucleus, where it binds an antioxidant response element (ARE) upstream numerous antioxidant-related genes.[18] In experimental models, disruption of Nrf2 has been shown to enhance susceptibility to allergic airway inflammatory responses induced by chronic exposure to diesel exhaust particulate matter.[20] While the role of Nrf2 in standard, adult exposure models is well-studied, the impact of Nrf2 signaling in maternal and fetal responses to *in utero* PM exposure, especially the ultrafine fraction, is yet to be clarified.

Therefore, to evaluate the effect of UFP exposure during pregnancy on neonatal outcomes in a model lacking an appropriate oxidative stress response, we exposed Nrf2 deficient ($Nrf2^{-/-}$) and wildtype (WT) dams to filtered air (control) or aerosolized ultrafine PM containing diesel exhaust. We evaluated the neonatal pulmonary immunophenotype and state of oxidative stress.

We hypothesized offspring of exposed dams lacking Nrf2 would have a reduced capacity to respond to the oxidative stress may be predisposed to enhanced respiratory morbidity.

4.2 Methods and Materials

4.2.1 Ultrafine Particle Exposure

Diesel Particulate Matter Standard Reference Material (SRM 2975) was purchased from the National Institute of Standards and Technology (Gaithersburg, MD). All other chemicals and reagents used were obtained commercially at the highest available purity. PM generation followed methods developed by Rychlik et al. [14], with adaptations to accommodate individual housing within whole body exposure chambers, as described by Behlen et al.[95] Briefly, HEPA filtered air was continuously pumped into two separate chambers (FA and PM) where pregnant dams were individually housed. For the PM chamber, UFPs were generated using a custom-built constant output atomizer. We employed a multicomponent aerosol mixture consisting of ammonium nitrate, ammonium sulfate, diesel exhaust PM (NIST, SRM 2975), and potassium chloride, with the mass fractions of 44, 39, 10, and 7%, respectively. Real-time particle size distribution was monitored using a differential mobility analyzer (DMA) in tandem with a condensation particle counter (CPC). The flowrate of HEPA-filtered air was adjusted to ensure consistent particle concentrations ~100 $\mu g/m^3$ within chambers throughout the exposure duration. This dose was selected based on previous reports from our research showing marked placental changes and enhanced viral infection severity in offspring.

Nrf2-deficient mice (Nrf2-/-) on C57Bl/6J background were obtained from Dr. Tom Kensler, which were generated as previously described[95]. Genotyping for homozygous wildtype ($Nrf2^{+/+}$) and null ($Nrf2^{-/-}$) mice was carried out following established methods (see supplemental

information). Mice were housed in a climate-controlled room with 12/12h light/dark cycle at an AAALAC approved facility at Texas A&M University. All procedures were approved by the Institutional Animal Care and Use Committee of Texas A&M University #2019-0025. Mice had access to standard chow, 19% protein extruded rodent diet (Teklad Global Diets), and water ad libitum except during exposure periods. A schematic of our exposure timeline is shown in Supplemental Figure 1. Male and female WT or Nrf2$^{-/-}$ mice were time-mated. The presence of a vaginal plug defined gestational day (GD) 0.5. Beginning on GD0.5, dams were randomized and placed into exposure chambers where they were exposed to either FA (n=5;5) or PM (n=4;7), listed as (n=WT; Nrf2$^{-/-}$) respectively, from 0800 to 1400 hours (6 hours) daily through GD18.5. Following exposure on GD18.5, mice were removed to individual housing and allowed to deliver spontaneously, denoted as PND1 (post-natal day). Pups were weighed and euthanized on PND5 for baseline evaluations.

4.2.2 Flow cytometry

PND5 lungs were perfused retrograde with sterile phosphate buffered saline for removal of red blood cells, mixed with a Miltenyi Biotic Flow Cytometry kit (Auburn, CA), dissociated with gentleMACS Octo Dissociator (Miltenyi Biotec, Auburn, CA), and strained through a 40-µm cell strainer (MACS SmartStrainers, Miltenyi Biotec, Auburn, CA). The single cell lung suspension was treated with RBC lysis buffer, washed, placed in 90% FBS and 10% DMSO freezing media, and frozen in a Mister Frosty (ThermoFisher, cat#: 5100-0001) down to -80°C and held there until later processing. Samples were

combined within litters and sexes to achieve appropriate cellularity. Processing was performed in a 96 well plate. Cells were incubated with Golgi Plug for 5 hours, washed with cell staining buffer,

blocked with anti-CD16/CD32 for 10 minutes, and incubated with cell surface fluorescent monoclonal antibodies for 20 minutes with the panels listed below. Cells were washed twice with cell staining buffer, resuspended in permeabilization wash buffer, incubated with intracellular fluorescent antibodies for 30 minutes, then washed in buffer twice again. Cells were resuspended in cell staining buffer and analyzed. All antibodies were obtained from BioLegend. T cell staining used Alexa Fluor 488 anti-mouse CD3 [100210] and PE anti-mouse CD69 [104507]. Th1 cell staining used Alexa Fluor 647 anti-rat IFN-ɣ [507809], APC/Fire 750 anti-mouse CD4 [100460], and PE/Cy7 anti-mouse CD8a [100722]. Th2 cell staining used Brilliant Violet 421 anti-mouse IL-4 [504119]. T regulatory cell staining used Alexa Fluor 647 anti-mouse CD25 [102019] and Brilliant Violet 421 anti-mouse FOXP3 [126419]. FMOs and positive and negative compensation beads were used to set gates for the above populations. Stained samples were measured using a Beckman Coulter Moflo Astrios high speed cell sorter outfitted with 405nm, 488nm, and 640nm lasers. The BV421 was excited using a 405nm laser and emission detected using a 448/59nm bandpass filter. The Alexa Fluor 488, and PE- Cy7 were excited using the 488nm laser and emissions were detected using 513/26nm, and 795/70nm bandpass filters, respectively. The Alexa Fluor 647 and APC-Fire 750 were excited using a 640nm laser and emission detected with a 671/30nm and 795/70nm bandpass filters, respectively. The Live/Dead fixable Red stain was excited using the 488 nm laser and emission detected using a 620/29nm bandpass filter. The samples were run at a flow rate less than 3000 events per second. The flow cytometry data was analyzed using FlowJo Software (Becton, Dickinson, and Company). Gating strategies are depicted in supplemental figures (Appendix 2, Sup. Fig. 4-5).

4.2.3 Gene Expression

Total RNA was extracted from PND5 lungs using TRIzol reagent according to the manufacturer's protocol (ThermoFisher Scientific). RNA was quantified with a DeNovix DS-11 FX+ Spectrophotometer/Fluorometer with ≥1.8 260/280 nm absorbance values. Following purification, cDNA was reverse transcribed (Qiagen QuantiTect® Reverse Transcription), and transcription levels of key genes related to oxidative stress were analyzed using SYBR Green qRT-PCR (Applied Biosystems™ Power SYBR™ Green PCR Master Mix) on a Roche LightCycler® 96 System. Relative expression was calculated using 2-ΔΔCT with Gapdh as the reference gene.

4.2.4 Thiol Redox Analysis

4.2.4.1 Sample Preparation

Thiol redox analysis followed Jones and Liang with slight modifications.[121] PND5 livers were snap frozen in liquid nitrogen until analysis. Approximately 10-50 mg of liver tissue was quickly weighed before being homogenized in 1 mL of buffer solution containing an internal standard, γ-glutamylglutamate (γ-Glu-Glu) and centrifuged at 10,000 g for 10 minutes at 4°C. 60 µL of 7.4 mg/mL iodoacetic acid (IAA) was added to 300 µL of the supernatant and immediately vortexed. pH was adjusted to ~9.0 ± 0.2 with ~425 µL of KOH/tetraborate to precipitate proteins, then incubated at room

temperature for 30 minutes before pH was confirmed. 300 µL dansyl chloride (DC) solution (20 mg/mL in acetone) was added to each sample, vortexed, and incubated at room temperature in complete darkness for 16-28 hours. 500 µL of HPLC-grade chloroform was added to samples, followed by vortexing and centrifugation. The upper aqueous layer was stored in -80°C until HPLC analysis.

4.2.4.2 HPLC Analysis

Samples were thawed on ice, centrifuged for 10 minutes, and aliquots were transferred to an HPLC autosampler vial. 35 µL was injected on a Supelcosil LC-NH2 column with internal dimensions of 5 µm, 4.6 mm X 25 cm (Supelco, Bellefonte, PA). Column oven operating temperature was held constant at 35°C. HPLC mobile phases included solvent A (80% v/v methanol/water) and solvent B (acetate-buffered methanol). Initial solvent conditions were 80% A, 20% B at 1 ml/minute for 10 minutes. A linear gradient to 20% A and 80% B was then run from 10-30 minutes. From 30 to 35 minutes, the flow gradient was maintained at 20% A and 80% B. From 35 to 42 minutes, conditions were returned to 80% A and 20% B. Detection of desired thiols was obtained by fluorescence monitoring. Approximate elution time frames of compounds of interest were as followed: cystine (CySS) from 9 to 9.5 min; cysteine (Cys) from 10 to 10.5 min; γ-GluGlu from 12 to 13 min; glutathione (GSH) from 19 to 19.5; and glutathione disulfide (GSSG) from 23.5 to 24 min.

4.2.5 Statistical Analysis

Statistical analysis was performed using Prism (v8, GraphPad Software, San Diego, CA) to determine differences in offspring outcomes based on exposure group. Two-way analysis of variance (ANOVA) with Tukey's multiple comparisons tests were conducted. An adjusted p value of <0.05 was considered statistically significant.

4.3. Results

4.3.1 In Utero UFP Exposure Alters Neonatal Weights Most Profoundly in Nrf2$^{-/-}$ Mice

Low birth weight is one of the common perinatal effects in children born to mothers exposed to particulate matter air pollution.[2,7] We monitored birth weights in neonates born to Nrf2$^{-/-}$ and wildtype (WT) dams exposed for the length of gestation to either filtered air (FA – 0 μg/m^3) or ultrafine particulate matter (PM, 111.87±4.40 μg/m^3, mean±SEM) (Appendix 2, Sup. Fig. 1). Regardless of exposure group or litter size, no statistical significance was detected between the average daily maternal weight gain during gestation (P=0.560) or the final weights of the pregnant dams before parturition (P=0.570) (Appendix 2, Sup. Fig. 2). Average litter sizes did not vary between exposures or genotypes (P=0.809), nor was there any correlation between litter size and pup weight (P=0.600) (data not shown). Initial weights of pups taken on PND5 showed Nrf2$^{-/-}$ pups with significantly reduced weight gain compared to WT pups (P=0.0001) (Fig. 9). PM exposure significantly reduced weight gain within WT and Nrf2-/- (P=0.045), although the reduction was milder compared to that induced by lack of Nrf2. Though both sexes mirror this overall trend, the male pups are significantly driving the differences between the control WT FA-exposed group and the Nrf2$^{-/-}$ PM-exposed group (P=0.003).

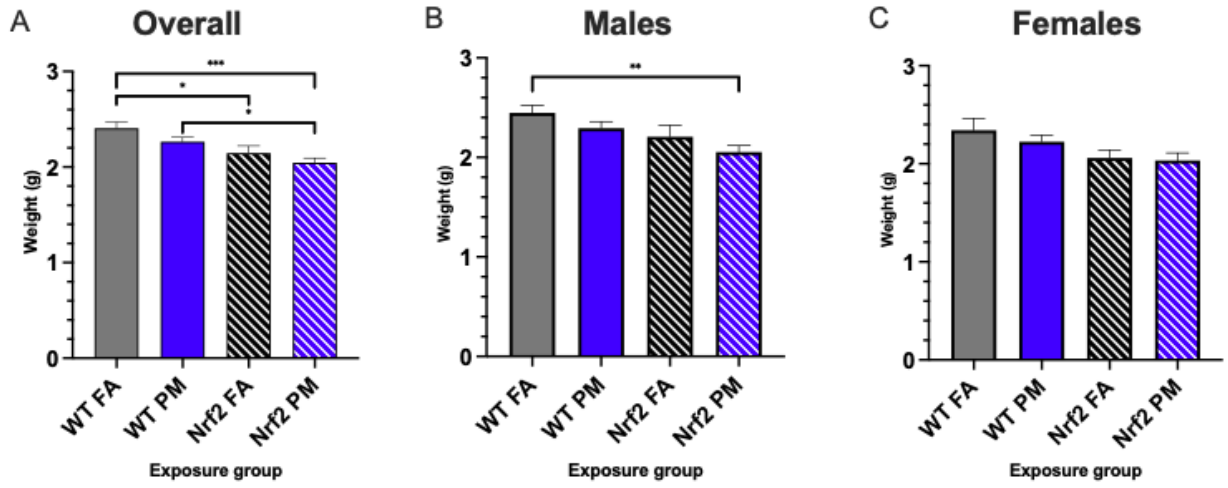

Figure 9: Neonatal weights taken at PND5 during collection (21 litters with total n=112). (A) Nrf2$^{-/-}$ offspring showed significantly decreased body weights from their wildtype counterparts

in both PM and FA exposed groups. Nrf2$^{-/-}$ PM-exposed offspring showed significantly decreased body weight versus the WT FA-exposed group. Male (B) and female (C) weight changes reflect overall trends. Offspring sample sizes, listed as (n=Male, Female), from 4-7 litters, include WT FA (n= 19,12), WT PM (n=16,12), Nrf2$^{-/-}$ FA (n=14,12), and Nrf2$^{-/-}$ PM (n=17,12). Error bars represent SEM. Data analyzed using two-way ANOVA with Tukey's multiple comparison test. (*p<0.05; **p<0.01; ***p<0.001)

4.3.2 Nrf2$^{-/-}$ Neonates Exhibit Th2 Pulmonary Immune Bias

Prenatal PM exposure is linked to a higher incidence of childhood asthma and respiratory infections, often driven by or compounded by a Th2-skewed immune response.[3,122] To evaluate the differences in neonatal pulmonary immunity between Nrf2$^{-/-}$ and WT FA- or PM-exposed mice, lungs were taken at PND5, and both a T regulatory panel and a Th1-Th2 panel evaluated all samples to examine the effect that UFP exposure would elicit from the immune system, particularly within its lymphocytes. The Th1 and Th2 panel looked at multiple markers: CD3, CD4, CD8, IFN-γ, IL-4, and IL-17A. From these, a Th1/2 ratio was examined to look for T helper cell bias. Overall CD4+ cell levels mildly, though not significantly, decreased in the Nrf2$^{-/-}$ PM group (P=0.100); CD8+ cells did not show any significant trends (P=0.315) (Appendix 2, Sup. Fig. 3).

Nrf2$^{-/-}$ PM-exposed neonates showed the highest numbers of both Th1 CD4+ cells, (positive for IFN-γ) and Th2 CD4+ cells (positive for IL-4). Within the Th1 subset, the combined data demonstrated that the Nrf2$^{-/-}$ PM CD4+ average of 9.83$\pm$1.71% significantly outweighed the 3.55$\pm$1.07% average of the Nrf2$^{-/-}$ FA group (P=0.025), a trend is also reflected in the sex-separated data, although without significance (P=0.114 and P=0.132 for males and females,

respectively) (Fig. 10A). The Nrf2$^{-/-}$ PM males and females averaged 9.87±2.38% and 12.15±2.76%, respectively, as compared to the lower Nrf2$^{-/-}$ FA males (3.40±1.36%) and females (5.09±0.92%). Within the Th2 subset, the Nrf2$^{-/-}$ PM-exposed neonates, when combined, had

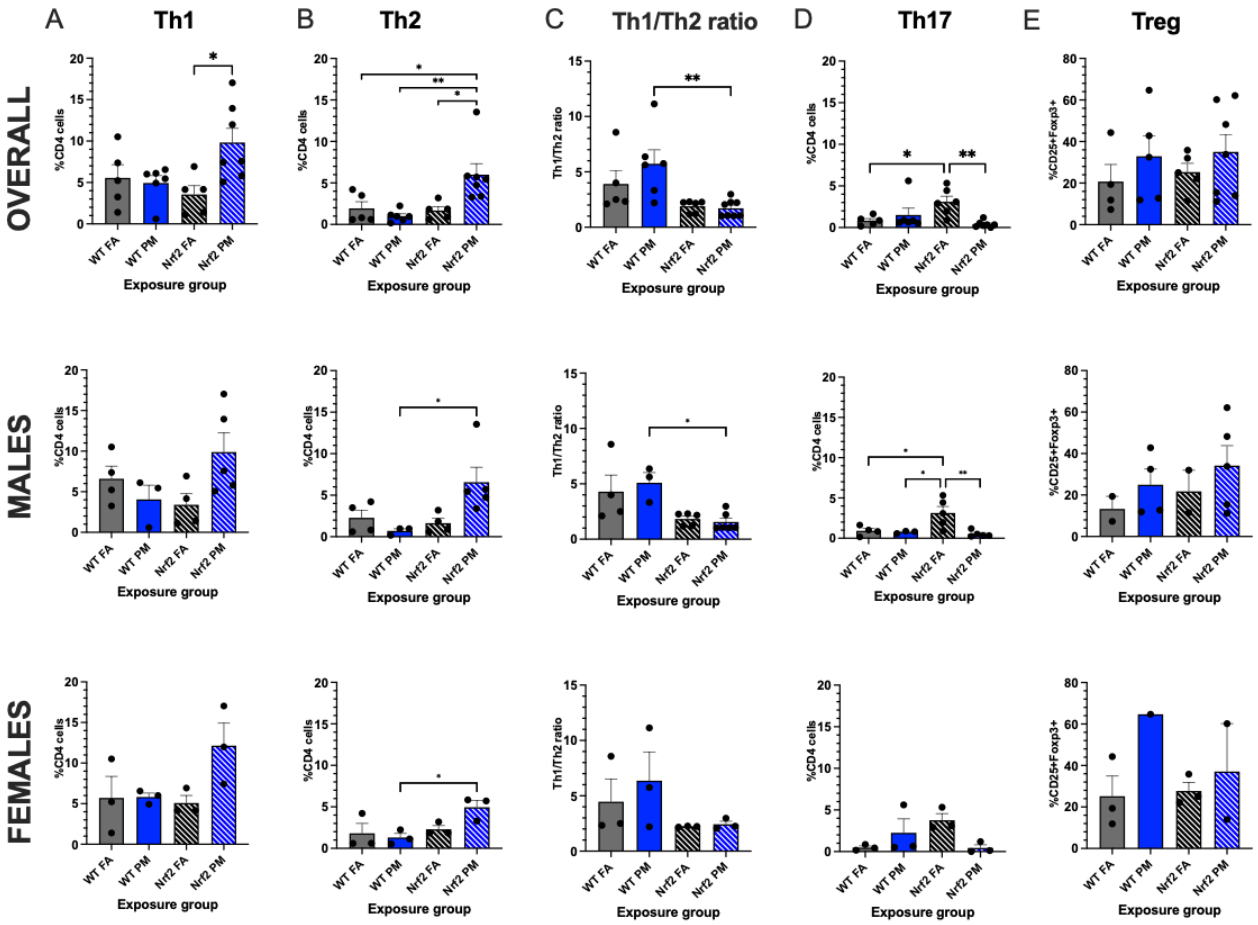

Figure 10: Flow cytometry analysis of neonatal lungs at PND5. Percentages of CD4+ cells with Th1 (A) and Th2 (B) differentiation significantly increase in Nrf2$^{-/-}$ PM-exposed mice. (C) Nrf2$^{-/-}$ mice experience a low Th1/2 ratio, indicating a Th2 bias, while the wildtype mice maintain a Th1 bias. (D) Th17 cells significantly increase in FA-exposed Nrf2$^{-/-}$ mice. (E) T regulatory cells do not differ significantly across groups. Th1/2 offspring sample sizes, listed as (n=Male, Female), from 4-7 litters, include WT FA (n= 3,3), WT PM (n=3,3), Nrf2$^{-/-}$ FA (n=5,3), and Nrf2$^{-/-}$ PM (n=6,3). Treg offspring sample sizes, listed as (n=Male, Female), from 4-7 litters, include WT FA

(n= 2,3), WT PM (n=4,1), Nrf2$^{-/-}$ FA (n=2,3), and Nrf2$^{-/-}$ PM (n=5,2). Error bars represent SEM. Data analyzed using two-way ANOVA with Tukey's multiple comparison test. (*p<0.05; **p<0.01)

---

significantly higher numbers of Th2 cells than the Nrf2$^{-/-}$ FA-exposed (P=0.016), WT PM-exposed (P=0.003), and WT FA-exposed groups (P=0.025) (Fig. 10B). The number of Nrf2$^{-/-}$ PM Th2 cells was significantly higher than the WT PM group in both males (6.57±1.79% versus 1.64±0.58%, P=0.037) and females (4.95±0.83% versus 2.30±0.45%, P=0.050).

These averages led the Th1/2 ratio to have a distinct separation by strain, wherein the ratio of the WT groups was greater than those of the Nrf2$^{-/-}$ groups, regardless of exposure group (Fig. 10C). A higher Th1/2 ratio represents skewing of the immune system towards a Th1 response, with the lower ratio conversely representing a Th2 biased immune response. Thus, the Nrf2$^{-/-}$ neonates display a Th2 immune bias by the Nrf2$^{-/-}$ PM ratio of 1.71±0.27%, decreased in comparison to the WT PM ratio of 5.73±1.26% (P=0.002) but similar to the Nrf2$^{-/-}$ FA ratio of 1.90±0.22%. The males' ratios follow similar patterns at 1.56±0.34%, 5.10±0.91%, and 1.83±0.26%, respectively (P=0.002), but the female ratios showed no significant differences (P=0.395).

Th17 CD4+ cells are most commonly recognized for their role in autoimmune phenotypes. As seen in Figure 10D, this subset demonstrated the most varied trends of the CD4+ cells, with an unexpectedly high count in the Nrf2$^{-/-}$ FA males (3.14±0.80%) and females (3.77±0.76%), with a combined average of 3.10±0.66%. This combined average is significantly higher than the Nrf2$^{-/-}$ PM and WT FA groups (P=0.008 and P=0.047, respectively), and the males in this group significantly exceeded their Nrf2$^{-/-}$ PM (P=0.009), WT FA (P=0.036), and WT PM (P=0.040)

counterparts. These findings may suggest a constitutively high level of Th17 cells in the Nrf2$^{-/-}$ strain that is suppressed by PM exposure.

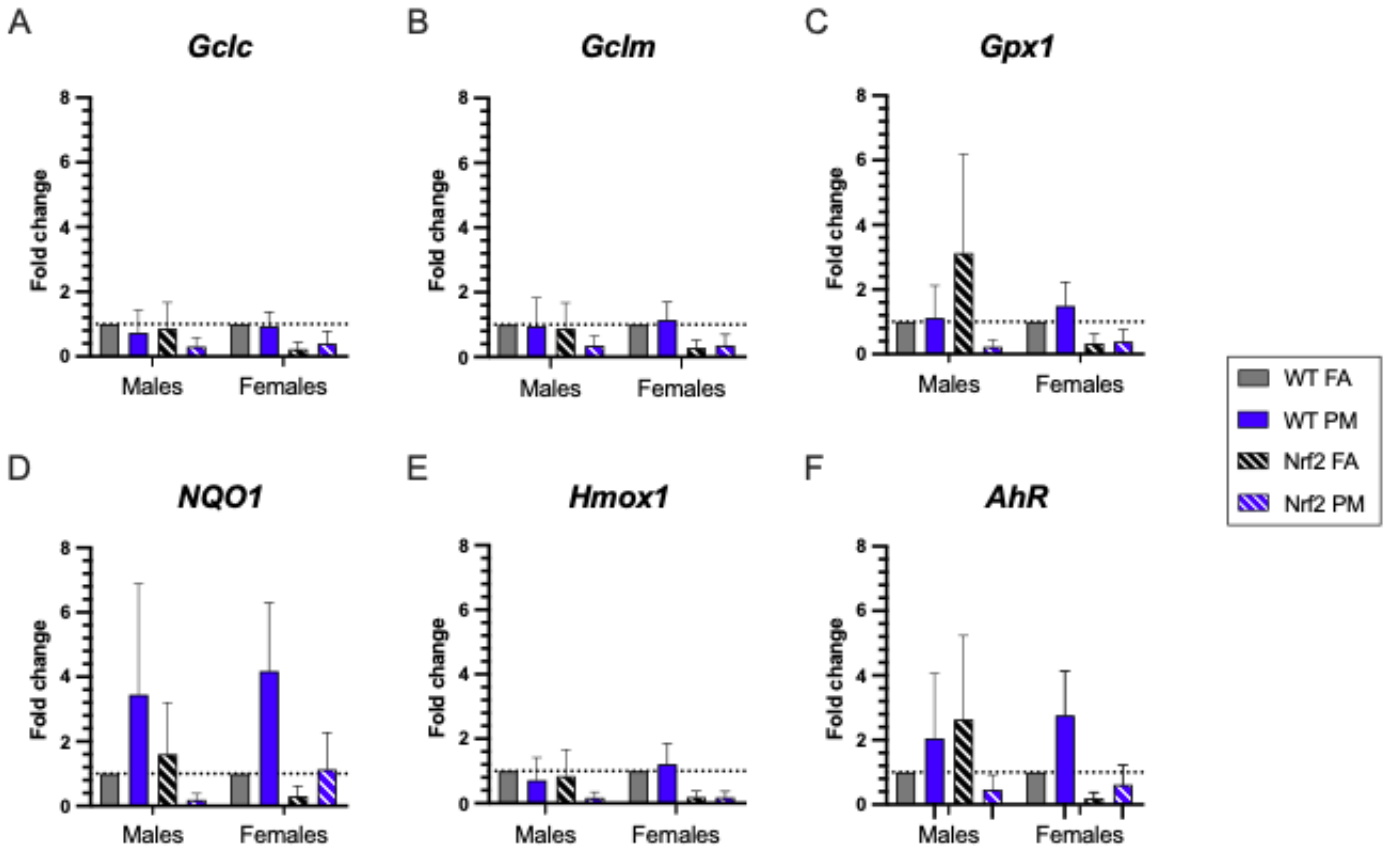

Figure 11: Pulmonary expression of oxidative stress-related genes. Nrf2$^{-/-}$ neonatal lung samples generally show consistently lower expression of oxidative stress-related genes than their wildtype counterparts. Females generally demonstrate higher expression in PM-exposed mice in both strains. The males demonstrate high expression of oxidative stress-related genes in the Nrf2$^{-/-}$ mice exposed to FA, contrasted by low expression in the Nrf2$^{-/-}$ PM-exposed males. Offspring sample sizes, listed as (n=Male, Female), from 4-7 litters, include WT FA (n= 19,12), WT PM (n=16,12), Nrf2$^{-/-}$ FA (n=14,12), and Nrf2$^{-/-}$ PM (n=17,12). Error bars represent SEM. Data analyzed using two-way ANOVA with Tukey's multiple comparison test.

The T regulatory panel in both strains shows that PM exposed groups have increased Treg levels compared to their FA strain counterparts (Fig. 10E), though there is no significance between

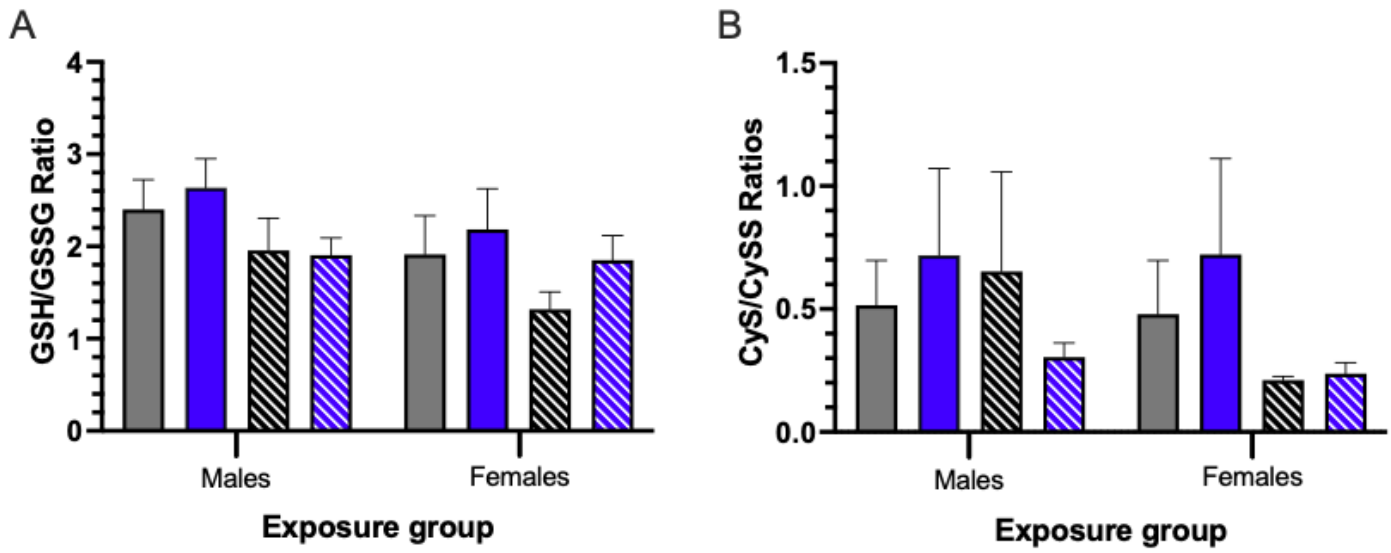

Figure 12: Oxidative stress biomarkers depicting thiol ratios of glutathione (GSH) to glutathione disulfide (GSSG) (A) and cysteine (CyS) to cystine (CySS) (B) in neonatal livers at PND5, representing systemic oxidative stress. Higher ratios indicate an increased capacity for reduction of reactive oxygen species. Though not significantly different, $Nrf2^{-/-}$ neonates generally have lower thiol ratios, and thus lower redox capacity, than their WT counterparts, and PM-exposed neonates generally have increased thiol ratios versus their FA-exposed counterparts. Offspring sample sizes, listed as (n=Male, Female), from 3 litters, include WT FA (n=5,5), WT PM (n=5,5), $Nrf2^{-/-}$ FA (n=5,5), and $Nrf2^{-/-}$ PM (n=5,5). Error bars represent SEM. Data analyzed using two-way ANOVA with Tukey's multiple comparison test.

---

any of the groups for combined averages (P=0.610), males (P=0.972), or females (P=0.324). The combined data shows the $Nrf2^{-/-}$ PM average of 35.00±8.34% to be higher than the $Nrf2^{-/-}$ FA

average of 25.32±4.21%, and the WT PM average of 32.90±9.90% to be higher than the WT FA average of 20.71±8.25%.

	Overall				Male				Female			
	WT FA	WT PM	Nrf2 FA	Nrf2 PM	WT FA	WT PM	Nrf2 FA	Nrf2 PM	WT FA	WT PM	Nrf2 FA	Nrf2 PM
GSH	72.87±12.23	72.87±9.33	43.33±9.91	47.91±4.32	91.95±19.84	82.84±8.96	56.28±18.25	47.14±5.57	53.79±9.88	62.89±16.17	30.38±4.95	48.68±7.26
GSSG	33.08±2.95	29.41±1.89	24.65±3.18	25.50±0.84	37.53±4.70	31.70±1.82	26.46±6.44	24.75±1.68	28.64±2.14	27.11±3.19	22.84±1.58	26.25±0.27
CyS	1.12±0.25	1.82±0.63	0.96±0.40	0.70±0.08	1.42±0.40	2.01±0.99	1.43±0.78	0.64±0.12	0.82±0.29	1.64±0.90	0.50±0.07	0.76±0.12
CySS	2.48±0.35	2.51±0.19	2.41±0.23	2.76±0.26	2.98±0.58	2.83±0.32	2.50±0.43	2.13±0.14	1.97±0.27	2.19±0.11	2.32±0.23	3.39±0.31

Table 2: Oxidative stress biomarkers depicting cysteine (CyS), cystine (CySS), glutathione (GSH), and glutathione disulfide (GSSG) values in neonatal livers at PND5, represented as mean ± SEM.

4.3.3 UFP Induces Increased Oxidative Stress Responses while Nrf2$^{-/-}$ Suppresses Overall Response

qRT-PCR was performed in PND5 lungs to evaluate oxidative stress-related gene expression (Fig. 11). We expected that Nrf2$^{-/-}$ neonates would have less ability to respond to oxidative stress and that PM exposure would enhance the response. The females responded in a characteristic manner, with the WT neonates exhibiting greater expression overall (vs. Nrf2$^{-/-}$) and PM eliciting more expression in both strains. *AhR* and *NQO1* had the highest fold change difference in the PM groups of both strains, in both males and females, but with no significance (*AhR:* Males, P=0.370, Females, P=0.410) (*NQO1*: Males, P=0.354, Females, P=0.379).

The males, however, demonstrated different responses, aside from the similar *AhR* and *NQO1* data. Within the WT neonates, the remaining four oxidative stress related genes of the PM group exhibited either similar expression or mildly decreased expression to the FA group. The Nrf2$^{-/-}$ FA

males showed an unexpected trend of having similar or increased fold change compared to the WT FA group. The Nrf2$^{-/-}$ PM males had appropriately low expression, similar to the Nrf2$^{-/-}$ PM females. This may be a sex-specific, strain-specific response in which our Nrf2$^{-/-}$ males have alternate pathways, such as *AhR*, used to activate an oxidative stress response. High variation may be due to the pooling of samples within litters.

4.3.4 Nrf2$^{-/-}$ Neonates Mildly Suppress Thiol Redox Capacity

We extrapolated the neonatal systemic oxidative stress state by measuring thiol redox capacity in PND5 livers by HPLC analysis. The ratios of glutathione (GSH) to glutathione disulfide (GSSG), and cysteine (CyS) to cystine (CySS) indicate the neonates' ability to reduce reactive oxygen species (ROS) by donating an electron from either GSH or CyS. The GSH/GSSG ratio showed both males and females had slightly decreased ratios in the Nrf2$^{-/-}$ strain when compared to their WT counterparts, but were not significantly different (Male, P=0.637; Female, P=0.745) (Table 1, Fig. 12). The CyS/CySS ratios were similar in females (P=0.638). Except for the Nrf2$^{-/-}$ males, all other FA/PM pairs showed a mild increase in ratios in the PM group, though not significantly different. Significance level may have been hampered by small sample sizes, and additional studies may be warranted.

4.4. Discussion

PM exposure confers significant detriments to human health, particularly during susceptible life stages, such as fetal development, with consequent negative health effects during infancy and childhood. The report on the State of Global Air 2020, included for the first time the burden of neonatal mortality from $PM_{2.5}$ exposure, largely driven through preterm birth and low infant birth

weight[2]. Moreover, it was estimated that air pollution also contributed to as much as 30% of lower-respiratory infections. Our previous research demonstrated offspring pulmonary immune suppression due to *in utero* UFP exposure with implications for infection risk[21]. The role of the current study was to elucidate the mechanisms by which *in utero* UFP exposure may predispose the neonatal immunophenotype to a more susceptible state, of which oxidative stress often plays a large role. Nrf2 is a key transcription factor that regulates over 1000 other genes and proteins to produce a protective antioxidant effect.[18] By incorporating a Nrf2 knockout mouse model into our established exposure paradigm, we demonstrated that the Nrf2 deficient neonates had an exacerbation of the growth inhibitory parameters following prenatal UFP exposure.

Birth weight can be used as an indicator of health in the neonate, during childhood, and even into adulthood, as low birth weight often accompanies numerous other comorbidities. Uwak et al. performed a meta-analysis demonstrating consistent association of prenatal air pollution exposure and low birth weight in numerous human case-control and cohort studies[7]. Our model demonstrated that the lack of Nrf2 exacerbates the growth inhibitory effects of prenatal PM exposure that was seen in both WT and Nrf2-/-. Previous literature has demonstrated that Nrf2 knockout mice had decreased fetal weights due to decreased placental efficiency[26], but Nezu et al. found no difference in fetal weights when Nrf2 was nullified in their non-eclampsia pregnant mouse model[27]. The role of Nrf2 within gestation is clearly intricate and requires further study, yet our results indicate that not only does Nrf2 deficiency cause low birth weight, but its effects can also be exacerbated by external factors such as UFP exposure.

A baseline pulmonary immunophenotype of the neonates was necessary to determine how infection severity may be enhanced in response to early life exposure. No significant differences in CD8+ or CD4+ cells were observed between any of the groups in combined or sex-separated

data. Adult Nrf2$^{-/-}$ mice also did not demonstrate differences in CD8+ cell expression in Ma et al.'s study.[28] CD4+ subsets in our study had several notable changes though. In particular, the Nrf2$^{-/-}$ PM-exposed neonates surpassed all other groups in increased levels of Th1 and Th2 differentiated CD4+ cells. They presented a phenotype with a prominent Th2-biased immune system, which can potentially predispose neonates to having more severe respiratory inflammation if challenged with viral infections or allergens. Yang et al. demonstrated an association to prenatal indoor $PM_{2.5}$ and tobacco smoke exposure and increased respiratory tract infections in children, potentially modified by maternal Nrf2 status.[29] This suggests that the priming of the immune system during prenatal exposure, plays an important role in the infant respiratory health. Two studies conducted by Perveen et al. indicate a correlation in the levels of protein kinase C isozyme zeta, found in cord blood T cells, and the risk of the neonate developing allergic-type symptoms later in life.[30,31] These cord blood cells may be the first step in elucidating the priming of the neonatal pulmonary T cells.

The balance between autoimmunity and immunosuppression is regulated by Th17 and T regulatory cells, respectively. Abnormal or deficient Nrf2 signaling has been documented as a contributor in some autoimmune diseases, such as asthma or multiple sclerosis.[32] Possible mechanisms of functional Nrf2 protecting against autoimmunity range from suppression of Th1 and Th17 cells to the reduction of oxidative stress that may potentially reduce the production of autoimmune self-antigens.[32] Adult Nrf2 deficient mice frequently develop lupus-like autoimmune diseases.[28] In this study, we saw a mild increase in the Treg cells in the PM-exposed neonates of both genotypes, but with no significant differences. Within the Th17 cells, we saw that the lack of Nrf2 increased the percentage of this subset in neonates; however, this effect was mitigated in the PM- exposed offspring, a finding that was also noted in our previous work by

Rychlik et al. [21] This may suggest the propensity of the Nrf2 knockout mouse towards autoimmune diseases naturally, with a potential mitigation of these effects by the PM by the slightly increased numbers of Tregs.

PM exposure is well documented to generate reactive oxygen species and create a state of oxidative stress in both humans and animal models. We evaluated six oxidative stress-related genes to determine if oxidative stress is a prominent mechanism by which UFPs exert their detrimental influence and which could be exacerbated by the lack of Nrf2. These genes are classically known to be induced, though not exclusively, by Nrf2.[33] The three genes related to glutathione (*Gclc, Gclm, Gpx1*) generally demonstrated lower expression in the Nrf2 deficient neonates, as expected, particularly in the females. *Hmox1* demonstrated similar patterns. Both *NQ01* and *AhR* demonstrated increased levels of expression in PM exposed mice in both genotypes, indicating a response to oxidative stress in our model. However, in the Nrf2 FA-exposed males, all oxidative stress related genes had a high level of constitutive expression, with the expression in *AhR*, *NQ01*, and *Gpx1* exceeding those levels of even the WT FA-exposed males. The high expression of *AhR* may account for the increased expression of the other related genes, as this gene can induce many other pathways, including upregulation of Nrf2 in WT mice.[34,35] This finding exhibits a distinct sex specific response of the Nrf2 male neonates as compared to the females, which will be crucial in interpreting future studies using Nrf2 deficient neonates. While significant trends were neither seen within the males nor females, this data shows that our model does induce oxidative stress and indicates lack of Nrf2 plays a role in such adverse health effects such as the reduced weight gain.

By utilizing hepatic tissue, we evaluated the systemic state of oxidative stress in the offspring compared to the pulmonary state. Though not significantly different, the lack of Nrf2 generally

resulted in a lower GSH/GSSG ratio, indicating that more GSH is available in the WT mice for a greater redox potential. Similarly, particularly in the female Nrf2 offspring, a decreased CyS/CySS ratio indicated an increased amount of oxidative stress and lack of response. Given Nfr2's key role as an antioxidant, these results are expected. Interestingly, however, in the Nrf2 FA-exposed males, a higher ratio was seen as compared to the PM exposed counterparts, similar even to the WT males. This mirrors the pulmonary gene expression data for the Nrf2 FA-exposed males and may reflect the alternative pathways utilized by these neonates to actually enhance their response to oxidative stress in the absence of Nrf2, which may be particular to our knockout genotype or to male Nrf2 neonates.

4.5. Conclusion

We demonstrated that the lack of maternal Nrf2 response enhances the growth inhibitory effects induced by gestational PM exposure, skews CD4+ T lymphocyte differentiation toward Th2, and reduces the capacity for oxidative stress responses. This information will be vital to further elucidating the mechanisms behind prenatal PM exposure, particularly how it predisposes children to future respiratory tract infections or conditions such as asthma.

CHAPTER V

SUMMARY OF KEY FINDINGS

Our research focused primarily on building on a robust prenatal UFP murine exposure model that would expose mice in a manner representative of what human mothers may face, with an additional viral challenge to mimic childhood respiratory disease. We hoped to establish a connection between prenatal UFP exposure and negative neonatal respiratory effects, with an initial effort to elucidate some of the possible mechanisms by which UFPs may exert their negative effects on the fetus through the mother.

5.1 Aim 1

In Aim 1, we performed two pilot studies while we refined our murine exposure system to maximize the amount of UFP exposure and examine the neonates at the optimum time for viral load and inflammatory changes. Though we started with a single dose of 100 ug/m^3/6 hours, a rough correlation to the WHO standards for $PM_{2.5}$, we realized that we needed a higher dose to stimulate exaggerated changes, and therefore added a five-fold dose level, HD. We altered the structure of the exposure chamber so that dams were individually housed and could no longer aggregate in corners of the chamber. We determined that 3 dpi was the optimum time to look for peak viral load and that 9 dpi was the optimum time to evaluate for more subacute inflammatory changes. We extended the exposure period to GD18.5, since mice could handle the stress of exposure for another day and rarely gave birth before GD19.5. Lastly, we switched from the BALB/c strain to the C57BL/6 strain, despite the Th1 nature of the latter since they are more sensitive to oxidative stress and thus were more likely to demonstrate changes from prenatal UFP

exposure. All of these changes were incorporated into our exposure model for Aim 2 to increase the neonatal response to UFP and maximize significant findings.

5.2 Aim 2

In Aim 2, we performed a full exposure study, wherein we exposed pregnant C57BL/6 females to UFPs throughout gestation, then infected the neonates with RSV at PND5. We successfully saw RSV pathogenicity in this strain of mouse, with effects compounded by UFP exposure. Histologic inflammation and viral load both had a positive association with increasing amounts of UFP exposure, though not significant. In the LD RSV group, particularly in the females, we saw an unusual thresholding trend, in which the LD RSV group frequently demonstrated an increased response as compared to the FA and HD RSV groups. The LD RSV group had an increased Th2/Th1 ratio, meaning a more Th2-biased immune response, and increased levels of T regulatory cells. The females in this group showed a reduced weight gain and an increased number of leukocytes in the BAL fluid. This thresholding effect was seen in a placental study done in our lab as well. This suggests that there may be an unknown mechanism that is activating between the low and high doses of UFP and provides a level of protection in the HD group not available in the LD group. Overall, we successfully developed a murine model in which prenatal PM exposure did enhance the severity of the RSV disease seen in the neonates.

5.3 Aim 3

In Aim 3, we strove to elucidate some of the mechanisms by which the prenatal UFP exposure may exert its effects on the neonate by examining the role of Nrf2 in protection against prenatal PM. Using a Nrf2 deficient mouse strain on a C57BL/6 background, we exposed this strain and a

wildtype strain to prenatal UFPs but did not challenge with RSV in this aim. We demonstrated that the Nrf2$^{-/-}$ neonates indeed had a reduced ability to respond to the pulmonary oxidative stress induced by the UFP exposure, though UFP exposure in both strains induced higher levels of oxidative stress. The hepatic redox capacity, taken as a representative of the systemic oxidative state, showed that Nrf2$^{-/-}$ neonates also had a reduced capacity to respond overall. Pulmonary flow cytometry demonstrated several distinct alterations in the PM-exposed groups. Nrf2$^{-/-}$ neonates overall had a more Th2 biased immune system. PM-exposed Nrf2$^{-/-}$ neonates showed increased levels of both Th1 and Th2 cells, so while their FA-exposed counterparts had a similar Th1/Th2 ratio, the PM-exposed group had a higher level of inflammation primed by the exposure. T regulatory cells were increased slightly in PM-exposed neonates regardless of strain, similar to a previous finding in our lab. Lastly, the Nrf2$^{-/-}$ FA-exposed neonates showed significantly higher levels of Th17, a cell type involved in autoimmunity, but these levels were suppressed by PM, again similar to previous findings in our lab. Overall, these findings show that UFP exposure does alter pulmonary T cell differentiation, likely leading to a more inflammatory cellular milieu that may explain the higher susceptibility of neonates to respiratory infection in early life. We demonstrated that Nrf2 plays an important role in the neonatal response to oxidative stress in response to prenatal UFP exposure.

5.4 Overall significance

Overall, we have demonstrated that prenatal UFP exposure has a negative effect upon neonatal health, particularly in response to respiratory infections. We have showed that Nrf2 plays a role in the protection of the infant against the oxidative stress and pulmonary T cell changes induced by prenatal UFP exposure. We hope that by demonstrating these findings, we can impress upon the

scientific community of the detrimental effects of UFPs on pregnant mothers, and thereby stimulate investigations into protective and preventative measures that women and children can take to ameliorate these effects.

5.5 Future studies

With the prenatal UFP exposure model developed, the possibilities for future studies are nearly boundless. First, the completion of the full prenatal UFP exposure and neonatal RSV challenge should be performed on the Nrf2 deficient mouse strain to fully understand the role of Nrf2 not only in PM exposure but in RSV challenge as well. Following this study, this model could be used for nearly any type of PM exposure, since the aerosolization is much more representative of natural human exposure. Other variables in this model that can be altered are exposures during various trimesters, concentration of exposure, focus on different organ systems within the mother or fetus, and of course, challenge with numerous different infectious agents, not necessarily viral or respiratory.

With the establishment of Nrf2 as a vital protective factor in prenatal PM exposure, this naturally brings to mind the possibility of increasing Nrf2 as a therapeutic or preventative measure in pregnant women. Triterpenoids, curcumin, and sulforaphane are all naturally derived Nrf2 activators found in common foods. Our lab has begun to look at the possibility of giving sulforaphane either during gestation, to protect against the PM exposure while it occurs, or during lactation, to ameliorate the effects of prenatal exposure during early infancy. This would be a simple addition to our model to give the pregnant or lactating dams sulforaphane in their diets during exposure.

Lastly, a popular field of research currently involves characterizing microbiomes, and it has been found that a "gut-lung axis" exists, wherein the microbiome of the gastrointestinal system and the microbiome of the lung have interplay with systemic mediators and can influence changes upon each other. Therefore, repeating these experiments, but examining the microbiome in these systems both before and after prenatal UFP exposure, both in the mother and the neonates, would be highly interesting and potentially relevant to future therapies targeting negative populations of bacteria in each system.

REFERENCES

(1) WHO Air Quality Guidelines for Particulate Matter, Ozone, Nitrogen Dioxide and Sulfur Dioxide: Global Update 2005, Summary of Risk Assessment. *World Heal. Organ.* **2005**. https://doi.org/10.1007/s12011-019-01864-7.

(2) Schraufnagel, D. E. The Health Effects of Ultrafine Particles. *Experimental and Molecular Medicine*. 2020, pp 311–317. https://doi.org/10.1038/s12276-020-0403-3.

(3) Jedrychowski, W. A.; Perera, F. P.; Spengler, J. D.; Mroz, E.; Stigter, L.; Zbieta Flak, E. ˙; Majewska, R.; Klimaszewska-Rembiasz, M.; Jacek, R. Intrauterine Exposure to Fine Particulate Matter as a Risk Factor for Increased Susceptibility to Acute Broncho-Pulmonary Infections in Early Childhood. *Int. J. Hyg. Environ. Health* **2013**, *216*, 395–401. https://doi.org/10.1016/j.ijheh.2012.12.014.

(4) Morales-Rubio, R. A.; Alvarado-Cruz, I.; Manzano-León, N.; Andrade-Oliva, M. D. L. A.; Uribe-Ramirez, M.; Quintanilla-Vega, B.; Osornio-Vargas, Á.; De Vizcaya-Ruiz, A. In Utero Exposure to Ultrafine Particles Promotes Placental Stress-Induced Programming of Renin-Angiotensin System-Related Elements in the Offspring Results in Altered Blood Pressure in Adult Mice. *Part. Fibre Toxicol.* **2019**, *16* (1), 1–16. https://doi.org/10.1186/s12989-019-0289-1.

(5) Valentino, S. A.; Tarrade, A.; Aioun, J.; Mourier, E.; Richard, C.; Dahirel, M.; Rousseau-Ralliard, D.; Fournier, N.; Aubrière, M. C.; Lallemand, M. S.; Camous, S.; Guinot, M.; Charlier, M.; Aujean, E.; Al Adhami, H.; Fokkens, P. H.; Agier, L.; Boere, J. A.; Cassee, F. R.; Slama, R.; Chavatte-Palmer, P. Maternal Exposure to Diluted Diesel Engine Exhaust Alters Placental Function and Induces Intergenerational Effects in Rabbits. *Part. Fibre Toxicol.* **2016**, *13* (1), 1. https://doi.org/10.1186/s12989-016-0151-7.

(6) Ohlwein, S.; Kappeler, R.; Kutlar Joss, M.; Künzli, N.; Hoffmann, B. Health Effects of Ultrafine Particles: A Systematic Literature Review Update of Epidemiological Evidence. *International Journal of Public Health*. Springer International Publishing May 1, 2019, pp 547–559. https://doi.org/10.1007/s00038-019-01202-7.

(7) Farina, F.; Lonati, E.; Milani, C.; Massimino, L.; Ballarini, E.; Donzelli, E.; Crippa, L.; Marmiroli, P.; Botto, L.; Corsetto, P. A.; Sancini, G.; Bulbarelli, A.; Palestini, P. In Vivo Comparative Study on Acute and Sub-Acute Biological Effects Induced by Ultrafine Particles of Different Anthropogenic Sources in BALB/c Mice. *Int. J. Mol. Sci.* **2019**, *20* (11). https://doi.org/10.3390/ijms20112805.

(8) Chen, C.; Yao, M.; Luo, X.; Zhu, Y.; Liu, Z.; Zhuo, H.; Zhao, B. Outdoor-to-Indoor Transport of Ultrafine Particles: Measurement and Model Development of Infiltration Factor *. **2020**. https://doi.org/10.1016/j.envpol.2020.115402.

(9) Topinka, J.; Rossner, P.; Milcová, A.; Schmuczerová, J.; Pěnčíková, K.; Rossnerová, A.; Ambrož, A.; Štolcpartová, J.; Bendl, J.; Hovorka, J.; Machala, M. Day-to-Day Variability of Toxic Events Induced by Organic Compounds Bound to Size Segregated Atmospheric Aerosol. *Environ. Pollut.* **2015**, *202*, 135–145. https://doi.org/10.1016/j.envpol.2015.03.024.

(10) Li, Z.; Tang, Y.; Song, X.; Lazar, L.; Li, Z.; Zhao, J. Impact of Ambient PM2.5 on Adverse Birth Outcome and Potential Molecular Mechanism. *Ecotoxicol. Environ. Saf.* **2019**, *169* (August 2018), 248–254. https://doi.org/10.1016/j.ecoenv.2018.10.109.

(11) Saenen, N. D.; Bové, H.; Steuwe, C.; Roeffaers, M. B. J.; Provost, E. B.; Lefebvre, W.; Vanpoucke, C.; Ameloot, M.; Nawrot, T. S. Children's Urinary Environmental Carbon Load: A Novel Marker Reflecting Residential Ambient Air Pollution Exposure? *American*

Journal of Respiratory and Critical Care Medicine. 2017, pp 873–881. https://doi.org/10.1164/rccm.201704-0797OC.

(12) Neven, K. Y.; Saenen, N. D.; Tarantini, L.; Janssen, B. G.; Lefebvre, W.; Vanpoucke, C.; Bollati, V.; Nawrot, T. S. Placental Promoter Methylation of DNA Repair Genes and Prenatal Exposure to Particulate Air Pollution: An ENVIRONAGE Cohort Study. *The Lancet Planetary Health*. 2018, pp e174–e183. https://doi.org/10.1016/S2542-5196(18)30049-4.

(13) Bekö, G.; Weschler, C. J.; Wierzbicka, A.; Karottki, D. G.; Toftum, J.; Loft, S.; Clausen, G. Ultrafine Particles: Exposure and Source Apportionment in 56 Danish Homes. *Environ. Sci. Technol.* **2013**, *47* (18), 10240–10248. https://doi.org/10.1021/es402429h.

(14) Rychlik, K. A.; Secrest, J. R.; Lau, C.; Pulczinski, J.; Zamora, M. L.; Leal, J.; Langley, R.; Myatt, L. G.; Raju, M.; C-A Chang, R.; Li, Y.; Golding, M. C.; Rodrigues-Hoffmann, A.; Molina, M. J.; Zhang, R.; Johnson, N. M. In Utero Ultrafine Particulate Matter Exposure Causes Offspring Pulmonary Immunosuppression. https://doi.org/10.1073/pnas.1816103116.

(15) Jaligama, S.; Saravia, J.; You, D.; Yadav, N.; Lee, G. I.; Shrestha, B.; Cormier, S. A. Regulatory T Cells and IL10 Suppress Pulmonary Host Defense during Early-Life Exposure to Radical Containing Combustion Derived Ultrafine Particulate Matter. https://doi.org/10.1186/s12931-016-0487-4.

(16) Colarusso, C.; De Falco, G.; Terlizzi, M.; Roviezzo, F.; Cerqua, I.; Sirignano, M.; Cirino, G.; Aquino, R. P.; Pinto, A.; D'Anna, A.; Sorrentino, R. The Inhibition of Caspase-1-Does Not Revert Particulate Matter (PM)-Induced Lung Immunesuppression in Mice. *Front. Immunol.* **2019**, *10*. https://doi.org/10.3389/fimmu.2019.01329.

(17) Luyten, L. J.; Saenen, N. D.; Janssen, B. G.; Vrijens, K.; Plusquin, M.; Roels, H. A.; Debacq-Chainiaux, F.; Nawrot, T. S. Air Pollution and the Fetal Origin of Disease: A Systematic Review of the Molecular Signatures of Air Pollution Exposure in Human Placenta. *Environmental Research*. 2018. https://doi.org/10.1016/j.envres.2018.03.025.

(18) Barker, D. J. . Fetal Origins of Coronary Heart Disease. *Br. Med. J.* **1995**, *311* (6998), 171–174. https://doi.org/10.1054/ebcm.1999.0268.

(19) Bhargava, Arpit; Shukla, Anushi; Bunkar, Neha; Shandilya, Ruchita; Lodhi, Lalit; Kumari, Roshani; Gupta, Pushpendra Kumar; Rahman, Akhlaqur; Chaudhury, Koael; Tiwari, Rajnarayan; Goryacheva, Irina Yu; Mishra, R. K. Exposure to Ultrafine Particulate Matter Induces NF-KB Mediate Epigenetic Modifications. *Environ. Pollut.* **2019**, *252*, 39–50.

(20) Janssen, B. G.; Byun, H. M.; Gyselaers, W.; Lefebvre, W.; Baccarelli, A. A.; Nawrot, T. S. Placental Mitochondrial Methylation and Exposure to Airborne Particulate Matter in the Early Life Environment: An ENVIRONAGE Birth Cohort Study. *Epigenetics* **2015**, *10* (6), 536–544. https://doi.org/10.1080/15592294.2015.1048412.

(21) Li, Z.; Fu, J.; Li, Z.; Tang, Y.; Hua, Q.; Liu, L.; Zhao, J. Air Pollution and Placental Mitochondrial DNA Copy Number: Mechanistic Insights and Epidemiological Challenges. *Environmental Pollution*. 2019. https://doi.org/10.1016/j.envpol.2019.113266.

(22) Tsamou, M.; Vrijens, K.; Madhloum, N.; Lefebvre, W.; Vanpoucke, C.; Nawrot, T. S. Air Pollution-Induced Placental Epigenetic Alterations in Early Life: A Candidate MiRNA Approach. *Epigenetics*. 2018, pp 135–146. https://doi.org/10.1080/15592294.2016.1155012.

(23) James M., R.; Robert N, T.; Alan, G. Clinical and Biochemical Evidence of Endothelial

Cell Dysfunction in the Pregnancy Syndrome Preeclampsia. *Am. J. Hypertens.* **1991**, *4* (8), 700–708. https://doi.org/10.1093/ajh/4.8.700.

(24) Bearblock, E.; Aiken, C. E.; Burton, G. J. Air Pollution and Pre-Eclampsia; Associations and Potential Mechanisms. *Placenta*. 2021, pp 188–194. https://doi.org/10.1016/j.placenta.2020.12.009.

(25) Assibey-Mensah, V.; Glantz, J. C.; Hopke, P. K.; Jusko, T. A.; Thevenet-Morrison, K.; Chalupa, D.; Rich, D. Q. Wintertime Wood Smoke, Traffic Particle Pollution, and Preeclampsia. *Hypertension*. 2020, pp 851–858. https://doi.org/10.1161/HYPERTENSIONAHA.119.13139.

(26) Nobles, C. J.; Williams, A.; Ouidir, M.; Sherman, S.; Mendola, P. Differential Effect of Ambient Air Pollution Exposure on Risk of Gestational Hypertension and Preeclampsia. *Hypertension*. 2019, pp 384–390. https://doi.org/10.1161/HYPERTENSIONAHA.119.12731.

(27) Wu, M.; Ries, J. J.; Proietti, E.; Vogt, D.; Hahn, S.; Hoesli, I. Development of Late-Onset Preeclampsia in Association with Road Densities as a Proxy for Traffic-Related Air Pollution. *Fetal Diagn. Ther.* **2016**, *39* (1), 21–27. https://doi.org/10.1159/000381802.

(28) Qin, Z.; Hou, H.; Fu, F.; Wu, J.; Han, B.; Yang, W.; Zhang, L.; Cao, J.; Jin, X.; Cheng, S.; Yang, Z.; Zhang, M.; Lan, X.; Yao, T.; Dong, Q.; Wu, S.; Zhang, J.; Xu, Z.; Li, Y.; Chen, Y. Fine Particulate Matter Exposure Induces Cell Cycle Arrest and Inhibits Migration and Invasion of Human Extravillous Trophoblast, as Determined by an ITRAQ-Based Quantitative Proteomics Strategy. *Reprod. Toxicol.* **2017**, *74*, 10–22. https://doi.org/10.1016/j.reprotox.2017.08.014.

(29) van den Hooven, E. H.; Pierik, F. H.; de Kluizenaar, Y.; Hofman, A.; van Ratingen, S. W.;

Zandveld, P. Y. J.; Russcher, H.; Lindemans, J.; Miedema, H. M. E.; Steegers, E. A. P.; Jaddoe, V. W. V. Air Pollution Exposure and Markers of Placental Growth and Function: The Generation R Study. *Environ. Health Perspect.* **2012**, *120* (12), 1753–1759. https://doi.org/10.1289/ehp.1204918.

(30) Zhang, M.; Mueller, N. T.; Wang, H.; Hong, X.; Appel, L. J.; Wang, X. Maternal Exposure to Ambient Particulate Matter ≤2.5 Mm during Pregnancy and the Risk for High Blood Pressure in Childhood. *Hypertension*. 2018, pp 194–201. https://doi.org/10.1161/HYPERTENSIONAHA.117.10944.

(31) Rosa, M. J.; Hsu, H. H. L.; Just, A. C.; Brennan, K. J.; Bloomquist, T.; Kloog, I.; Pantic, I.; Mercado García, A.; Wilson, A.; Coull, B. A.; Wright, R. O.; Téllez Rojo, M. M.; Baccarelli, A. A.; Wright, R. J. Association between Prenatal Particulate Air Pollution Exposure and Telomere Length in Cord Blood: Effect Modification by Fetal Sex. *Environmental Research*. 2019, pp 495–501. https://doi.org/10.1016/j.envres.2019.03.003.

(32) Saenen, N. D.; Martens, D. S.; Neven, K. Y.; Alfano, R.; Bové, H.; Janssen, B. G.; Roels, H. A.; Plusquin, M.; Vrijens, K.; Nawrot, T. S. Air Pollution-Induced Placental Alterations: An Interplay of Oxidative Stress, Epigenetics, and the Aging Phenotype? *Clin. Epigenetics* **2019**, *11* (1), 1–14. https://doi.org/10.1186/s13148-019-0688-z.

(33) Harnung Scholten, R.; Møller, P.; Jovanovic Andersen, Z.; Dehlendorff, C.; Khan, J.; Brandt, J.; Ketzel, M.; Knudsen, L. E.; Mathiesen, L. Telomere Length in Newborns Is Associated with Exposure to Low Levels of Air Pollution during Pregnancy. *Environ. Int.* **2021**, *146* (October 2020). https://doi.org/10.1016/j.envint.2020.106202.

(34) Wu, J.; Zhong, T.; Zhu, Y.; Ge, D.; Lin, X.; Li, Q. Effects of Particulate Matter (PM) on Childhood Asthma Exacerbation and Control in Xiamen, China.

https://doi.org/10.1186/s12887-019-1530-7.

(35) Glinianaia, Svetlana V.; Rankin, Judith; Bell, Ruth; Pless-Mulloli, T. D. H.; Public. Does Particulate Air Pollution Contribute to Infant Death? A Systematic Review. *Environ. Health Perspect.* **2004**, *112* (14), 1365–1370. https://doi.org/10.1289/ehp.6857.

(36) Defranco, E.; Hall, E.; Hossain, M.; Chen, A.; Haynes, E. N.; Jones, D.; Ren, S.; Lu, L.; Muglia, L. Air Pollution and Stillbirth Risk: Exposure to Airborne Particulate Matter during Pregnancy Is Associated with Fetal Death. **2015**. https://doi.org/10.1371/journal.pone.0120594.

(37) Percy, Z.; Defranco, E.; Xu, F.; Hall, E. S.; Haynes, E. N.; Jones, D.; Muglia, L. J.; Chen, A. Trimester Specific PM 2.5 Exposure and Fetal Growth in Ohio, HHS Public Access. *Env. Res* **2019**, *171*, 111–118. https://doi.org/10.1016/j.envres.2019.01.031.

(38) Zhu, Xiaoxia; Liu, Ying; Chen, Yanyan; Yao, Cijiang; Che, Zhen; Cao, J. Maternal Exposure to Fine Particulate Matter (PM2.5) and Pregnancy Outcomes: A Meta-Analysis. *Environ. Sci. Pollut. Res.* **2015**, *22*, 3383–3396.

(39) Stieb, D. M.; Chen, L.; Eshoul, M.; Judek, S. Ambient Air Pollution, Birth Weight and Preterm Birth: A Systematic Review and Meta-Analysis. *Environ. Res.* **2012**, *117*, 100–111. https://doi.org/10.1016/j.envres.2012.05.007.

(40) Chun, H. K.; Leung, C.; Wen, S. W.; McDonald, J.; Shin, H. H. Maternal Exposure to Air Pollution and Risk of Autism in Children: A Systematic Review and Meta-Analysis. *Environ. Pollut.* **2020**, *256*, 113307. https://doi.org/10.1016/j.envpol.2019.113307.

(41) McGuinn, L. A.; Bellinger, D. C.; Colicino, E.; Coull, B. A.; Just, A. C.; Kloog, I.; Osorio-Valencia, E.; Schnaas, L.; Wright, R. J.; Téllez-Rojo, M. M.; Wright, R. O.; Horton, M. K. Prenatal PM2.5 Exposure and Behavioral Development in Children from

Mexico City. *NeuroToxicology*. 2020, pp 109–115. https://doi.org/10.1016/j.neuro.2020.09.036.

(42) Korten, I.; Ramsey, K.; Latzin, P. Air Pollution during Pregnancy and Lung Development in the Child. *Paediatric Respiratory Reviews*. W.B. Saunders Ltd January 1, 2017, pp 38–46. https://doi.org/10.1016/j.prrv.2016.08.008.

(43) W., J.; F.P., P.; U., M.; D., M.-B.; E., M.; E., F.; S., E.; J.D., S.; R., J.; A., S.; A., M. Early Wheezing Phenotypes and Severity of Respiratory Illness in Very Early Childhood. Study on Intrauterine Exposure to Fine Particle Matter. *Environ. Int.* **2009**, *35* (6), 877–884.

(44) Hüls, A.; Vanker, A.; Gray, D.; Koen, N.; MacIsaac, J. L.; Lin, D. T. S.; Ramadori, K. E.; Sly, P. D.; Stein, D. J.; Kobor, M. S.; Zar, H. J. Genetic Susceptibility to Asthma Increases the Vulnerability to Indoor Air Pollution. *European Respiratory Journal*. 2020. https://doi.org/10.1183/13993003.01831-2019.

(45) Soh, S. E.; Goh, A.; Teoh, O. H.; Godfrey, K. M.; Gluckman, P. D.; Shek, L. P. C.; Chong, Y. S. Pregnancy Trimester-Specific Exposure to Ambient Air Pollution and Child Respiratory Health Outcomes in the First 2 Years of Life: Effect Modification by Maternal Pre-Pregnancy BMI. *Int. J. Environ. Res. Public Health* **2018**, *15* (5). https://doi.org/10.3390/ijerph15050996.

(46) Lu, C.; Peng, W.; Kuang, J.; Wu, M.; Wu, H.; Murithi, R. G.; Johnson, M. B.; Zheng, X. Preconceptional and Prenatal Exposure to Air Pollution Increases Incidence of Childhood Pneumonia: A Hypothesis of the (Pre-)Fetal Origin of Childhood Pneumonia. *Ecotoxicology and Environmental Safety*. 2021. https://doi.org/10.1016/j.ecoenv.2020.111860.

(47) MacIntyre, E. A.; Gehring, U.; Mölter, A.; Fuertes, E.; Klümper, C.; Krämer, U.; Quass,

U.; Hoffmann, B.; Gascon, M.; Brunekreef, B.; Koppelman, G. H.; Beelen, R.; Hoek, G.; Birk, M.; de Jongste, J. C.; Smit, H. A.; Cyrys, J.; Gruzieva, O.; Korek, M.; Bergström, A.; Agius, R. M.; de Vocht, F.; Simpson, A.; Porta, D.; Forastiere, F.; Badaloni, C.; Cesaroni, G.; Esplugues, A.; Fernández-Somoano, A.; Lerxundi, A.; Sunyer, J.; Cirach, M.; Nieuwenhuijsen, M. J.; Pershagen, G.; Heinrich, J. Air Pollution and Respiratory Infections during Early Childhood: An Analysis of 10 European Birth Cohorts within the ESCAPE Project. *Environ. Health Perspect.* **2014**, *122* (1), 107–113. https://doi.org/10.1289/ehp.1306755.

(48) Baiz, N.; Slama, R.; Béné, M.; Charles, M.; Kolopp-Sarda, M.; Magnan, A.; Thiebaugeorges, O.; Faure, G.; Annesi-Maesano, I. Maternal Exposure to Air Pollution before and during Pregnancy Can Induce Changes in Newborn's Cord Blood Lymphocytes Involved in Asthma and Allergies. *Allergy Eur. J. Allergy Clin. Immunol.* **2011**, *66*, 707.

(49) Herr, Caroline EW; Dostal, Miroslav; Ghosh, Rakesh; Ashwood, Paul; Lipsett, Michael; Pinkerton, Kent E; Sram, Radim; Hertz-Picciotto, I. Air Pollution Exposure during Critical Time Periods in Gestation and Alterations in Cord Blood Lymphocyte Distribution: A Cohort of Livebirths. *Environ. Heal.* **2010**, *9*.

(50) Fedulov, A. V; Leme, A.; Yang, Z.; Dahl, M.; Lim, R.; Mariani, T. J.; Kobzik, L. Pulmonary Exposure to Particles during Pregnancy Causes Increased Neonatal Asthma Susceptibility. https://doi.org/10.1165/rcmb.2007-0124OC.

(51) Reiprich, M.; Rudzok, S.; Sch??tze, N.; Simon, J. C.; Lehmann, I.; Trump, S.; Polte, T. Inhibition of Endotoxin-Induced Perinatal Asthma Protection by Pollutants in an Experimental Mouse Model. *Allergy Eur. J. Allergy Clin. Immunol.* **2013**, *68* (4), 481–

489. https://doi.org/10.1111/all.12121.

(52) Manners, S.; Alam, R.; Schwartz, D. A.; Gorska, M. M. A Mouse Model Links Asthma Susceptibility to Prenatal Exposure to Diesel Exhaust. **2013**. https://doi.org/10.1016/j.jaci.2013.10.047.

(53) Yoshida, S.; Takano, H.; Nishikawa, M.; Miao, H.; Ichinose, T. *Effects of Fetal Exposure to Urban Particulate Matter on the Immune System of Male Mouse Offspring*; 1238; Vol. 35.

(54) Paul, E.; Franco-Montoya, M. L.; Paineau, E.; Angeletti, B.; Vibhushan, S.; Ridoux, A.; Tiendrebeogo, A.; Salome, M.; Hesse, B.; Vantelon, D.; Rose, J.; Canouï-Poitrine, F.; Boczkowski, J.; Lanone, S.; Delacourt, C.; Pairon, J. C. Pulmonary Exposure to Metallic Nanomaterials during Pregnancy Irreversibly Impairs Lung Development of the Offspring. *Nanotoxicology* **2017**, *11* (4), 484–495. https://doi.org/10.1080/17435390.2017.1311381.

(55) Tang, W.; Huang, S.; Du, L.; Sun, W.; Yu, Z.; Zhou, Y.; Chen, J.; Li, X.; Li, X.; Yu, B.; Chen, D. Expression of HMGB1 in Maternal Exposure to Fine Particulate Air Pollution Induces Lung Injury in Rat Offspring Assessed with Micro-CT. *Chem. Biol. Interact.* **2018**, *280*, 64–69. https://doi.org/10.1016/j.cbi.2017.12.016.

(56) Tang, W.; Du, L.; Sun, W.; Yu, Z.; He, F.; Chen, J.; Li, X.; Li, X.; Yu, L.; Chen, D. Maternal Exposure to Fine Particulate Air Pollution Induces Epithelial-to-Mesenchymal Transition Resulting in Postnatal Pulmonary Dysfunction Mediated by Transforming Growth Factor-β/Smad3 Signaling. *Toxicol. Lett.* **2017**, *267*, 11–20. https://doi.org/10.1016/j.toxlet.2016.12.016.

(57) Hamada, K.; Suzaki, Y.; Leme, A.; Ito, T.; Miyamoto, K.; Kobzik, L.; Kimura, H. Exposure of Pregnant Mice to an Air Pollutant Aerosol Increases Asthma Susceptibility in

Offspring. *J. Toxicol. Environ. Heal. Part A* **2007**, *70* (8), 688–695. https://doi.org/10.1080/15287390600974692.

(58) Mauad, T.; Rodriguez, D. H.; Rivero, F.; Carvalho De Oliveira, R.; Julia De Faria, A.; Lichtenfels, C.; Guimarães, E. T.; Afonso De Andre, P.; Kasahara, D. I.; Maria De Siqueira Bueno, H.; Hilário, P.; Saldiva, N. Chronic Exposure to Ambient Levels of Urban Particles Affects Mouse Lung Development. https://doi.org/10.1164/rccm.200803-436OC.

(59) Kulas, J. A.; Hettwer, J. V.; Sohrabi, M.; Melvin, J. E.; Manocha, G. D.; Puig, K. L.; Gorr, M. W.; Tanwar, V.; McDonald, M. P.; Wold, L. E.; Combs, C. K. In Utero Exposure to Fine Particulate Matter Results in an Altered Neuroimmune Phenotype in Adult Mice. *Environ. Pollut.* **2018**, *241*, 279–288. https://doi.org/10.1016/j.envpol.2018.05.047.

(60) Cory-Slechta, D. A.; Allen, J. L.; Conrad, K.; Marvin, E.; Sobolewski, M. Developmental Exposure to Low Level Ambient Ultrafine Particle Air Pollution and Cognitive Dysfunction. *NeuroToxicology*. 2018, pp 217–231. https://doi.org/10.1016/j.neuro.2017.12.003.

(61) Corson, L.; Zhu, H.; Quan, C.; Grunig, G.; Ballaney, M.; Jin, X.; Perera, F. P.; Factor, P. H.; Chen, L. C.; Miller, R. L. Prenatal Allergen and Diesel Exhaust Exposure and Their Effects on Allergy in Adult Offspring Mice. *Allergy, Asthma Clin. Immunol.* **2010**, *6* (1), 1–11. https://doi.org/10.1186/1710-1492-6-7.

(62) Sharkhuu, T.; Doerfler, D. L.; Krantz, Q. T.; Luebke, R. W.; Linak, W. P.; Gilmour, M. I. Effects of Prenatal Diesel Exhaust Inhalation on Pulmonary Inflammation and Development of Specific Immune Responses. *Toxicol. Lett.* **2010**, *196* (1), 12–20. https://doi.org/10.1016/j.toxlet.2010.03.017.

(63) Gutierrez-Vasquez, Cristina; Quintana, F. J. . Regulation of the Immune Response by the Aryl Hydrocarbon Receptor. *Immunity* **2018**, *48* (1), 19–33. https://doi.org/10.1016/j.immuni.2017.12.012.Regulation.

(64) Ege, M. J.; Bieli, C.; Frei, R.; van Strien, R. T.; Riedler, J.; Üblagger, E.; Schram-Bijkerk, D.; Brunekreef, B.; van Hage, M.; Scheynius, A.; Pershagen, G.; Benz, M. R.; Lauener, R.; von Mutius, E.; Braun-Fahrländer, C.; the PARSIFAL Study team. Prenatal Farm Exposure Is Related to the Expression of Receptors of the Innate Immunity and to Atopic Sensitization in School-Age Children. *J. Allergy Clin. Immunol.* **2006**, *117* (4), 817–823. https://doi.org/10.1016/j.jaci.2005.12.1307.

(65) Barros, T. De; Lopes, M.; Groth, E. E.; Veras, M.; Furuya, T. K.; Souza, N. De; Costa, X.; Lopes, F. D.; Almeida, F. M. De; Cardoso, W. V; Hilario, P.; Saldiva, N.; Chammas, R.; Mauad, T.; Paulo, U. D. S.; Paulo, S.; Paulo, U. D. S.; Paulo, U. D. S.; Paulo, S. Pre- and Postnatal Exposure of Mice to Concentrated Urban PM2.5 Decreases the Number of Alveoli and Leads to Altered Lung Function at an Early Stage of Life. *Environ. Pollut.* **2019**, *241*, 511–520. https://doi.org/10.1016/j.envpol.2018.05.055.Pre-.

(66) Thevenot, P. T.; Saravia, J.; Jin, N.; Giaimo, J. D.; Chustz, R. E.; Mahne, S.; Kelley, M. A.; Hebert, V. Y.; Dellinger, B.; Dugas, T. R.; Demayo, F. J.; Cormier, S. A. Radical-Containing Ultrafine Particulate Matter Initiates Epithelial-to-Mesenchymal Transitions in Airway Epithelial Cells. https://doi.org/10.1165/rcmb.2012-0052OC.

(67) Saravia, Jordy; You, Dahui; Thevenot, Paul; Lee, Greg I.; Shrestha, Bishwas; Lomnicki, Slawo; Cormier, S. A. . Early-Life Exposure to Combustion-Derived Particulate Matter Causes Pulmonary Immunosuppression. *Mucosal Immunol.* **2014**, *7* (3), 694–704. https://doi.org/10.1038/mi.2013.88.Early-life.

(68) Lee, G. I.; Saravia, J.; You, D.; Shrestha, B.; Jaligama, S.; Hebert, V. Y.; Dugas, T. R.; Cormier, S. A. *Exposure to Combustion Generated Environmentally Persistent Free Radicals Enhances Severity of Influenza Virus Infection*; 2014. https://doi.org/10.1186/s12989-014-0057-1.

(69) El-Sayed, Y. S.; Shimizu, R.; Onoda, A.; Takeda, K.; Umezawa, M. Carbon Black Nanoparticle Exposure during Middle and Late Fetal Development Induces Immune Activation in Male Offspring Mice. *Toxicology* **2015**, *327*, 53–61. https://doi.org/10.1016/j.tox.2014.11.005.

(70) Wang, Pingli; You, Dahui; Saravia, Jordy; Shen, Huahao; Cormier, S. A. Maternal Exposure to Combustion Generated PM Inhibits Pulmonary Th1 Maturation and Concomitantly Enhances Postnatal Asthma Development in Offspring. *Part. Fibre Toxicol.* **2013**, *10*, 29.

(71) Hall, Caroline Breese; Weinberg, Geoffrey A; Iwane, Marika K; Blumkin, Aaron K; Edwards, Kathryn M; Staat, Mary A; Auinger, Peggy; Griffin, Marie R; Poehling, Katherine A; Erdman, Dean; Grijalva, Calos G; Zhu, Yuwei; Szilagyi, P. *The Burden of Respiratory Syncytial Virus Infection in Young Children Caroline*; 2009.

(72) Jorquera, P. A.; Anderson, L.; Tripp, R. A. Human Respiratory Syncytial Virus: An Introduction; Humana Press, New York, NY, 2016; pp 1–12. https://doi.org/10.1007/978-1-4939-3687-8_1.

(73) Borchers, A. T.; Chang, C.; Gershwin, M. E.; Gershwin, L. J. Respiratory Syncytial Virus - A Comprehensive Review. *Clin. Rev. Allergy Immunol.* **2013**, *45* (3), 331–379. https://doi.org/10.1007/s12016-013-8368-9.

(74) Bohmwald, K.; Espinoza, J. A.; Rey-Jurado, E.; Gómez, R. S.; González, P. A.; Bueno, S.

M.; Riedel, C. A.; Kalergis, A. M.; Singh, S. K. Human Respiratory Syncytial Virus: Infection and Pathology. **2016**. https://doi.org/10.1055/s-0036-1584799.

(75) Cormier, S. A.; You, D.; Honnegowda, S. The Use of a Neonatal Mouse Model to Study Respiratory Syncytial Virus Infections. https://doi.org/10.1586/eri.10.125.

(76) Collins, P. L.; Graham, B. S. Viral and Host Factors in Human Respiratory Syncytial Virus Pathogenesis. *J. Virol.* **2008**. https://doi.org/10.1128/JVI.01625-07.

(77) Muenchhoff, M.; Goulder, P. J. R. Sex Differences in Pediatric Infectious Diseases. *J. Infect. Dis.* **2014**, *209* (SUPPL. 3), S120. https://doi.org/10.1093/infdis/jiu232.

(78) Singh, A. K.; Jain, B.; Verma, A. K.; Kumar, A.; Dangi, T.; Dwivedi, M.; Singh, K. P.; Jain, A. Hospital Outbreak of Human Respiratory Syncytial Virus (HRSV) Illness in Immunocompromised Hospitalized Children during Summer. *Clin. Respir. J.* **2015**, *9* (2), 180–184. https://doi.org/10.1111/crj.12121.

(79) Kensler, T. W.; Wakabayashi, N. Nrf2: Friend or Foe for Chemoprevention? *Carcinogenesis* **2010**, *31* (1), 90–99. https://doi.org/10.1093/carcin/bgp231.

(80) Silva-Islas, C. A.; Maldonado, P. D. Canonical and Non-Canonical Mechanisms of Nrf2 Activation. *Pharmacological Research*. Academic Press August 1, 2018, pp 92–99. https://doi.org/10.1016/j.phrs.2018.06.013.

(81) Shen, Y.; Liu, X.; Shi, J.; Wu, X. Involvement of Nrf2 in Myocardial Ischemia and Reperfusion Injury. *Int. J. Biol. Macromol.* **2019**, *125*, 496–502. https://doi.org/10.1016/j.ijbiomac.2018.11.190.

(82) Pozo, D.; Conte, C.; De, V. P.; Cruz, L.; Song, X.; Long, D. Nrf2 and Ferroptosis: A New Research Direction for Neurodegenerative Diseases. **2020**. https://doi.org/10.3389/fnins.2020.00267.

(83) Kitamura, H.; Motohashi, H. NRF2 Addiction in Cancer Cells. *Cancer Sci.* **2018**, *109* (4), 900–911. https://doi.org/10.1111/cas.13537.

(84) Rangasamy, Tirumalai; Guo, Jia; Mitzner, Wayne A.; Roman, Jessica; Singh, Anju; Fryer, Allison D.; Yamamoto, Masayuki; Kensler, Thomas W.; Tuder, Rubin M.; Georas, Steve N.; Biswal, S. Disruption of Nrf2 Enhances Susceptibility to Severe Airway Inflammation and Asthma in Mice. *Journal of Experimental Medicine*. 2005.

(85) Hua, C.-C.; Chang, L.-C.; Tseng, J.-C.; Chu, C.-M.; Liu, Y.-C.; Shieh, W.-B. Functional Haplotypes in the Promoter Region of Transcription Factor Nrf2 in Chronic Obstructive Pulmonary Disease. *Dis. Markers* **2010**, *28*, 185–193. https://doi.org/10.3233/DMA-2010-0700.

(86) Acosta-Herrera, M.; Pino-Yanes, M.; Blanco, J.; Ballesteros, J. C.; Ambrós, A.; Corrales, A.; Gandía, F.; Subirá, C.; Domínguez, D.; Baluja, A.; Añón, J. M.; Adalia, R.; Pérez-Méndez, L.; Flores, C.; Villar, J.; Fernández, R. L.; Espinosa, E.; Campo, R. del; Fernández, R.; Rodríguez, J. A.; álvarez, J.; González, E.; Hernández, O.; Solano, R.; Pérez-Crespo, J.; Arellano, P.; Zavala, E.; Martínez, J.; Torres, A.; Badia, J.; Alba, F.; Corpas, R.; Muriel, A.; Sagredo, V.; Taboada, F.; Albaiceta, G. M.; Bobillo, F.; Tamayo, L.; Labattut, A. G.; Carriedo, D.; Collado, J.; Diaz, F. J.; Valledor, M.; Antuña, M.; de Frutos, M.; López, M. J.; Cortina, J. J.; Saldaña, T.; Caballero, A.; álvarez, T.; álvarez, B.; Sandoval, J. Common Variants of NFE2L2 Gene Predisposes to Acute Respiratory Distress Syndrome in Patients with Severe Sepsis. *Crit. Care* **2015**, *19* (1), 1–8. https://doi.org/10.1186/s13054-015-0981-y.

(87) Cho, H. Y.; Imani, F.; Miller-DeGraff, L.; Walters, D.; Melendi, G. A.; Yamamoto, M.; Polack, F. P.; Kleeberger, S. R. Antiviral Activity of Nrf2 in a Murine Model of

Respiratory Syncytial Virus Disease. *Am. J. Respir. Crit. Care Med.* **2009**, *179* (2), 138–150. https://doi.org/10.1164/rccm.200804-535OC.

(88) Li, N.; Alam, J.; Venkatesan, M. I.; Eiguren-Fernandez, A.; Schmitz, D.; Di Stefano, E.; Slaughter, N.; Killeen, E.; Wang, X.; Huang, A.; Wang, M.; Miguel, A. H.; Cho, A.; Sioutas, C.; Nel, A. E. Nrf2 Is a Key Transcription Factor That Regulates Antioxidant Defense in Macrophages and Epithelial Cells: Protecting against the Proinflammatory and Oxidizing Effects of Diesel Exhaust Chemicals. *J. Immunol.* **2004**, *173* (5), 3467–3481. https://doi.org/10.4049/jimmunol.173.5.3467.

(89) Mizumura, K.; Maruoka, S.; Shimizu, T.; Gon, Y. Role of Nrf2 in the Pathogenesis of Respiratory Diseases. *Respir. Investig.* **2020**, *58* (1), 28–35. https://doi.org/10.1016/j.resinv.2019.10.003.

(90) Lin, C. Y.; Yao, C. A. Potential Role of NRF2 Activators with Dual Antiviral and Anti-Inflammatory Properties in the Management of Viral Pneumonia. *Infect. Drug Resist.* **2020**, *13*, 1735–1741. https://doi.org/10.2147/IDR.S256773.

(91) Liu, Q.; Gao, Y.; Ci, X. Review Article Role of Nrf2 and Its Activators in Respiratory Diseases. **2019**. https://doi.org/10.1155/2019/7090534.

(92) da Costa e Oliveira, J. R.; Base, L. H.; de Abreu, L. C.; Filho, C. F.; Ferreira, C.; Morawska, L. Ultrafine Particles and Children's Health: Literature Review. *Paediatr. Respir. Rev.* **2019**. https://doi.org/10.1016/j.prrv.2019.06.003.

(93) Uwak, I.; Olson, N.; Fuentes, A.; Moriarty, M.; Pulczinski, J.; Lam, J.; Xu, X.; Taylor, B. D.; Taiwo, S.; Koehler, K.; Foster, M.; Chiu, W. A.; Johnson, N. M. Application of the Navigation Guide Systematic Review Methodology to Evaluate Prenatal Exposure to Particulate Matter Air Pollution and Infant Birth Weight. *Environment International*.

2021. https://doi.org/10.1016/j.envint.2021.106378.

(94) Wu, G.; Brown, J.; Zamora, M. L.; Miller, A.; Satterfield, M. C.; Meininger, C. J.; Steinhauser, C. B.; Johnson, G. A.; Burghardt, R. C.; Bazer, F. W.; Li, Y.; Johnson, N. M.; Molina, M. J.; Zhang, R. Adverse Organogenesis and Predisposed Long-Term Metabolic Syndrome from Prenatal Exposure to Fine Particulate Matter. *Proceedings of the National Academy of Sciences of the United States of America*. 2019, pp 11590–11595. https://doi.org/10.1073/pnas.1902925116.

(95) Behlen, Jonathan C; Lau, Carmen H; Li, Yixin; Dhagat, Prit; Stanley, Jone A; Rodrigues Hoffman, Aline; Golding, Michael C; Zhang, Renyi; Johnson, N. M. Gestational Exposure to Ultrafine Particles Reveals Sex- and Dose-Specific Changes in Offspring Birth Outcomes, Placental Morphology, and Gene Networks. *Toxicol. Sci.* **2021**.

(96) You, D.; Siefker, D. T.; Shrestha, B.; Saravia, J.; Cormier, S. A. Building a Better Neonatal Mouse Model to Understand Infant Respiratory Syncytial Virus Disease. *Respir. Res.* **2012**, *16*. https://doi.org/10.1186/s12931-015-0244-0.

(97) Byrne, A. J.; Weiss, M.; Mathie, S. A.; Walker, S. A.; Eames, H. L.; Saliba, D.; Lloyd, C. M.; Udalova, I. A. A Critical Role for IRF5 in Regulating Allergic Airway Inflammation. *Mucosal Immunol.* **2017**, *10* (3), 716–726. https://doi.org/10.1038/mi.2016.92.

(98) Health Effects Institute. State of Global Air 2019. *Heal. Eff. Institute.* **2019**, 24. https://doi.org/https://www.stateofglobalair.org/sites/default/files/soga_2019_report.pdf.

(99) Johnson, N. M.; Hoffmann, A. R.; Behlen, J. C.; Lau, C.; Pendleton, D.; Harvey, N.; Shore, R.; Li, Y.; Chen, J.; Tian, Y.; Zhang, R. Air Pollution and Children's Health—a Review of Adverse Effects Associated with Prenatal Exposure from Fine to Ultrafine Particulate Matter. *Environ. Health Prev. Med.* **2021**, *26* (1), 1–29.

https://doi.org/10.1186/s12199-021-00995-5.

(100) L.A., D.; M., K.; W., D. F.; J.A., M.; P.E., T.; M.J., S. Air Pollution and Acute Respiratory Infections among Children 0-4 Years of Age: An 18-Year Time-Series Study. *Am. J. Epidemiol.* **2014**, *180* (10), 968–977.

(101) Zhang, R.; Wang, G.; Guo, S.; Zamora, M. L.; Ying, Q.; Lin, Y.; Wang, W.; Hu, M.; Wang, Y. Formation of Urban Fine Particulate Matter. *Chem. Rev.* **2015**, *115* (10), 3803–3855. https://doi.org/10.1021/acs.chemrev.5b00067.

(102) Zhang, R.; Khalizov, A.; Wang, L.; Hu, M.; Xu, W. Nucleation and Growth of Nanoparticles in the Atmosphere. *Chem. Rev.* **2012**, *112* (3), 1957–2011. https://doi.org/10.1021/cr2001756.

(103) Guo, S.; Hu, M.; Zamora, M. L.; Peng, J.; Shang, D.; Zheng, J.; Du, Z.; Wu, Z.; Shao, M.; Zeng, L.; Molina, M. J.; Zhang, R. Elucidating Severe Urban Haze Formation in China. *Proc. Natl. Acad. Sci. U. S. A.* **2014**, *111* (49), 17373–17378. https://doi.org/10.1073/pnas.1419604111.

(104) Guo, S.; Hu, M.; Peng, J.; Wu, Z.; Zamora, M. L.; Shang, D.; Du, Z.; Zheng, J.; Fang, X.; Tang, R.; Wu, Y.; Zeng, L.; Shuai, S.; Zhang, W.; Wang, Y.; Ji, Y.; Li, Y.; Zhang, A. L.; Wang, W.; Zhang, F.; Zhao, J.; Gong, X.; Wang, C.; Molina, M. J.; Zhang, R. Remarkable Nucleation and Growth of Ultrafine Particles from Vehicular Exhaust. *Proceedings of the National Academy of Sciences of the United States of America*. 2020, pp 3427–3432. https://doi.org/10.1073/pnas.1916366117.

(105) Bové, H.; Bongaerts, E.; Slenders, E.; Bijnens, E. M.; Saenen, N. D.; Gyselaers, W.; Van Eyken, P.; Plusquin, M.; Roeffaers, M. B. J.; Ameloot, M.; Nawrot, T. S. Ambient Black Carbon Particles Reach the Fetal Side of Human Placenta. *Nature Communications*. 2019.

https://doi.org/10.1038/s41467-019-11654-3.

(106) Veras, M. M.; Damaceno-Rodrigues, N. R.; Caldini, E. G.; Maciel Ribeiro, A. A. C.; Mayhew, T. M.; Saldiva, P. H. N.; Dolhnikoff, M. Particulate Urban Air Pollution Affects the Functional Morphology of Mouse Placenta. *Biol. Reprod.* **2008**, *79* (3), 578–584. https://doi.org/10.1095/biolreprod.108.069591.

(107) Russell, C. J.; Hurwitz, J. L. Sendai Virus as a Backbone for Vaccines against RSV and Other Human Paramyxoviruses. *Expert Review of Vaccines*. 2016, pp 189–200. https://doi.org/10.1586/14760584.2016.1114418.

(108) Fang, J.; Song, X.; Xu, H.; Wu, R.; Song, J.; Xie, Y.; Xu, X.; Zeng, Y.; Wang, T.; Zhu, Y.; Yuan, N.; Jia, J.; Xu, B.; Huang, W. Associations of Ultrafine and Fine Particles with Childhood Emergency Room Visits for Respiratory Diseases in a Megacity. *Thorax* **2021**, 1–7. https://doi.org/10.1136/thoraxjnl-2021-217017.

(109) Bohmwald, K.; Espinoza, J. A.; Rey-Jurado, E.; Gómez, R. S.; González, P. A.; Bueno, S. M.; Riedel, C. A.; Kalergis, A. M. Human Respiratory Syncytial Virus: Infection and Pathology. https://doi.org/10.1055/s-0036-1584799.

(110) Gitiban, N.; Jurcisek, J. A.; Harris, R. H.; Mertz, S. E.; Durbin, R. K.; Bakaletz, L. O.; Durbin, J. E. Chinchilla and Murine Models of Upper Respiratory Tract Infections with Respiratory Syncytial Virus. *J. Virol.* **2005**, *79* (10), 6035–6042. https://doi.org/10.1128/JVI.79.10.6035-6042.2005.

(111) Becker, Y. Respiratory Syncytial Virus (RSV) Evades the Human Adaptive Immune System by Skewing the Th1/Th2 Cytokine Balance toward Increased Levels of Th2 Cytokines and IgE, Markers of Allergy-a Review. *Virus Genes* **2006**, *33*, 235–252. https://doi.org/10.1007/s11262-006-0064-x.

(112) Kabe, Yasuaki; Ando, Kozue; Hirao, Stoshi; Yoshida, Makoto; Handa, H. Redox Regulation of NF-KB Activation: Distinct Redox Regulation between the Cytoplasm and the Nucleus. *Antioxidants Redox Signal.* **2005**, *7* (3–4). https://doi.org/10.1111/j.1475-4959.2010.00371.x.

(113) High, M.; Cho, H. Y.; Marzec, J.; Wiltshire, T.; Verhein, K. C.; Caballero, M. T.; Acosta, P. L.; Ciencewicki, J.; McCaw, Z. R.; Kobzik, L.; Miller-DeGraff, L.; Gladwell, W.; Peden, D. B.; Serra, M. E.; Shi, M.; Weinberg, C.; Suzuki, O.; Wang, X.; Bell, D. A.; Polack, F. P.; Kleeberger, S. R. Determinants of Host Susceptibility to Murine Respiratory Syncytial Virus (RSV) Disease Identify a Role for the Innate Immunity Scavenger Receptor MARCO Gene in Human Infants. *EBioMedicine*. 2016, pp 73–84. https://doi.org/10.1016/j.ebiom.2016.08.011.

(114) Zhang, R.; Li, Y.; Zhang, A. L.; Wang, Y.; Molina, M. J. Identifying Airborne Transmission as the Dominant Route for the Spread of COVID-19. *Proceedings of the National Academy of Sciences of the United States of America*. 2020, pp 14857–14863. https://doi.org/10.1073/pnas.2009637117.

(115) WHO. *WHO's Global Air-Quality Guidelines*; 2021.

(116) Bernstein, J. A.; Alexis, N.; Barnes, C.; Bernstein, I. L.; Bernstein, J. A.; Nel, A.; Peden, D.; Diaz-Sanchez, D.; Tarlo, S. M.; Williams, P. B. Health Effects of Air Pollution. *J. Allergy Clin. Immunol.* **2004**, *114* (5), 1116–1123. https://doi.org/10.1016/j.jaci.2004.08.030.

(117) Lavigne, E.; Donelle, J.; Hatzopoulou, M.; Van Ryswyk, K.; Van Donkelaar, A.; Martin, R. V.; Chen, H.; Stieb, D. M.; Gasparrini, A.; Crighton, E.; Yasseen, A. S.; Burnett, R. T.; Walker, M.; Weichenthal, S. Spatiotemporal Variations in Ambient Ultrafine Particles and

the Incidence of Childhood Asthma. *American Journal of Respiratory and Critical Care Medicine*. 2019, pp 1487–1495. https://doi.org/10.1164/rccm.201810-1976OC.

(118) Wright, R. J.; Coull, B. A. Small but Mighty: Prenatal Ultrafine Particle Exposure Linked to Childhood Asthma Incidence. *American Journal of Respiratory and Critical Care Medicine*. 2019, pp 1448–1450. https://doi.org/10.1164/rccm.201903-0506ED.

(119) Park, S. H.; Jang, J. H.; Chen, C. Y.; Na, H. K.; Surh, Y. J. A Formulated Red Ginseng Extract Rescues PC12 Cells from PCB-Induced Oxidative Cell Death through Nrf2-Mediated Upregulation of Heme Oxygenase-1 and Glutamate Cysteine Ligase. *Toxicology* **2010**, *278* (1), 131–139. https://doi.org/10.1016/j.tox.2010.04.003.

(120) Y.-J., L.; T., K.; A., A. Nrf2 Is a Protective Factor against Oxidative Stresses Induced by Diesel Exhaust Particle in Allergic Asthma. *Oxid. Med. Cell. Longev.* **2013**, *2013*.

(121) Jones, D. P.; Liang, Y. Measuring the Poise of Thiol/Disulfide Couples in Vivo. *Free Radic. Biol. Med.* **2009**, *47* (10), 1329–1338. https://doi.org/10.1016/j.freeradbiomed.2009.08.021.

(122) Castañeda, A. R.; Bein, K. J.; Smiley-Jewell, S.; Pinkerton, K. E. Fine Particulate Matter (PM 2.5) Enhances Allergic Sensitization in BALB/c Mice. https://doi.org/10.1080/15287394.2016.1222920.

(123) Kweider, N.; Huppertz, B.; Rath, W.; Lambertz, J.; Caspers, R.; ElMoursi, M.; Pecks, U.; Kadyrov, M.; Fragoulis, A.; Pufe, T.; Wruck, C. J. The Effects of Nrf2 Deletion on Placental Morphology and Exchange Capacity in the Mouse. *J. Matern. Neonatal Med.* **2017**, *30* (17), 2068–2073. https://doi.org/10.1080/14767058.2016.1236251.

(124) Nezu, M.; Souma, T.; Yu, L.; Sekine, H.; Takahashi, N.; Zu-Sern Wei, A.; Ito, S.; Fukamizu, A.; Zsengeller, Z. K.; Nakamura, T.; Hozawa, A.; Ananth Karumanchi, S.;

Suzuki, N.; Yamamoto, M. Nrf2 Inactivation Enhances Placental Angiogenesis in a Preeclampsia Mouse Model and Improves Maternal and Fetal Outcomes. *Sci. Signal.* **2017**, *10* (479), 1–10. https://doi.org/10.1126/scisignal.aam5711.

(125) Ma, Q.; Battelli, L.; Hubbs, A. F. Multiorgan Autoimmune Inflammation, Enhanced Lymphoproliferation, and Impaired Homeostasis of Reactive Oxygen Species in Mice Lacking the Antioxidant-Activated Transcription Factor Nrf2. *American Journal of Pathology*. 2006, pp 1960–1974. https://doi.org/10.2353/ajpath.2006.051113.

(126) S.-I., Y.; B.-J., K.; S.-Y., L.; H.-B., K.; C.M., L.; J., Y.; M.-J., K.; H.-S., Y.; E., L.; Y.-H., J.; H.Y., K.; J.-H., S.; J.-W., K.; D.J., S.; G.C., J.; W.-K., K.; J.Y., S.; S.-Y., L.; H.J., Y.; D.I., S.; S.A., H.; K.-Y., C.; Y.H., S.; K., A.; K.W., K.; E.-J., K.; S.-J., H. Prenatal Particulate Matter/Tobacco Smoke Increases Infants' Respiratory Infections: COCOA Study. *Allergy, Asthma Immunol. Res.* **2015**, *7* (6), 573–582.

(127) Cuadrado, A.; Manda, G.; Hassan, A.; Alcaraz, M. J.; Barbas, C.; Daiber, A.; Ghezzi, P.; León, R.; López, M. G.; Oliva, B.; Pajares, M.; Rojo, A. I.; Robledinos-Antón, N.; Valverde, A. M.; Guney, E.; Schmidt, H. H. H. W. Transcription Factor NRF2 as a Therapeutic Target for Chronic Diseases: A Systems Medicine Approach. *Pharmacological Reviews*. 2018, pp 348–383. https://doi.org/10.1124/pr.117.014753.

(128) Morzadec, C.; Macoch, M.; Sparfel, L.; Kerdine-Römer, S.; Fardel, O.; Vernhet, L. Nrf2 Expression and Activity in Human T Lymphocytes: Stimulation by T Cell Receptor Activation and Priming by Inorganic Arsenic and Tert-Butylhydroquinone. *Free Radic. Biol. Med.* **2014**, *71*, 133–145. https://doi.org/10.1016/j.freeradbiomed.2014.03.006.

(129) Taguchi, Keiko; Kensler, T. W. . Nrf2 in Liver Toxicology. *Arch. Pharm. Res.* **2020**, *43*, 337–349.

(130) Vogel, C. F. A.; Van Winkle, L. S.; Esser, C.; Haarmann-Stemmann, T. The Aryl Hydrocarbon Receptor as a Target of Environmental Stressors – Implications for Pollution Mediated Stress and Inflammatory Responses. *Redox Biology*. 2020. https://doi.org/10.1016/j.redox.2020.101530.

APPENDIX 1

SUPPLEMENTAL FIGURES AND TABLES FROM CHAPTER III

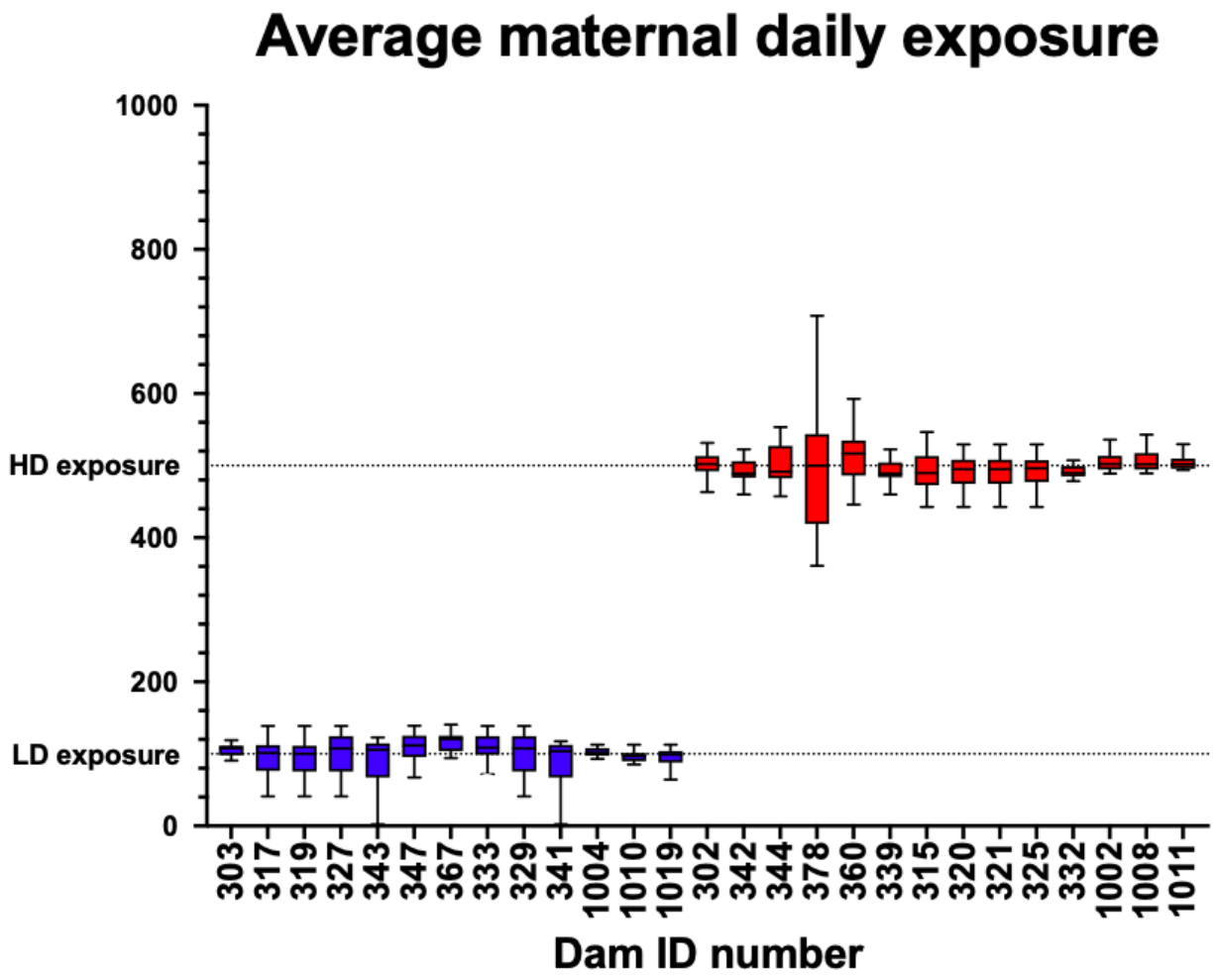

Supplemental Figure 1. Beginning on GD0.5, dams were randomized and placed into exposure chambers where they were exposed to either FA (n=14), LD (n=12), or HD (n=13) 6 hours daily through GD18.5. Average maternal dam exposure to ultrafine particles (UFP) in the low dose (LD) and high dose (HD) groups over the course of gestation averaged 101.70±2.76 $\mu g/m^3$ and 495.89±10.53 $\mu g/m^3$, respectively. Error bars represent variation of exposure during the entire length of gestation.

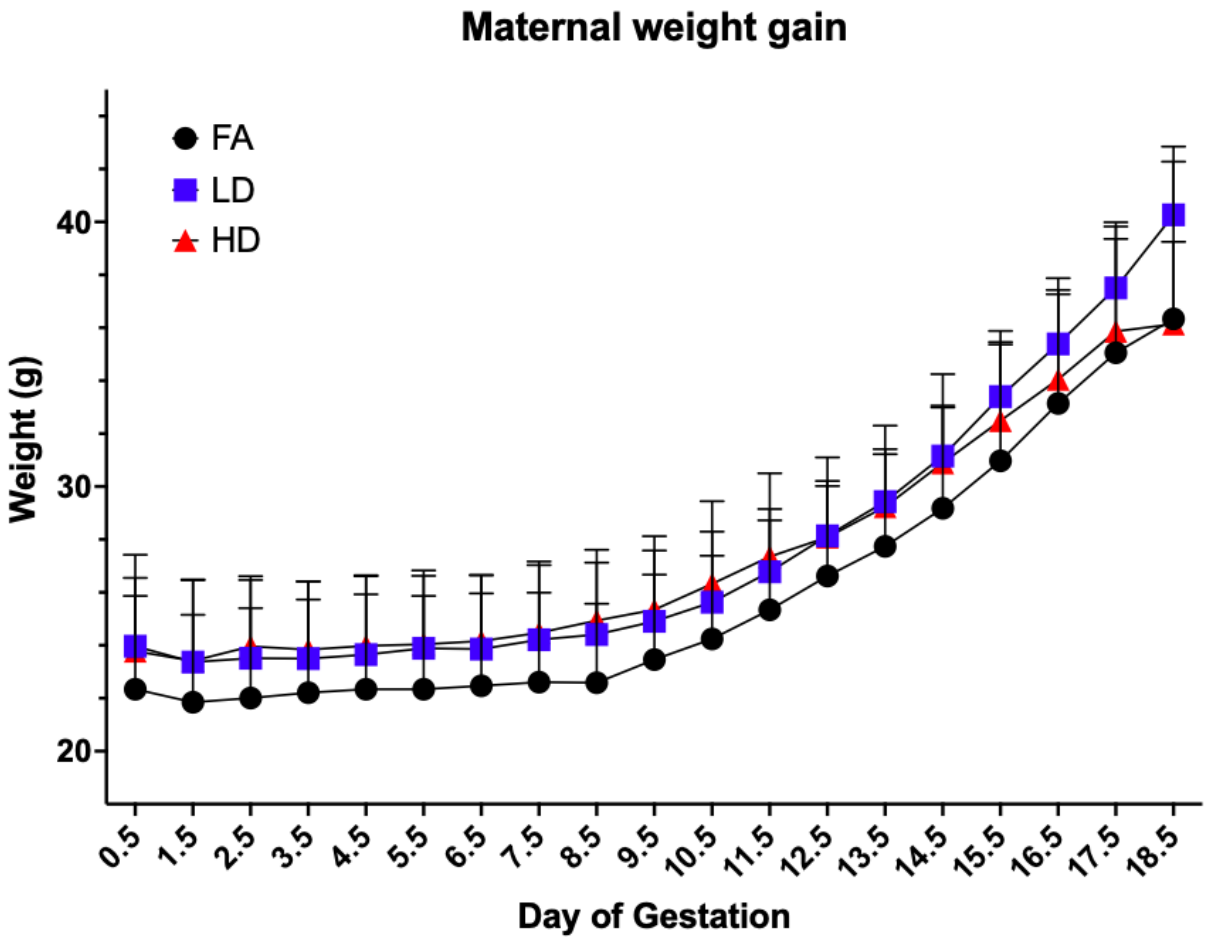

Supplemental Figure 2. Average maternal weight gain during gestation did not significantly differ within or between exposure groups (P=0.107). Dam sample sizes included FA (n=14), LD (n=12), or HD (n=13). Error bars represent SEM.

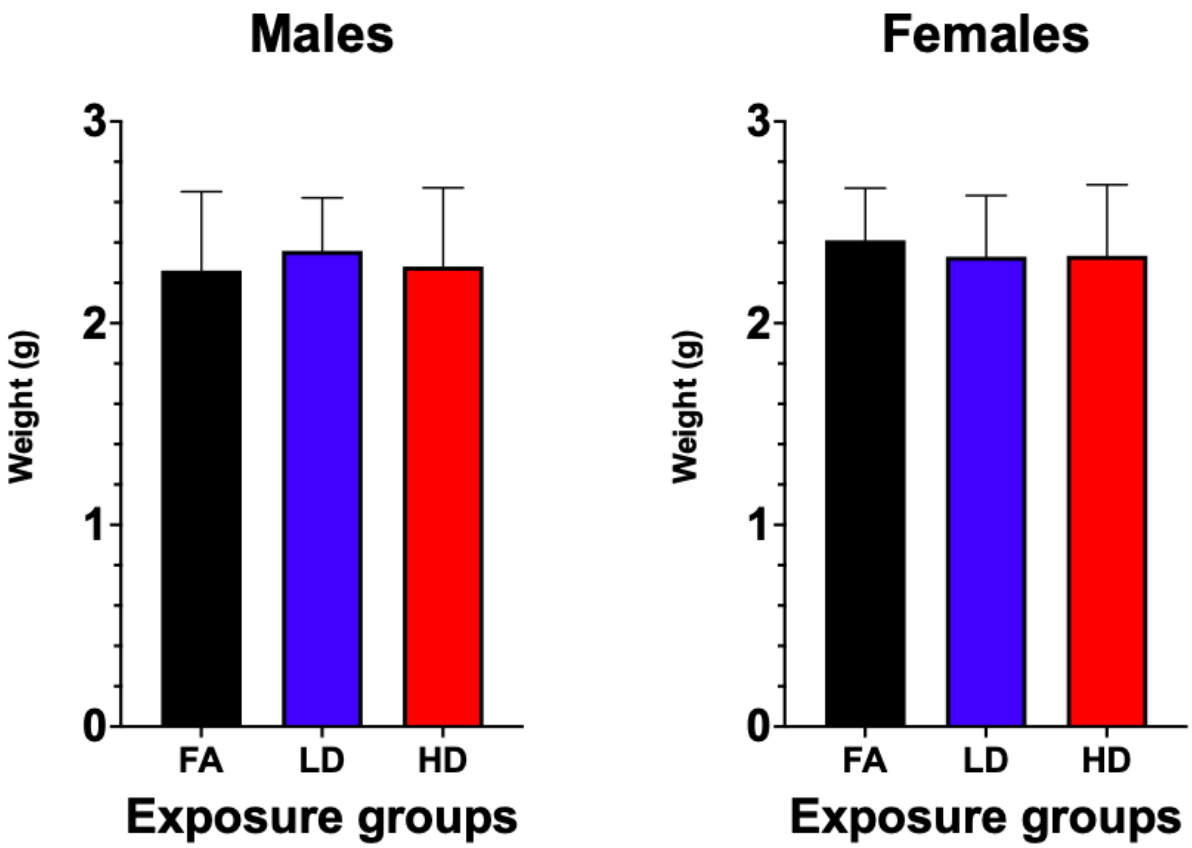

Supplemental Figure 3. Neonatal weights at PND5 for males and females (n=257 from 39 litters). No significant difference was observed among groups (P=0.899). Offspring sample sizes, listed as (n=Male, Female), from 10-12 litters, includes FA (54, 36), LD (53, 37), and HD (42, 35) groups. Error bars represent SEM.

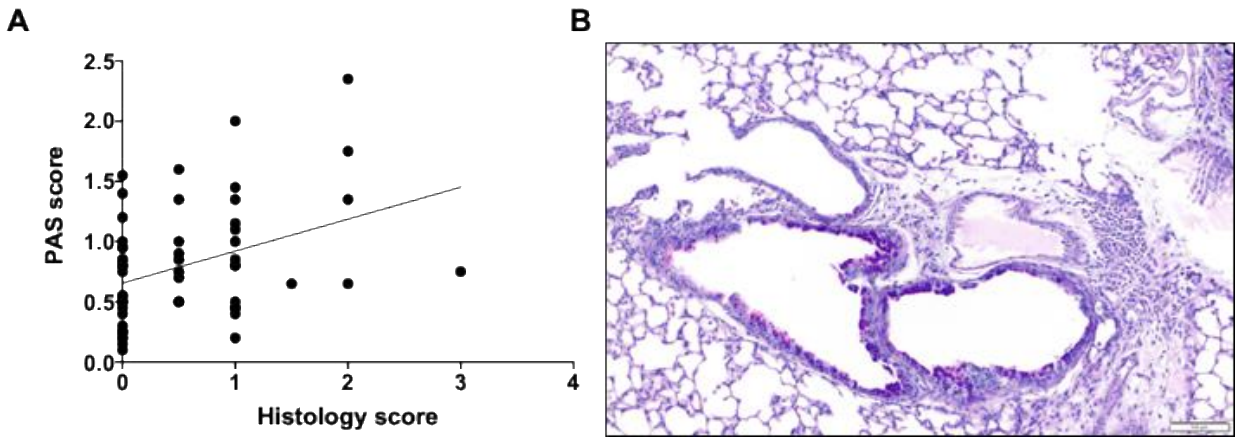

Supplemental Figure 4. (A) A weak correlation of the PAS score of neonatal lungs with their respective histologic inflammation score (R^2=0.144). (B) A lung score of 1 (mild inflammation) with a high PAS score.

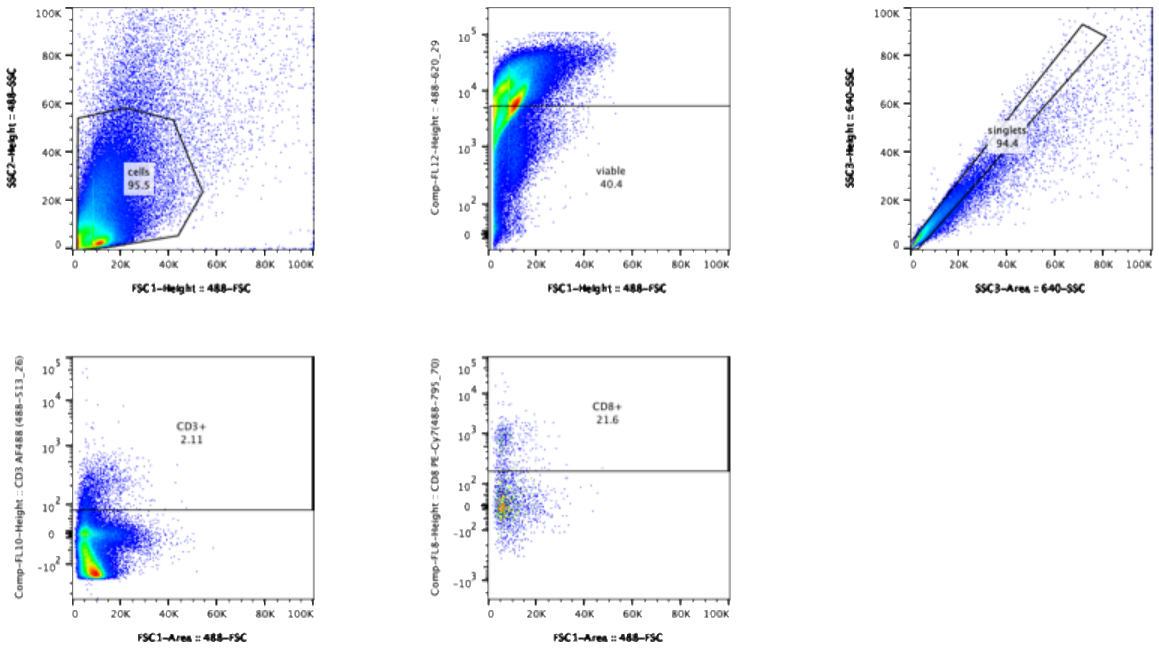

Supplemental Figure 5. CD8+ gating strategy, HD sample. Gating from left to right, top to bottom: Cells, Singlets, Viable cells, CD3+ cells, CD8+ cells.

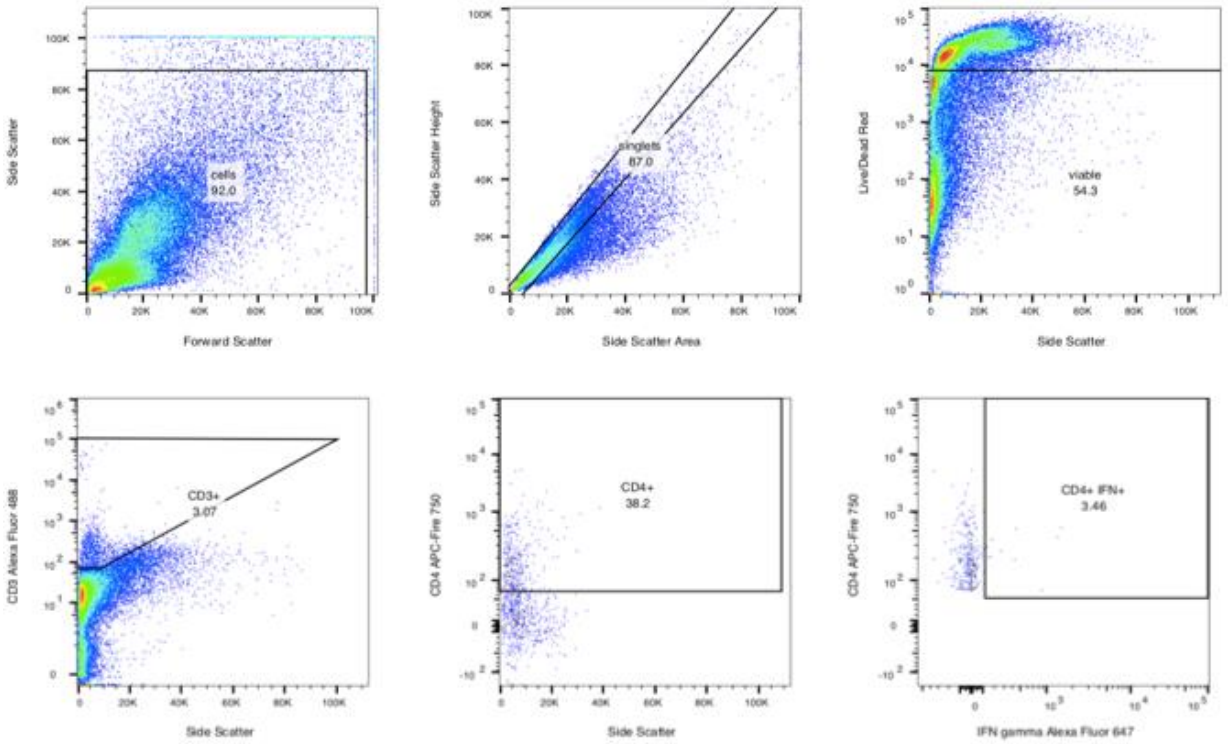

Supplemental Figure 6. Th1 gating strategy, FA sample. Gating from left to right, top to bottom: Cells, Singlets, Viable cells, CD3+ cells, CD4+ cells, Th1-biased cells.

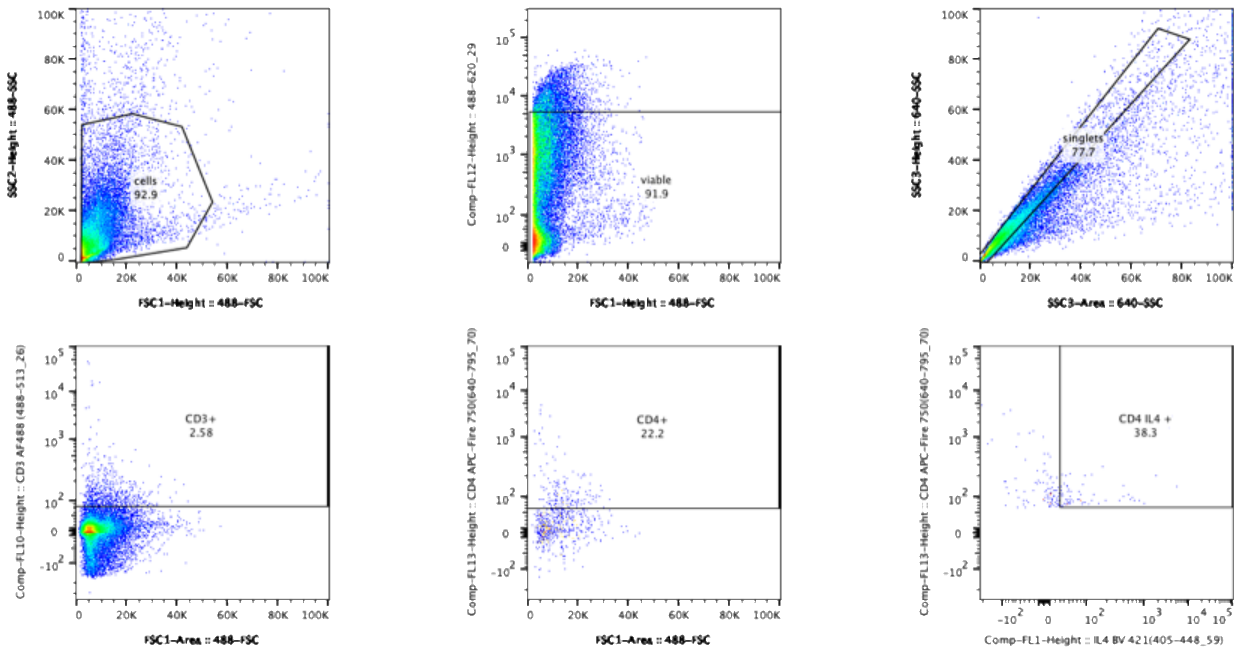

Supplemental Figure 7. Th2 gating strategy, HD sample. Gating from left to right, top to bottom: Cells, Singlets, Viable cells, CD3+ cells, CD4+ cells, Th2-biased cells.

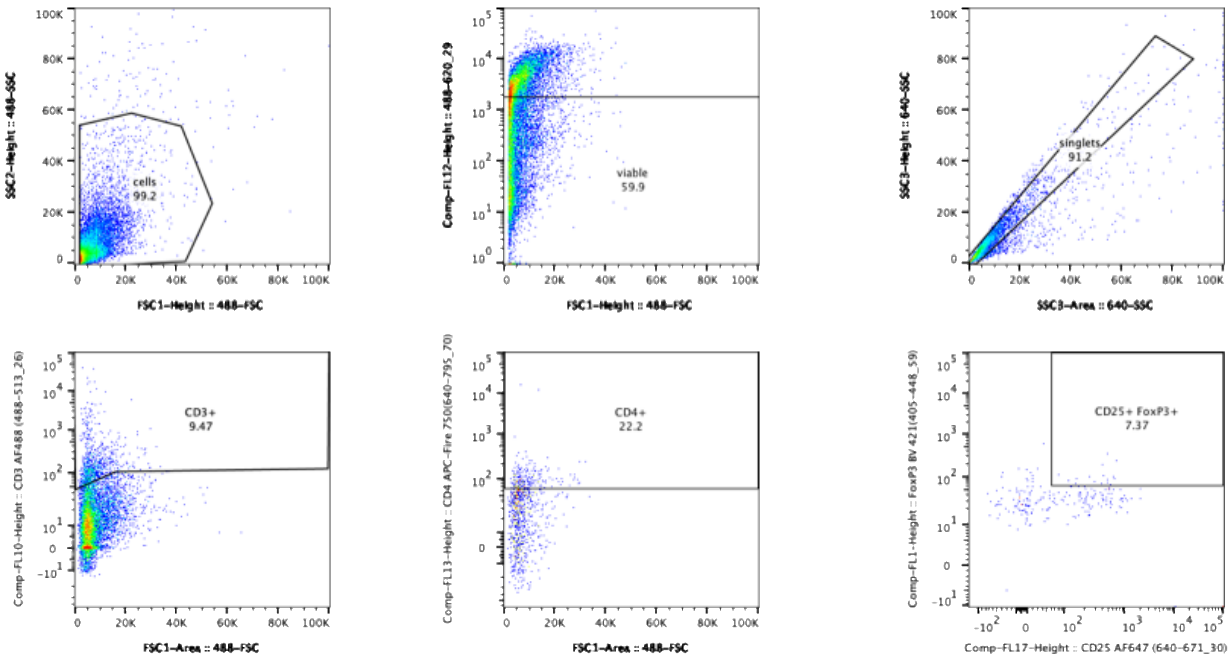

Supplemental Figure 8. T regulatory cell gating strategy, HD sample. Gating from left to right, top to bottom: Cells, Singlets, Viable cells, CD3+ cells, CD4+ cells, CD25+FoxP3+ cells.

Supplemental Table 1. Histologic PAS score was graded on a scale from 0-4 based on the percentage of goblet cells per complete bronchiole [97]. Scores are expressed as the mean ± SEM. Offspring sample sizes (n= Male, Female) from 3-6 litters include FA Sham (7, 4), LD Sham (5, 4), HD Sham (5, 4), FA RSV (3, 4), LD RSV (7, 3), and HD RSV (6, 5).

	Overall	Males	Females
FA Sham	0.74 ± 0.13	0.84 ± 0.16	0.62 ± 0.09
FA RSV	0.76 ± 0.16	0.71 ± 0.28	0.68 ± 0.18
LD Sham	0.79 ± 0.16	0.89 ± 0.25	0.66 ± 0.11
LD RSV	0.91 ± 0.17	0.97 ± 0.24	0.77 ± 0.20
HD Sham	0.86 ± 0.14	0.95 ± 0.24	0.74 ± 0.10
HD RSV	0.76 ± 0.19	0.93 ± 0.33	0.56 ± 0.17

APPENDIX 2

SUPPLEMENTAL FIGURES AND TABLES FROM CHAPTER IV

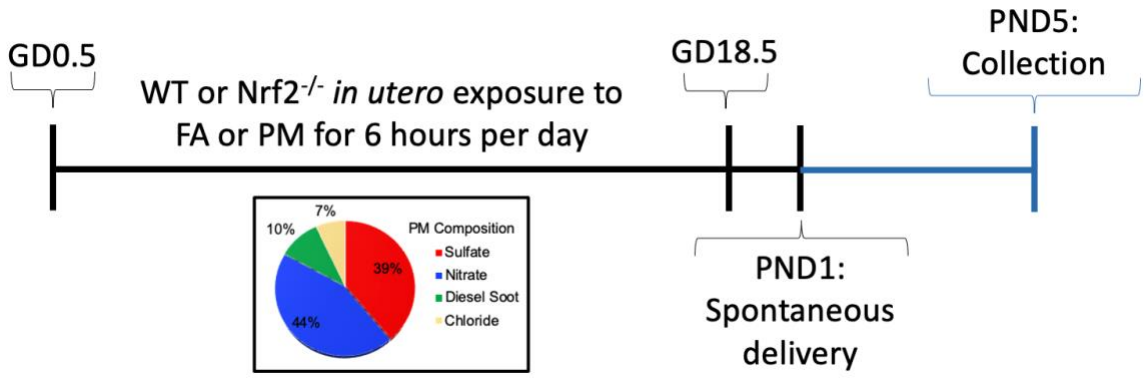

Supplemental Figure 1: Experimental timeline for mouse exposure model. GD: gestation day; FA: filtered air; PM: particulate matter; PND: postnatal day.

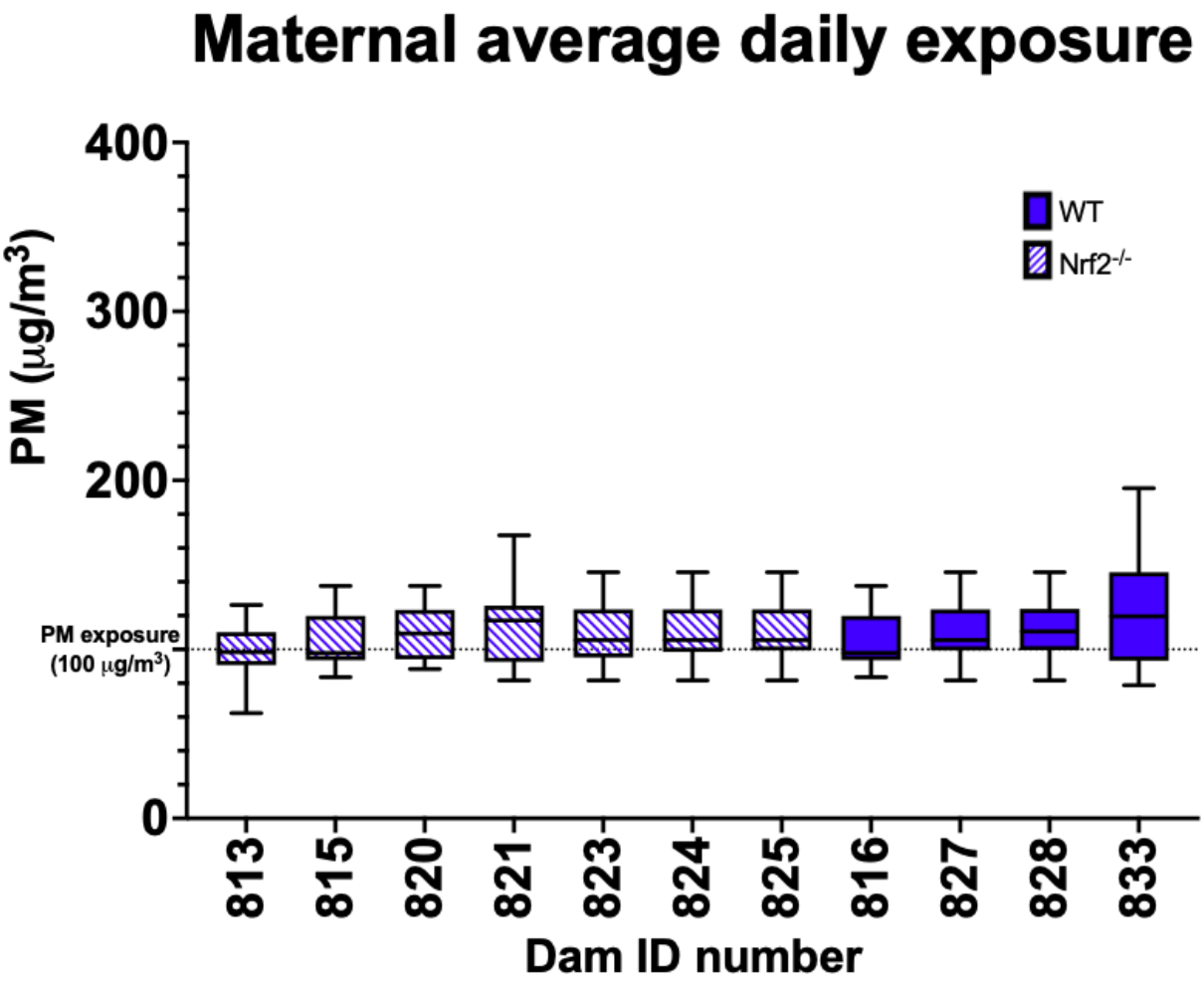

Supplemental Figure 2: Average maternal exposure to particulate matter (PM) in the low dose (LD) averaged 111.88±4.40 μg/m^3. Error bars represent minimum and maximum variation of exposure during the entire period of gestation.

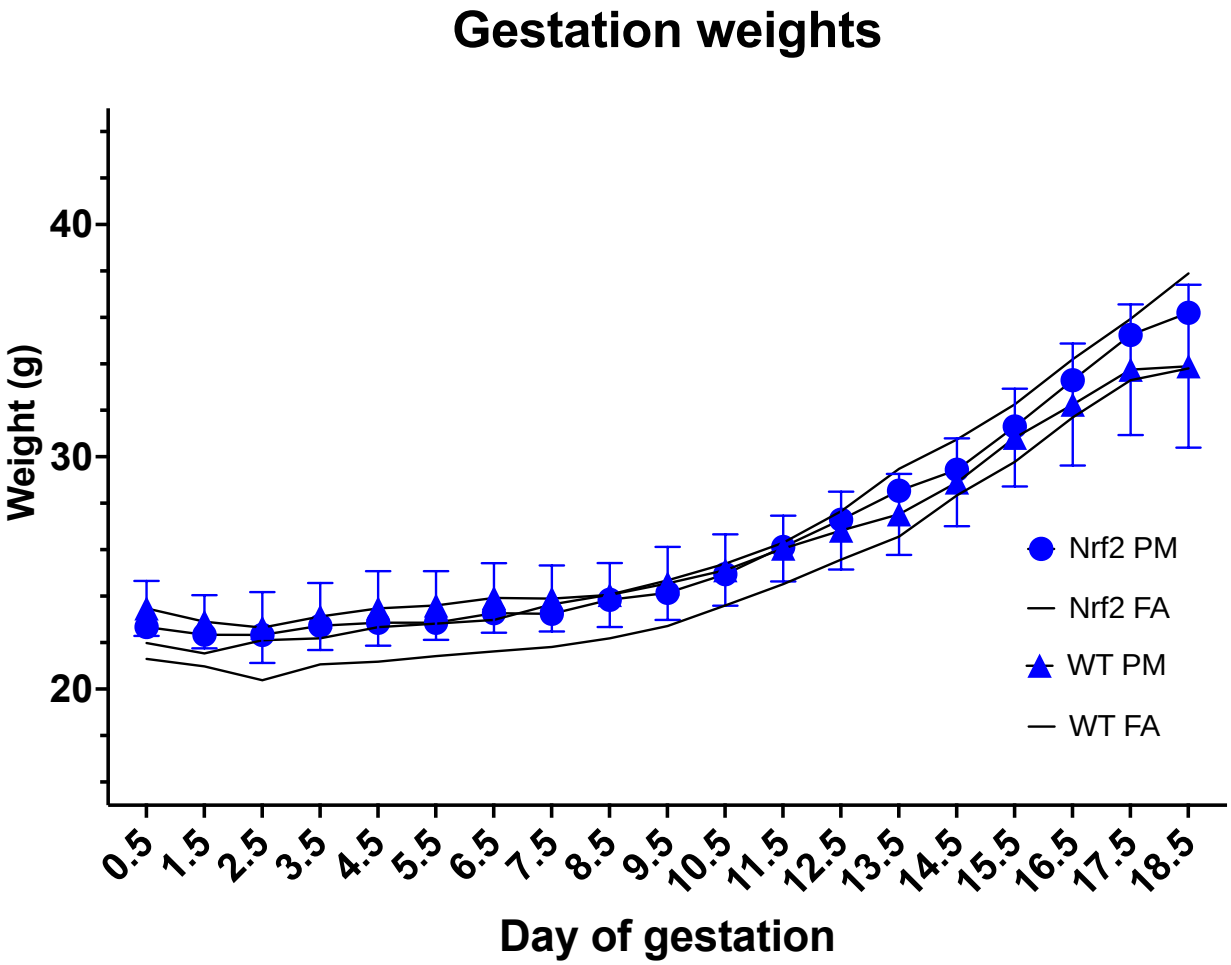

Supplemental Figure 3: Maternal weight gain during gestation did not significantly differ within or between exposure groups. Dam sample size includes WT FA (n=5), WT PM (n=4), $Nrf2^{-/-}$ FA (n=5), and $Nrf2^{-/-}$ PM (n=7).

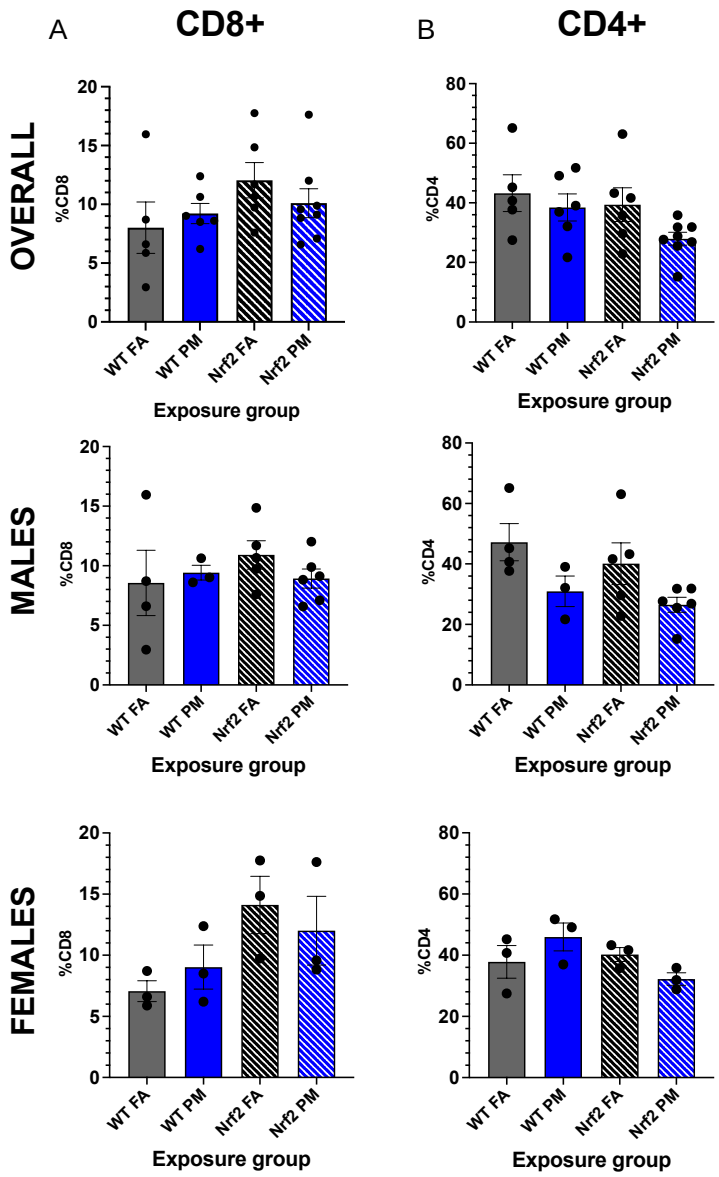

Supplemental Figure 4: CD8+ (A) and CD4+ (B) cells separated by sex. No significant differences are noted, though the overall level of CD4+ cells appears slightly lower in PM-exposed Nrf2$^{-/-}$ neonates (males and females) and WT neonates (males). Offspring sample sizes, listed as (n=Male, Female), from 4-7 litters, include WT FA (n= 3,3), WT PM (n=3,3), Nrf2$^{-/-}$ FA (n=5,3), and Nrf2$^{-/-}$ PM (n=6,3). Error bars represent SEM. Data analyzed using two-way ANOVA with Tukey's multiple comparison test.

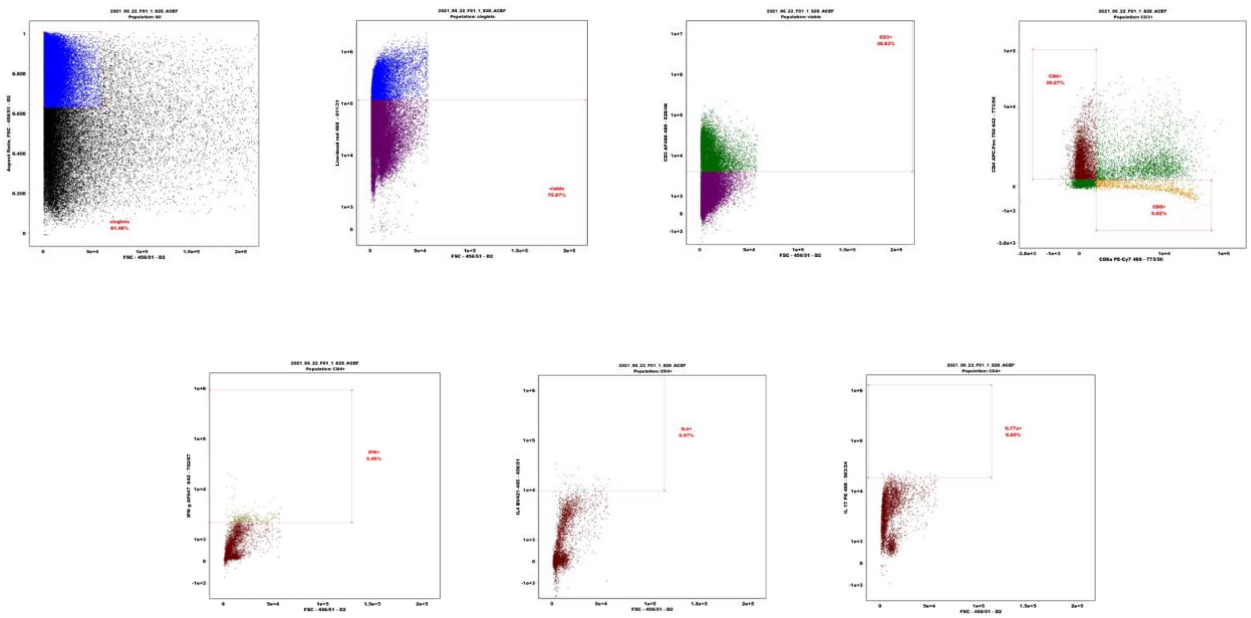

Supplemental Figure 5: CD4+ subsets gating strategy, FA sample. Gating from left to right, top to bottom: Cells, Singlets, Viable cells, CD3+ cells, CD4+ cells, FoxP3+ cells (last two).

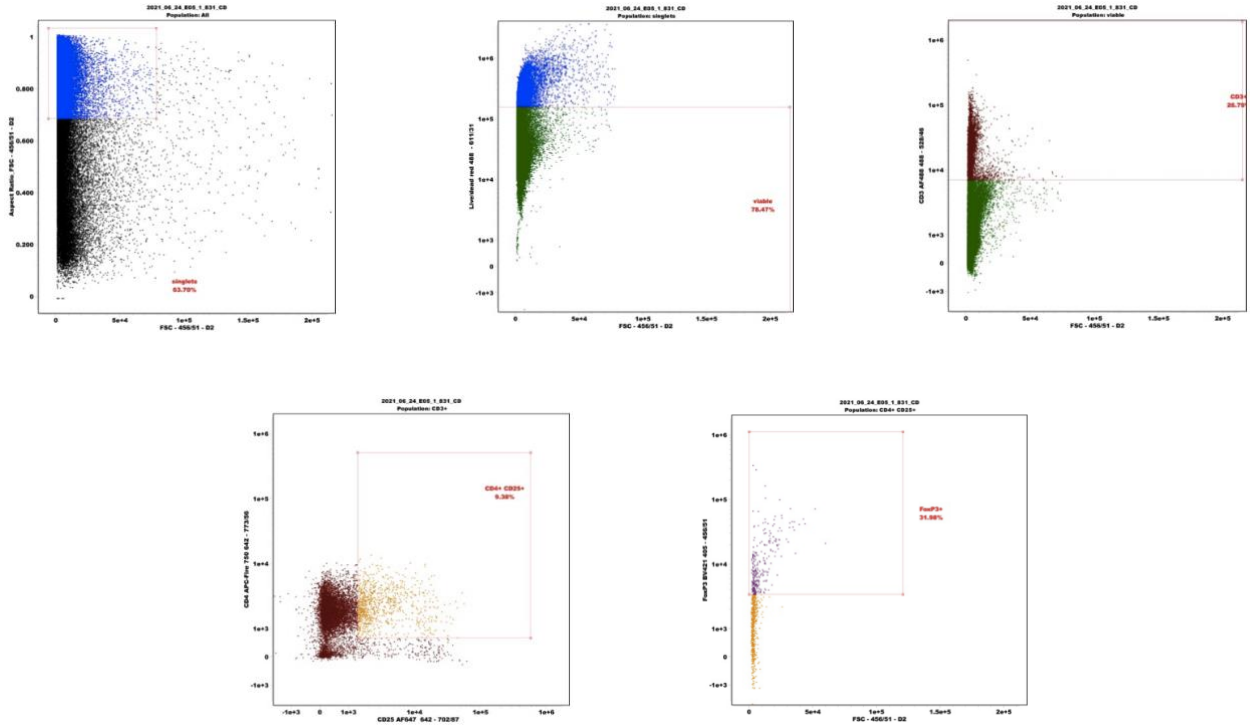

Supplemental Figure 6: CD4+ subsets gating strategy, FA sample. Gating from left to right, top to bottom: Cells, Singlets, Viable cells, CD3+ cells, CD4+ cells, FoxP3+ cells (last two).